NOTICE

The quality of this microform is heavily dependent upon the quality of the original thesis submitted for microfilming. Every effort has been made to ensure the highest quality of reproduction possible.

If pages are missing, contact the university which granted the degree.

Some pages may have indistinct print especially if the original pages were typed with a poor typewriter ribbon or if the university sent us an inferior photocopy.

Reproduction in full or in part of this microform is governed by the Canadian Copyright Act, R.S.C. 1970, c. C-30, and subsequent amendments.

AVIS

La qualité de cette microforme dépend grandement de la qualité de la thèse soumise au microfilmage. Nous avons tout fait pour assurer une qualité supérieure de reproduction.

S'il manque des pages, veuillez communiquer avec l'université qui a conféré le grade.

La qualité d'impression de certaines pages peut laisser à désirer, surtout si les pages originales ont été dactylographiées à l'aide d'un ruban usé ou si l'université nous a fait parvenir une photocopie de qualité inférieure.

La reproduction, même partielle, de cette microforme est soumise à la Loi canadienne sur le droit d'auteur, SRC 1970, c. C-30, et ses amendements subséquents.

ISBN 0-315-53266-1

THE PETROLOGY AND MINERALOGY OF THE CLINTON-COLDEN GABBRO-ANORTHOSITE INTRUSION, SLAVE PROVINCE, N.W.T.

R.I. MACFIE

Thesis submitted to
the School of Graduate Studies and Research
in partial fulfillment of the requirements for the M.Sc.
degree in Geology

Ottawa-Carleton Geoscience Centre and
Université d'Ottawa/University of Ottawa

ABSTRACT

The Clinton-Colden gabbro-anorthosite intrusion occurs in the eastern Slave Province near the boundary with the Churchill Province. It is approximately 20 km^2 in area and consists of meta-gabbro to meta-anorthosite, varying in an extremely irregular manner depending upon the closeness of packing of plagioclase. It differs from typical Archean anorthositic intrusions in that it is not layered and has a low $Mg/Mg+Fe^{+2}$ ratio of 0.348.

The gabbro-anorthosite body intrudes meta-volcanic rocks consisting of tholeiitic mafic flows and sills and a calc-alkaline series of intermediate and felsic flows and sills. The volcanic package includes mafic sills containing coarse-grained plagioclase phenocrysts. U-Pb zircon age of 2686+/-3 Ma has been obtained for the gabbro-anorthosite intrusion, while a rhyolite in the volcanic sequence has an age of 2671+2/-4 Ma, clearly indicating that the gabbro-anorthosite intrusion crystallized before volcanism had ceased.

The gabbro-anorthosite consists predominantly of unzoned coarse-grained sub-equidimensional calcic (An_{65-85}) plagioclase grains. These grains retain nearly pristine igneous compositions and morphology, except near veins where extensive alteration of plagioclase to fine epidote has occurred. Plagioclase grains are enclosed in very coarse oikocrysts consisting of calcic amphibole with actinolitic cores and hornblendic rims. Grain boundaries between amphibole oikocrysts and enclosed plagioclase grains are characterized by growth of fine amphibibole (hornblende to tschermakite) grains extending into and replacing the plagioclase grains.

The non-magmatic chemistry of the amphibole oikocrysts (low Ti, Al-poor cores) and the rare occurrence of uralite cores, having augite bulk compositions and partially overgrown by actinolite oikocrysts, indicate that the oikocrystic amphibole pseudomorphically replaced oikocrystic clinopyroxene. During the hydration of clinopyroxene to produce actinolite, Al was supplied from sites of replacement of calcic plagioclase by tschermakite and hornblende. Diffusion of Al into the actinolite pseudomorphs resulted in a compositional gradient from aluminous hornblende rims to less aluminous, typically actinolite, cores.

The magmatic mineral assemblage included an oikocrystic Fe-Ti oxide, perhaps titanomagnetite, which has been partially oxidized to skeletal trellis networks of ilmenite and rutile. Evidence of other magmatic phases (apart from rare zircon), for instance cummingtonite after orthopyroxene or serpentine after olivine, is not observed. This could be a result of homogenization of ferromagnesian material during the alteration process. Fine-grained secondary calcic amphibole obscures the nature of the alteration processes in some rocks.

The hydrating phase could have been of deuteric or non-marine external origin. It circulated in a pervasive set of sub-rectilinear fractures which could be of cooling-shrinkage or tectonic origin. The mineralogy of the intrusion indicates postmagmatic re-equilibration at the greenschist-amphibolite facies transition, at between 5 and 9 kb.

The plagioclase of the intrusion crystallized from a body of magma larger than the gabbro-anorthosite as presently exposed. In the absence of geological or geophysical evidence of a larger body in the subsurface, it is presumed that the plagioclase-rich magma separated

from its parental system. REE evidence is compatible with, but not demonstrative of, a genetic relationship between the gabbro-anorthosite intrusion and volcanic rocks of the Clinton-Colden greenstone belt.

SOMMAIRE

L'intrusion Clinton-Colden, qui se trouve dans la partie est de la province de l'Esclave, tout près de la frontière avec la province de Churchill est composée de métagabbro et de méta-anorthosite qui affleurent sur près de 20 km^2 et qui varient compositionellement de facon tres irreguliere selon la degré d'entassement du plagioclase. Cette intrusion se distingue clairement des autres complexes anorthositiques archéens par son absence de litage et son pauvrete relatif en magnesium ($Mg/Mg+Fe^{+2} = 0.348$).

L'intrusion est encaissée par et recoupe une séquence de roches métavolcaniques composée surtout de laves et filons mafiques et tholéiitiques mais aussi de laves et filons intérmediaires et calco-alcalins. Certains des filons mafiques de cette séquence possèdent de gros phénocristaux de plagioclase. L'âge absolu de l'intrusion, obtenu par radiométrie U-Pb pratiquée sur zircon, est de 2686+/-3 Ma alors qu'une rhyolite des roches encaissantes et âgée de 2671+2/-4 Ma. Ceci demontre clairement que l'intrusion fut solidifiée avant la fin du volcanisme dans la région.

Les roches de l'intrusion sont dominées par des gros phénocristaux quasi-équidimensionels de plagioclase avec une composition homogène et calcique (An_{89-95}). Ces phénocristaux retiennent bien leur composition et morphologie primitive sauf en bordure de veines tardives ou le plagioclase est transformé à l'épidote. Les phénocristaux de plagioclase sont renfermés par des très gros oikocristaux d'amphibole calcique qui ont des coeurs actinolitques et des bordures hornblendiques. L'interface entre ces amphiboles et les plagioclases et souvent ornée par de fines aiguilles d'amphibole (hornblende à

tschermakite) qui croissent vers le plagioclase par remplacement de ce dernier-ci.

Le chimisme des oikocristaux d'amphibole, plus particulièrement leur faible teneur en Ti et leurs coeurs actinolitiques ainsi que la présence occasionelle de vestiges d'uralite ayant des compositions d'augite au coeurs de certains oikocristaux, laisse croire que ces oikocristaux d'amphibole proviennent d'un remplacement pseudomorphique d'oikocristaux de clinopyroxène. L'approvisionnement en aluminium necessaire a l'hyratation du clinopyroxène á l'actinolite fut assuré par le remplacement simultané du plagioclase calcique par la tschermakite et la hornblende. La diffusion de l'aluminium vers les oikocristaux explique la zonation compositionelle de ceux-cis; des bordures hornblendiques enrichies en aluminium, aux coeurs actinolitiques appauvries en celui-ci.

Parmi les minéraux primitifs de l'intrusion on compte des oxydes de fer-titane, eux aussi oikocristiques, qui ont maintenant étés oxydes à des treillis squelettiques d'ilmenite et de rutile. On ne retrouve aucune autre evidence de phases primitives (sauf peut-être quelques rares zircons) comme par exemple la cummingtonite (suite à un orthopyroxene) ou la serpentine (suite à l'olivine). Ceci est peut-être une consequence de l'effet homogénéisant du processus d'altération. La présence de fines amphiboles calciques secondaires obscurcit la nature de l'altération dans plusiers roches.

La phase volatile hydratante responsable de cette altération peut aussi bien être d'origine deutérique ou non-marine. Elle fut circulée par un réseau pénétrant de fractures d'origine tectonique ou encore de contraction. La mineralogie de l'intrusion nous indique que le

ré-équilibre postmagmatique correspond aux conditions du facies transitionel schistes vert-amphibolites, à des pression de 5 a 9 kb.

Les roches enrichies en plagioclase de cette intrusion proviennent certainement de la cristallisation d'un volume de magma supérieur à celui présentement exposé. En l'absence de toute évidence géologique ou géophysique pour attester la présence, en profondeur, d'une salle magmatique plus volumineuse, on doit supposer que cette intrusion enrichie en feldspath fut à un moment donné, séparée de sa salle magmatique originale. Le chimisme des éléments terre-rares suggère, mais ne démontre pas de facon non-équivoque, un lien génétique entre l'intrusion de gabbro-anorthosite et les roches volcaniques encaissantes de la ceinture métavolcanique de Clinton-Colden.

ACKNOWLEDGEMENTS

The writer acknowledges the invaluable guidance of André E. Lalonde throughout the duration of this study. R. Kretz reviewed an early version of the thesis, and A.D. Fowler read a portion of it. The editorial effort expended by W.F. Fahrig is greatly appreciated. J.B. Henderson, who discovered the Clinton-Colden intrusion in 1984, provided advice and encouragement, and read a portion of the thesis. Discussions with D. Lentz regarding various aspects of the project were of great assistance. Field work was supported by the Geological Survey of Canada (Project 84005), and assistance in the field was provided by N. Wodicka and S. Leclair. Much of the data on the volcanic rocks of the area was collected by N. Wodicka and incorporated in her B.Sc. thesis at the University of Ottawa.

R. Hartree, J. Loop, G. Mrazek, J-F. Tardif and E. Hearn of the University of Ottawa provided technical assistance. The U-Pb age for the Clinton-Colden intrusion was obtained thanks to the co-operation of O. van Breemen of the Geological Survey of Canada.

This project was completed in part as a result of the patience and support of my wife, Martha.

TABLE OF CONTENTS

TABLE OF CONTENTS (cont'd)

TABLE OF CONTENTS (cont'd.)

LIST OF FIGURES

LIST OF FIGURES (cont'd.)

LIST OF TABLES

CHAPTER 1

INTRODUCTION

1.1 Introduction and purpose of study

The Clinton-Colden gabbro-anorthosite intrusion occurs near Clinton-Colden Lake in the Slave structural province, N.W.T. It is an Archean mafic intrusion, with less than 50 wt.% SiO_2 and consisting essentially of calcic plagioclase (An>60) and amphibole. It displays spectacular, coarse, poikilitic textures and an extremely heterogeneous distribution of rock types. The predominant ferromagnesian phase is coarse amphibole which encloses plagioclase grains in a poikilitic manner. Macroscopically this amphibole appears to be primary, and the intrusion was first named the Clinton-Colden hornblende gabbro-anorthosite intrusion (Macfie, 1987). However, detailed investigation of the amphibole indicates that it replaces pyroxene. Therefore the intrusion is now referred to simply as gabbro-anorthosite.

The intrusion contains abundant anorthosite. Archean anorthosite is known from a number of areas, including Greenland (e.g. the Fiskenaesset intrusion (Weaver et al., 1981)), India, Africa, Labrador (e.g. the Tessiuyakh intrusion (Wiener, 1981)), and Ontario (e.g. the Bad Vermilion Lakes complex (Ashwal et al., 1983) and the Shawmere complex (Simmons et al., 1980)). In general Archean anorthosite occurs as plagioclase-rich units in layered complexes of more mafic overall composition. The Clinton-Colden gabbro-anorthosite intrusion shares a number of characteristics with "typical" Archean anorthosite intrusions, but it differs in some important respects. The most

striking dissimilarity is that it is not layered, and is not associated with large amounts of more mafic rock.

The principal objective of this study was to investigate the origin of the 'hornblende gabbro' which, were it of magmatic origin, would represent a petrological anomaly. The second objective was to study the mineralogy of the amphibole in the intrusion. The intrusion's age, and its relationship with the greenstone belt which it intrudes, were also objects of study.

1.2 Location and access

The Clinton-Colden gabbro-anorthosite intrusion lies approximately 380 km north-east of Yellowknife, in the Slave structural province of the Canadian shield (Fig. 1.1). The intrusion is located approximately one km inland from the south-east shore of Clinton-Colden Lake in the Artillery Lake map area (NTS 75 O), about 20 km west of the Thelon tectonic zone, the boundary between the Slave and Churchill structural provinces (Fig. 1.1). Small aircraft provide the only practical means of access to the area, although an arduous passage is possible by canoe from the East Arm of Great Slave Lake, through the Lockhart River and Artillery and Ptarmigan Lakes, to Clinton-Colden Lake.

1.3 Previous work

The Clinton-Colden greenstone belt was recognized by Wright (1957, 1967) during reconnaissance mapping of parts of the districts of Mackenzie and Keewatin. The northern segment of the belt was included in 1:250,000 scale mapping of the Healey Lake map area (Henderson et al., 1982) and the southern part was covered in 1984 during mapping of

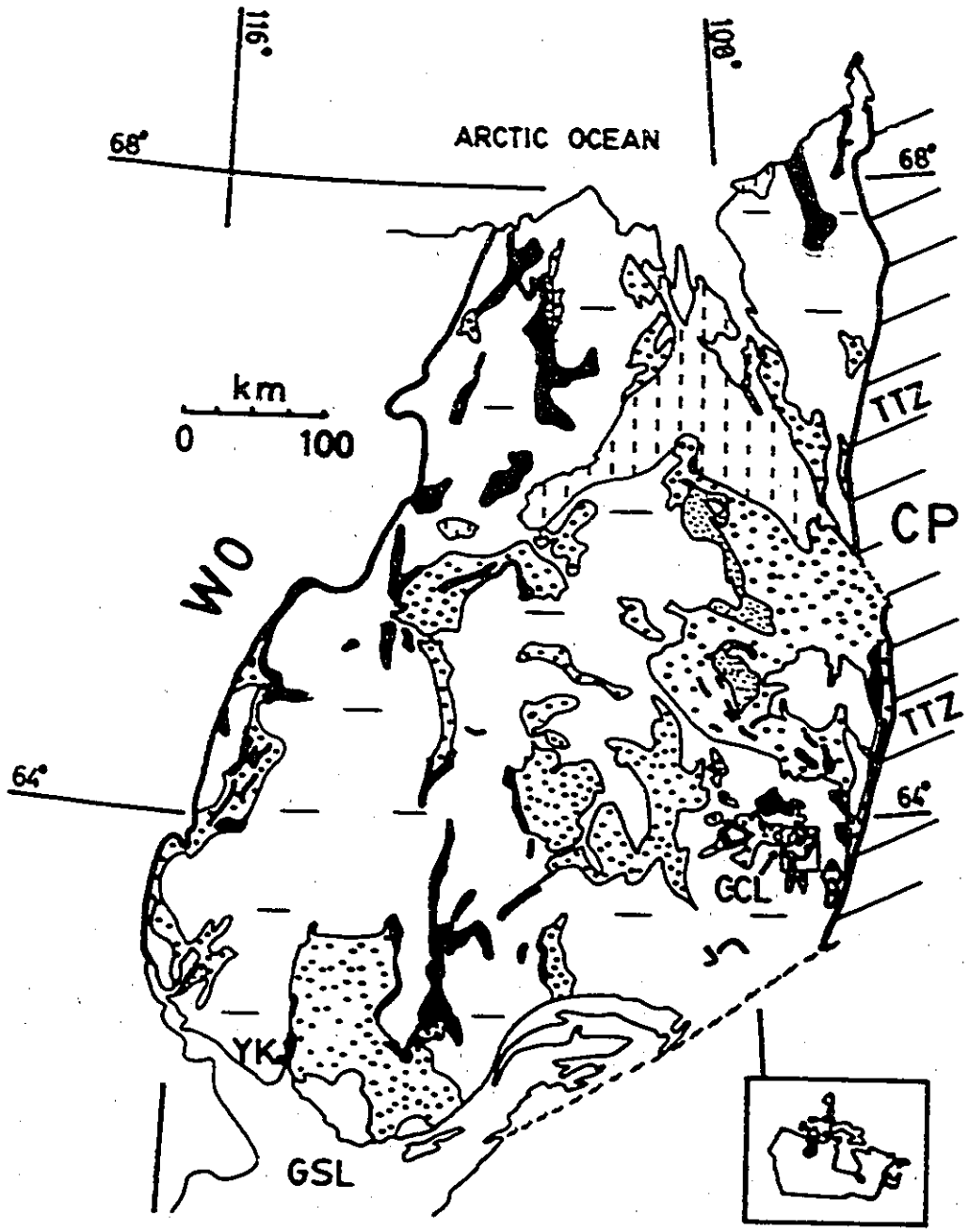

Fig. 1.1: Geology of the Slave structural province and the location of Clinton-Colden Lake. Proterozoic sedimentary rocks of the Kilohigok basin in vertical dashed lines; Archean mafic and undivided volcanic belts in black, intermediate to felsic volcanic belts in light stipple, metagreywacke-mudstone in heavy stipple, undifferentiated granitoid bodies and granitoid gneisses in horizontal dashed lines. WO=Wopmay orogen, CP=Churchill province, TTZ=Thelon tectonic zone, C-CL=Clinton-Colden Lake, GSL=Great Slave Lake, YK=Yellowknife. Area in box around southeastern Clinton-Colden Lake=location map in Fig. 2.1 Simplified after Henderson (1985).

the Artillery Lake map area (Henderson and Macfie, 1985). The Clinton-Colden gabbro-anorthosite intrusion was first recognized during the course of the latter project. A detailed study of volcanic rocks adjacent to the Clinton-Colden gabbro-anorthosite intrusion was undertaken by Wodicka (1987). Volcanic rocks of the northern part of the greenstone belt were studied by Lougheed (1986).

CHAPTER 2

GEOLOGY OF THE SLAVE PROVINCE AND THE CLINTON-COLDEN LAKE GREENSTONE BELT

2.1 The Slave structural province

The Slave province of the Canadian shield is a block of Archean (3.5-2.5 Ga) (Kusky, 1989) crust bounded by the Churchill province in the east and by the Wopmay orogen in the west (Hoffman, 1980). The geology of the province, briefly summarized below, is described in greater detail by Henderson (1981), Padgham (1985), and by others referred to in those works.

The province is underlain by Archean supracrustal rocks of the Yellowknife Supergroup, including predominantly mafic (Yellowknife-type) volcanic belts, predominantly felsic and intermediate volcanic belts (Hackett River-type), and turbidites (Padgham, 1985). Tholeiitic to calc-alkaline mafic volcanic rocks are more abundant in the west, while felsic and intermediate dominated belts are more common in the east. The former consist of 70-80% basalt and andesite (Padgham, 1985). These supracrustal rocks were intruded by granitoid plutons which have created thermal metamorphic aureoles, ranging up to sillimanite grade in places, upon surrounding rocks. Sialic basement to the supracrustal rocks is probably present in places (Henderson, 1981; Easton, 1985).

At least two models exist for the origin of the volcanic belts. The more widely held view is that they were deposited at the margins of rift-basins in a pre-existing sialic block (Henderson, 1981). By contrast, it has been suggested (Folinsbee

et al., 1968; Hoffman, 1986; Kusky, 1989) that the volcanic rocks are oceanic in origin, and that the Slave province grew by tectonic accretion of oceanic material. An implication of this hypothesis is that little or no pre-Yellowknife Supergroup sialic crust existed. Rationalizing oceanic volcanism and the presence of pre-Yellowknife sialic basement, Fyson and Helmstaedt (1988) have suggested that the volcanic belts represent oceanic crust, but that the oceanic basins formed following rifting of sialic basement.

Geochronological work suggests that the volcanic sequences were deposited mainly between 2.69 Ga and 2.66 Ga, and that for the eastern and central Slave province two episodes of volcanic activity occurred, one during the period of 2698-2687 Ma and one during 2675-2663 Ma (Mortensen et al., 1988).

2.2 General geology of the Clinton-Colden Lake area

The study area of this project is in the eastern part of the Slave province, within the westernmost part of an area showing the effects of the Proterozoic collision (ca. 1.9 Ga) of the Slave province with the Churchill province. As a result, rocks of the area have foliation trajectories transitional from the curvilinear Slave province pattern to the Thelon-parallel trend of the easternmost part of the province. The rocks in this area were weakly altered following the emplacement of a crustal sheet thrust over the area from the east (Henderson et al., 1982). This thrusting event is associated with the major Proterozoic event to have affected the eastern margin of the Slave province: the collision between the Slave and Churchill provinces between 1970 Ma and

1950 Ma (van Breemen et al., 1987a). Farther to the east, closer to the boundary between the two structural provinces, the overthrusting resulted in the crystallization of kyanite in the underlying Yellowknife metapelites (Henderson and Macfie, 1985; James, 1985). In the Clinton-Colden area it resulted only in minor amphibolitization of Proterozoic diabase dykes.

2.3 The southeastern Clinton-Colden Lake area

2.3.1 Introduction and geochronology

The area around eastern Clinton-Colden Lake is underlain by a variety of Archean rocks and by two sets of Proterozoic mafic dykes (Henderson et al., 1987; Macfie, 1987; Henderson et al., 1982). The oldest rocks are volcanic and associated hypabyssal rocks of the Clinton-Colden greenstone belt, which covers an area of approximately 400 km^2 and extends roughly 75 km in a north-westerly direction (Fig. 1.1).

Zircons from rhyolite in the central part of the greenstone belt have yielded a U-Pb age of 2671+2/-4 Ma (van Breemen and Henderson, 1988). This may be compared with a date of 2692+/-2 Ma obtained from rhyolite of the Back River complex about 100 km to the north (van Breemen et al., 1987b). Volcanic rocks of the southern part of the greenstone belt are cut by the Clinton-Colden gabbro-anorthosite intrusion, for which a U-Pb (zircon) age of 2686+/-3 Ma has been obtained for a sample from Station G-92 (Fig. 2.2) (Macfie et al., in press) The gabbro-anorthosite was therefore emplaced before the cessation of volcanism in the area. This date is of interest with regard to the general geochronology of the eastern Slave province, and

is discussed in Chapter 6.

Both the greenstone belt and the gabbro-anorthosite are bounded to the south, and are intruded successively by, a diorite to quartz diorite body and a suite of granitoid rocks ranging in composition from granodiorite to tonalite. Similar nearby granitoid rocks have been dated at 2617+/-7 Ma (Charloit granodiorite) and 2616+7/-6 Ma (plutons of the Tarantula suite) (van Breemen and Henderson, 1988). The oldest Proterozoic rocks comprise several 20-60 m thick vertical dykes with trends parallel to the 2.4 Ga Mackay swarm (Fahrig and West, 1986). The youngest rocks in the area are two 20 m thick Mackenzie dykes having an age of approximately 1.27-1.28 Ga (Heamen and LeCheminant, 1988).

2.3.2 Volcanic rocks of the region

The volcanic rocks are predominantly mafic and intermediate in composition, with minor amounts of felsic material (Fig. 2.1). They contain no primary minerals, but for ease of presentation the prefix meta- is not used in the following discussion. Their stratigraphy has been obscured by deformation and metamorphism. Petrography of the volcanic rocks has been dealt with in some detail by Wodicka (1987), and the descriptions which follow derive in part from that work which contains full descriptions and illustrations.

Volcanic-derived sedimentary units, mostly debris flows, are locally recognizable. Also common are sills and dykes of material presumed to represent hypabyssal equivalents of the volcanic units. The original relationship between the volcanic rocks and meta-greywackes found approximately 8 km to the northwest is not

apparent. Basement to the supracrustal rocks is not observed.

Mafic volcanic rocks consist of pillowed and massive flows. They occur throughout the area, and, while difficult to distinguish in the field from volcanic rocks of more intermediate composition, appear to underlie approximately 70% of the area based upon observations made by the author. Included here are mafic sills, which are difficult to distinguish from massive flows, in part because of metamorphism. Massive sills or flows containing plagioclase phenocrysts up to two centimetres in size, along with occasional glomerocrysts, are common but are volumetrically minor. Mafic rocks are included with intermediate rocks in Figure 2.1.

Intermediate volcanic rocks, identified in the field by their colour index and later confirmed by chemical analysis, make up approximately 25% of the Clinton-Colden greenstone belt. Like the mafic volcanic rocks, they occur throughout the area, interspersed with their mafic counterparts. They are predominantly of pyroclastic origin.

Felsic volcanic rocks make up approximately 5% of the Clinton-Colden greenstone belt. They consist of crystal tuffs, along with probable massive dome or flow units. They occur at three locations within the area mapped by Wodicka (1987) and this author. Such felsic centres have been identified elsewhere in the volcanic belt (Henderson and Macfie, 1985; Henderson et al., 1982).

2.3.3 Clinton-Colden gabbro-anorthosite intrusion

The Clinton-Colden gabbro-anorthosite intrusion cuts the volcanic rocks of the southernmost part of the greenstone belt (Fig. 2.1). It

is described in detail in Chapter 4. Dykes of rock identical to rocks of the gabbro-anorthosite intrusion locally cut the volcanic rocks. Many 0.5 to 5 m thick mafic dykes, some of which are plagioclase-phyric, cut the gabbro-anorthosite. These dykes are cut by the Mackay-trend and Mackenzie dykes, and in general resemble the sills or dykes which cut the volcanic rocks, although they are less common in the gabbro-anorthosite. Such dykes are rare in the granitoid rocks of the area, and their distribution suggests that most were syn-volcanic.

2.3.4 Diorite to quartz diorite intrusion

A composite body ranging in composition from diorite to quartz diorite partially bounds the volcanic belt and the gabbro-anorthosite intrusion in the south (Fig. 2.1). It consists of small (100 m scale) plugs or sheets (three dimensional geometry unknown) consisting of plagioclase, green hornblende and quartz. Hornblende varies from 30 to 80%; quartz from 1 to 15%. Optical determinations indicate that plagioclase compositions range from An_{43} to An_{51}. Zircon is present in some phases of the body. The rock is fine to coarse grained, medium being typical. Alteration is slight, being restricted to minor replacement of plagioclase by fine epidote in some rocks.

Sharp contacts between phases of the body are exposed in several places. Distribution of phases is irregular, and their distinction is based upon grain size and quartz content. Rocks of this body are distinguished from the granitoid suite described below on the basis of colour of hornblende (green versus brown), absence of biotite and microcline, more calcic plagioclase and more mafic composition. Dykes related to the granitoid suite cut the diorite body.

Rocks of the dioritic body are easily distinguished from those of the gabbro-anorthosite intrusion on the basis of texture (granular versus poikilitic, medium grained versus very coarse), absence of hydrothermal alteration, presence of homogeneous, unaltered hornblende rather than the complex amphiboles of the gabbro-anorthosite, and different mineralogy, particularly anorthite and quartz content. Dykes of the dioritic rock cut both the gabbro-anorthosite intrusion and the volcanic rocks. Angular xenoliths derived from the gabbro-anorthosite body are common in the diorite-quartz diorite body.

Mafic dykes cutting the dioritic body are much less common than those cutting the volcanic rocks and the gabbro-anorthosite intrusion. Xenoliths of amphibolite and schistose rocks which may be metasediment are common within both the dioritic body and the granitoid suite described below.

2.3.5 Granitoid rocks

An extensive area underlain by granitoid rocks lies to the east and south of the Clinton-Colden area (Henderson and Macfie, 1986), bounding and intruding the above units (Fig. 2.1). They comprise tonalite with minor granodiorite, consisting of varying amounts of plagioclase, quartz, biotite, hornblende, muscovite, microcline and opaque minerals. Minor epidote and chlorite are present, particularly near contacts with the more mafic units described above. While rocks of the suite vary in colour (pink to white), mineralogy (biotite-only to hornblende-only) and grain size, variation is gradational and intrusive relationships between phases were not observed.

2.3.6 Metamorphism

Metamorphism of the volcanic and sedimentary rocks in the eastern Clinton-Colden Lake area, as in most parts of the Slave province (Henderson, 1981; Padgham, 1985), took place largely during intrusion of granitoid plutonic bodies. The volcanic rocks of the area vary from greenschist facies in the northeast to amphibolite facies in the west and south, i.e. towards the large area of granitoid rocks (Henderson and Macfie, 1985; Wodicka, 1987) (Fig. 2.1). The mineralogy of the meta-volcanic rocks has been documented by Wodicka (1987). At greenschist facies mafic volcanic rocks consist of albite, quartz, epidote, chlorite, calcite and, locally, actinolite. At higher grade they also contain hornblende and cummingtonite. Highest grade occurs adjacent to the granitoid intrusions. Variable silicification and carbonatization of the volcanic rocks has occurred, and, in general the volcanic rocks have been thoroughly recrystallized.

Evidence of minor contact metamorphism by the Clinton-Colden intrusion is also present in adjacent volcanic rocks. A 200 m-wide aureole of massive, garnet-bearing amphibolite occurs along the margin of the Clinton-Colden intrusion (Fig. 2.1). The garnet is red almandine-spessartine having the composition

$Si_{6.06}Al_{3.92}Ti_{0.01}Mg_{0.02}Fe^{+2}_{3.58}Mn_{1.25}Ca_{0.9}$

(analyses given in Appendix 3). It occurs in mafic to intermediate flows and fragmental rocks. At one location, where a screen of gabbro derived from the Clinton-Colden intrusion is enclosed in younger granitoid rocks, a volcanic xenolith in the gabbro screen is

garnet-bearing. Probably the highest metamorphic grade, represented by the presence of garnet, was caused by the emplacement of the Clinton-Colden intrusion. Wodicka (1987) suggests that the growth of cummingtonite rims on blue-green hornblende in an area within the garnet-bearing aureole reflects an increase in temperature. Like garnet, cummingtonite is not observed adjacent to the granitoid rocks, nor within the Clinton-Colden intrusion. This may reinforce the suggestion that a thermal peak was achieved following the intrusion of the Clinton-Colden intrusion, producing both garnet and cummingtonite in adjacent rocks which had already been metamorphosed at amphibolite (hornblende-producing) facies during an undetermined metamorphic event, perhaps resulting from early plutonism in the area. The presence of a significant amount of Mn in the almandine provides additional evidence that it was produced during contact metamorphism (Deer et al., 1966).

Later minor metamorphic effects are evident in the rocks of the area. Shear zones, trending approximately parallel to the Thelon tectonic zone, are characterized in the volcanic and granitoid rocks of the area by a biotite-chlorite assemblage, and a biotite foliation is present in the granitoid rocks. Garnets in the aureole around the gabbro-anorthosite intrusion are deformed where they are found in minor shear zones. The orientation of these structural features indicates that they formed during Proterozoic movement along the Thelon tectonic zone (Henderson et al., 1987).

While growth of biotite in Thelon-parallel shears is common, evidence of high pressure metamorphism following thrusting along the Thelon tectonic zone is not found in the area. To the northeast, in the Healey Lake map area (Henderson et al., 1982) and the Moraine Lake

map area (James, 1985), kyanite occurs in meta-pelites, and it occurs approximately 40 km to the east at Sifton Lake in the western margin of the Thelon tectonic zone (Henderson and Macfie, 1985). However, it is not found in the area of Clinton-Colden Lake. The Clinton-Colden area probably lies to the west of the area most strongly affected by the west-directed Thelon thrust sheet. However, it does lie to the east of the isograd, mapped in the Healey Lake Area to the north (van Breemen et al., 1987b), marking the limit of amphibole growth in Proterozoic diabase dykes. Similar amphibole growth is seen in the Mackay-trend dykes in the southeastern Clinton-Colden Lake area. If these are indeed Mackay dykes, this metamorphic event may be related to early movement on the Thelon tectonic zone, suggested by Henderson et al. (1987) to have occurred between 2.2 and 2.4 Ga.

There has been no metamorphism after 1.27 Ga as the Mackenzie dykes are not altered.

2.3.7 Regional tectonics

Two major deformation events have affected rocks in the Clinton-Colden area. Early deformation of the volcanic pile was later followed by deformation resulting from activity along the Thelon tectonic zone. However, discriminating between effects of these events is difficult, in part due to poor development of foliation in the volcanic rocks.

The dips of volcanic and sedimentary strata and foliations are steep (Fig. 2.1), indicating that a major folding event has affected these rocks, and an absence of fold closures suggests that the folds have subhorizontal axes. Foliations in the volcanic rocks are parallel

to the contact with the adjacent granitoid rocks, and rare top indicators (pillowed flows) indicate that the volcanic units face away from the granitoid rocks. This pattern is common in Archean greenstone belts (e.g. Ayre et al., 1987), and is commonly attributed to diapiric intrusion of granitoid masses. Such a process has been suggested for Slave province greenstone belts as well (Drury, 1977), and may account for early folding in the Clinton-Colden greenstone belt. The data are insufficient to evaluate other mechanisms, such as imbricate thrusting during emplacement of the greenstone belt as accreted oceanic material at the margin of a growing Slave province (Hoffman, 1986; Kusky, 1989).

Many late shear zones and foliations striking approximately 015°, and occurring in all rocks except Mackenzie dykes, are attributed to movement along the Thelon tectonic zone. Shear zones range in thickness from a few centimetres to more than ten metres. Shear zones and foliations in the volcanic rocks, diorite and granitoids contain chlorite, biotite and hornblende. The Clinton-Colden gabbro-anorthosite intrusion contains a network of anastomosing shear zones, also attributed to activity along the Thelon tectonic zone. The coarse-grained intrusion acted as a relatively rigid body deforming along discrete anastomosing shear zones, while granitoid and other bodies in the area deformed both pervasively (becoming foliated) and along shear zones. A Mackay-trend metadiabase dyke which is unfoliated where it passes through the Clinton-Colden intrusion possesses a Thelon-trend foliation where it passes through adjacent rocks of the granitoid suite. This dyke cleanly cuts major shear zones with Thelon trends within the Clinton-Colden intrusion. Although the Thelon-parallel orientation of the shear zones cut by the dyke might be

fortuitous, if, for instance, the shears are Archean syn-volcanic feature, they nonetheless provide strong evidence of a protracted history of deformation along the Thelon tectonic zone since the Mackay swarm (2.4 Ga) predates the period of major activity along that zone. They also indicate that the major deformation of the gabbro-anorthosite body occurred before 2.4 Ga, since shear zones in that body are not observed to cut the dyke. The true extent of later deformation is difficult to assess since exposure of the dyke is limited. Many minor mafic dykes of probable syn-volcanic origin within the intrusion are cut by Thelon-trend shear zones of unknown age.

Granitoid rocks are invariably foliated, as are Mackay-trend dykes where they are found in foliated rocks. The foliation in the granitoid rocks is usually parallel to the contact with rocks of the greenstone belt, a result of diapiric intrusion and/or rheological control during later regional deformation. Mackenzie diabase dykes are undeformed, indicating that tectonic activity had ceased by 1.27 Ga.

CHAPTER 3

PETROGRAPHY AND MINERALOGY OF THE CLINTON-COLDEN GABBRO-ANORTHOSITE INTRUSION

3.1 Introduction

The Clinton-Colden gabbro-anorthosite intrusion consists predominantly of amphibole and plagioclase. The intrusion is texturally unusual, and shows signs of having been emplaced as a crystal mush consisting of >50% plagioclase crystals suspended in mafic magma. As a result, it is not layered and its composition varies irregularly, depending upon the distribution of plagioclase phenocrysts.

3.2 Rock types and compositional variation

The intrusion originally ranged in composition from leucocratic anorthosite to gabbro. Although coarse poikilitic amphibole constitutes the main ferromagnesain phase present in the intrusion, there is convincing evidence that it in fact pseudomorphically replaced clinopyroxene (see Chapter 4). Thus the body was originally gabbro, following Streckeisen (1976). It was previously mis-identified as hornblende gabbro, based upon the assumption that abundant coarse oikocrystic amphibole was primary (Macfie, 1987).

The intrusion consists of approximately 65% leucogabbro (Fig. 3.1), 20% gabbro (Fig. 3.2), and 15% anorthosite (Fig. 3.3). Grain size in anorthosite and gabbro ranges from <1 mm to >40 cm, with coarse grained rocks (5 to 10 mm) making up approximately 70% of the intrusion. Classification according to grain size is complicated by the occurrence of coarse amphibole grains enclosing plagioclase. Rocks dominated by

Fig. 3.1: Leucogabbro consisting of agglomerations of plagioclase grains in coarse oikocrystic and fine secondary calcic amphibole. Station G-72.

Fig. 3.2: Gabbro consisting of plagioclase laths in coarse amphibole oikocrysts. Station G-84.

Fig. 3.3: Typical anorthosite, composed of close-packed coarse plagioclase (in this case altered to fine epidote) with minor interstitial material consisting of coarse actinolitic to aluminous calcic amphibole and fine aluminous amphibole. Station G-28.

plagioclase have average grain sizes defined by that mineral, while rocks containing abundant amphibole are usually coarser. In general all rocks contain large amphibole grains, while plagioclase tends to be smaller. The size of plagioclase grains appears to vary independently of that of hornblende oikocrysts, which are almost always very large.

Unlike most Archean anorthosites, the intrusion is unlayered, and the distribution of rock types is remarkably irregular (Fig. 3.4, 3.5). Rock types are defined on the basis of plagioclase abundance at the scale being considered. Outcrops tens of metres in size may have overall anorthositic compositions, but may display areas metres or centimetres across where gabbro or amphibole-rich rock predominate. In detail (metres to centimetres) the intrusion consists of gabbro to anorthosite, depending upon the closeness of packing of plagioclase grains. Because layering is not present and compositional variation is irregular, the assignment of rock names is rather arbitrary. In the southern third of the intrusion, leucogabbro makes up approximately 75% of the rock, the remainder being anorthosite. Towards the north, gabbro predominates, with numerous ten-metre-wide zones of melanogabbro. Variation between rock types is generally gradual in detail, but it is not unusual to find gabbro and anorthosite occurring within 50 cm of one another. Even the most leucocratic anorthosite contains pockets of very mafic rock (Fig. 3.5). In most cases zones of one rock type are small, usually not more than two to three metres wide.

3.3 Mineralogy of the intrusion

3.3.1 Introduction

Chemical analyses of minerals of the intrusion were obtained with

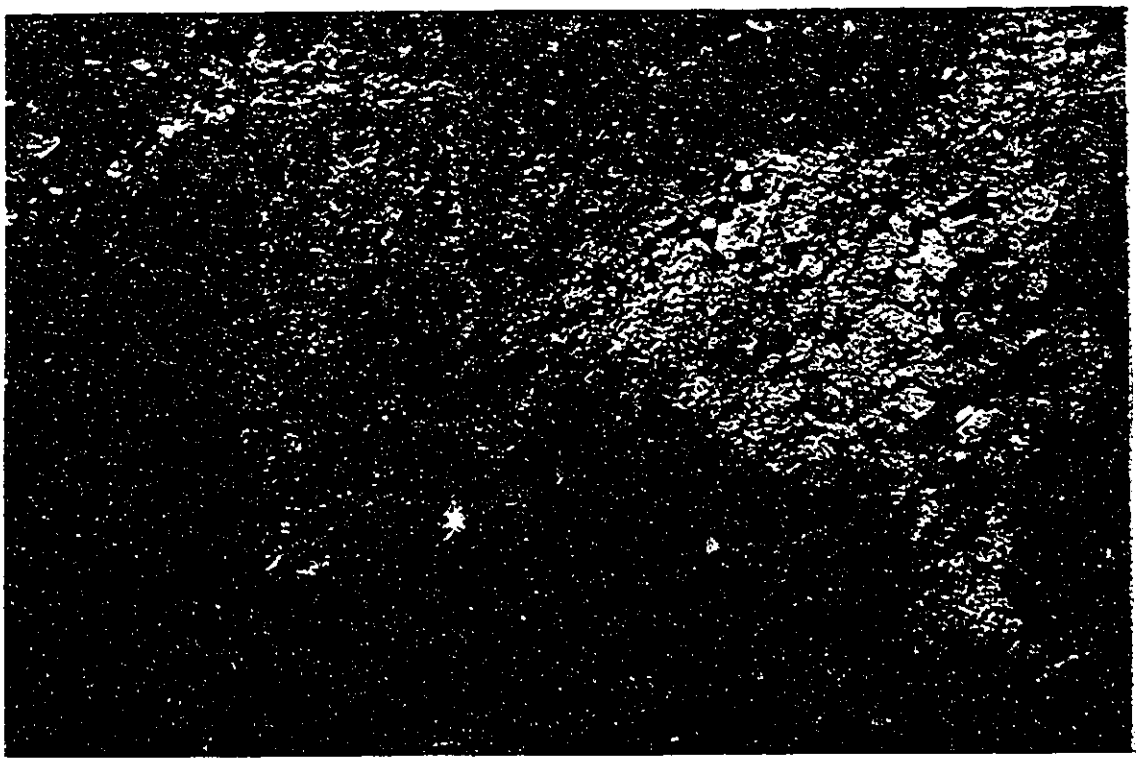

Fig. 3.4: Example of variation in the intrusion, here variation in size of plagioclase grains, which are enclosed in coarse calcic amphibole. Pen is 14 cm long. Station T-5.

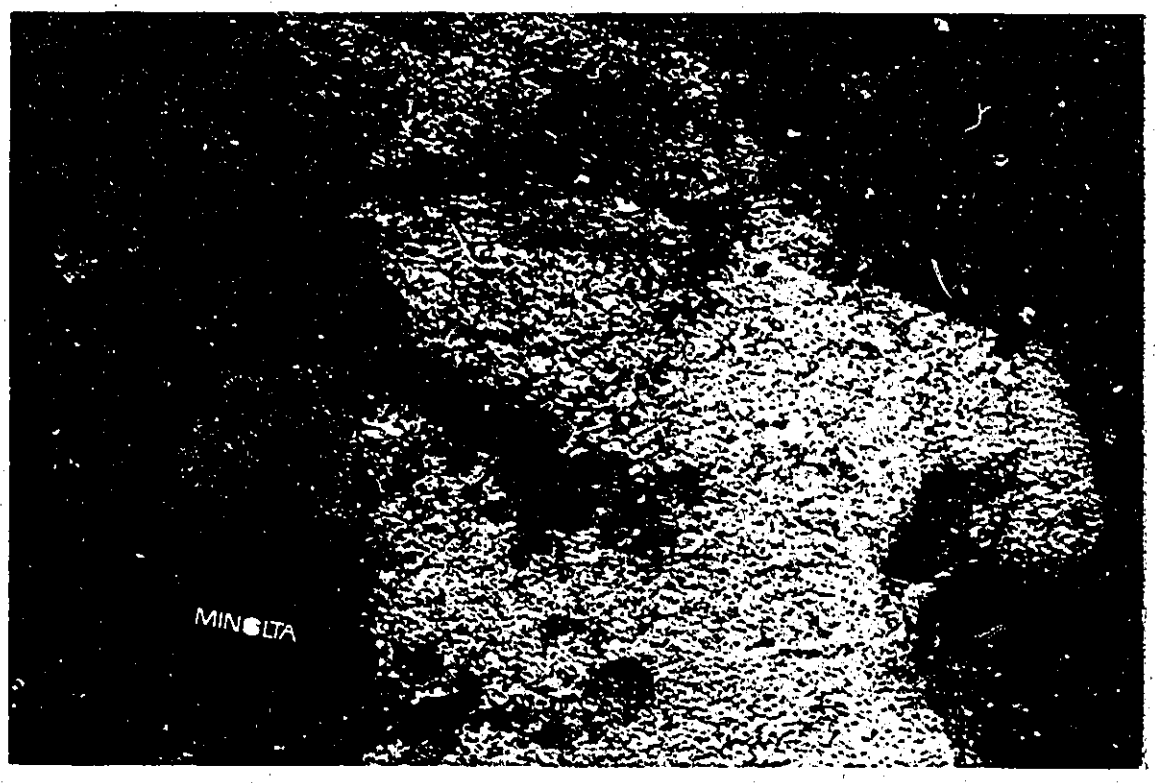

Fig. 3.5: Variation from anorthosite to leucogabbro, showing pockets of mafic material (now calcic amphibole) within predominantly plagioclase-rich rock. Station G-92.

the CAMEBAX electron microprobe of the McGill University microprobe laboratory. Operating conditions are described in Appendix 1.

Assignment of elements to sites in the amphibole structure was accomplished following the method of Deer et al. (1966), assisted by the computer program MINFILE by A.N. Afifi and E.J. Essene (University of Michigan). MINFILE was also used to calculate the chemical formula for epidote and to assign elements to sites in the plagioclase structure, using the number of oxygen atoms specified by Deer et al. (1966).

Essential and accessory minerals were identified where possible. Almost all minerals have been affected by alteration processes. As a result, determination of the original assemblage is based partly on indirect evidence.

Modal analysis is difficult due to the coarseness of most rocks. Therefore, percentages of minerals presented below are visual estimates.

Minerals which occur in the intrusion in large amounts are plagioclase, calcic amphibole ranging in composition from actinolite to tschermakite, opaque oxides (ilmenite, rutile, hematite and titanomagnetite) (2-5%), and epidote species (2-5%). Other minerals present in trace amounts are chlorite, titanite, calcite, quartz, apatite, zircon and a very fine-grained fibrous material resembling uralite. Very minor, fine-grained apatite, calcite and sulphides are disseminated in some rocks of the intrusion, and generally occur in association with fine secondary amphibole. A single centimetre-wide aggregate of fine molybdenite was observed.

3.3.2 Plagioclase

Plagioclase, the best preserved primary phase, constitutes more than 50% of the Clinton-Colden intrusion. It generally occurs as abundant euhedral to subhedral phenocrysts distributed in an irregular manner, with a variable amount of interstitial mafic material. Fine epidote alteration is sometimes present, but in many rocks the plagioclase is nearly pristine. Anorthite contents range from An_{35} to An_{25}, except where adjacent to epidote (Table 3.1, sample J-445).

Plagioclase grain size typically exceeds 0.5 cm, (Fig. 3.6, 3.7). Isolated phenocrysts are commonly euhedral to subhedral. Most grains are subequidimensional, but in some rocks tabular grains occur (Fig. 3.2). In hand samples plagioclase ranges in colour from dark grey to white. Colour in hand samples is a function of the degree of epidote alteration, darker plagioclase being relatively unaltered.

Individual plagioclase grains show only slight and subtle non-oscillatory marginal zoning, rims being slightly more sodic ($<An_5$ difference) than cores (Table 3.1, sample J-445). Within individual samples, plagioclase compositions of nearly homogeneous plagioclase grains can differ by An_{10} or more. Albite twinning is present in almost all grains, and Carlsbad twinning is common, being shown by approximately 10 percent of the grains (Fig. 3.7). No systematic variation was observed in the composition and textures of plagioclase from one rock sample to another.

In the Clinton-Colden intrusion plagioclase retains it primary morphology and composition. Features indicative of metamorphic equilibration or recrystallization of plagioclase, such as sub-domain development, granulation, growth of plagioclase over other minerals, or

Table 3.1: Microprobe analyses of plagioclase, classified according to sample number, grain number in each sample, and relative location in grain (c=core, m=margin). Points analysed in sample J-445 lie successively closer to an epidote grain (analysis given in Appendix 3): c=core, a=approaching epidote, e=adjacent to epidote. Recalculated on basis of 32 oxygens. All Fe expressed as FeO. Symbol "-" means <0.005, rounds to zero.

	G-87			G-92				
	1c	1m	2m	1c	2c	2m	3c	3m
SiO2	48.78	48.75	51.41	48.18	47.59	47.31	48.11	47.92
TiO2	0.04	0.04	0.03	0.02	0.03	0.03	0.03	0.07
Al2O3	32.01	32.23	30.71	31.99	32.11	32.32	31.75	32.39
FeO	0.05	0.08	0.03	0.11	0.01	0.22	0.30	0.30
MnO	-	-	-	-	0.01	-	-	-
MgO	0.26	0.38	-	0.01	0.10	-	0.19	-
CaO	14.92	13.95	13.23	15.52	15.60	15.51	15.42	15.37
Na2O	2.81	2.66	4.05	2.61	2.57	2.66	2.50	2.59
K2O	0.11	0.43	0.03	0.03	0.02	0.03	0.02	0.02
Total	98.98	98.52	99.49	98.47	98.04	98.08	98.32	98.66
Ab	0.25	0.25	0.36	0.15	0.23	0.24	0.23	0.23
Or	0.06	0.03	—	-	-	-	-	-
An	0.74	0.72	0.64	0.85	0.77	0.76	0.77	0.77
#Si+4	9.00	9.02	9.38	8.95	8.89	8.84	8.96	8.89
#Ti+4	0.01	0.01	0.00	0.00	0.00	0.00	0.00	0.01
#Al+3	6.96	7.03	6.61	7.01	7.07	7.12	6.97	7.08
#Fe+2	0.01	0.01	0.00	0.02	0.00	0.03	0.05	0.05
#Mn+2	-	-	-	-	0.00	-	-	-
#Mg+2	0.07	0.10	-	0.00	0.03	-	0.05	-
#Ca+2	2.95	2.77	2.59	3.09	3.12	3.11	3.08	3.06
#Na+1	1.01	0.95	1.43	0.94	0.93	0.96	0.90	0.93
#K	0.03	0.10	0.01	0.01	0.00	0.01	0.00	0.00
#TOTAL	20.03	19.99	20.03	20.02	20.04	20.08	20.01	20.02
#O-2	32.00	32.00	32.00	32.00	32.00	32.00	32.00	32.00

	G-92				G-95			J-445	
	4c	4m	5c	5m	1m	2c	3c	1c	1a
SiO2	48.08	49.18	48.62	48.54	53.91	48.77	48.26	50.15	49.80
TiO2	-	0.09	-	0.07	0.03	-	-	0.05	-
Al2O3	32.45	32.28	31.79	31.76	28.90	32.23	32.23	31.19	31.37
FeO	0.15	0.27	0.25	0.07	0.29	0.09	0.08	0.07	0.09
MnO	-	0.01	-	0.01	0.05	0.01	-	0.02	0.03
MgO	-	-	0.01	-	-	-	-	-	0.02
CaO	14.52	15.02	15.15	14.52	10.97	15.01	15.17	13.76	13.85
Na2O	2.64	2.96	3.00	3.10	4.85	2.99	2.66	3.61	3.46
K2O	0.05	0.02	0.02	0.05	0.03	0.02	0.02	0.04	0.02
Total	97.89	99.83	98.84	98.12	99.03	99.12	98.42	98.89	98.64
Ab	0.24	0.26	0.26	0.28	0.44	0.26	0.24	0.32	0.31
Or	-	-	-	-	-	-	-	-	-
An	0.76	0.74	0.74	0.72	0.55	0.74	0.76	0.68	0.69
#Si+4	8.96	9.00	9.00	9.03	9.82	8.99	8.96	9.23	9.19
#Ti+4	-	0.01	-	0.01	0.00	-	-	0.01	-
#Al+3	7.12	6.97	6.94	6.96	6.20	7.00	7.05	6.77	6.82
#Fe+2	0.02	0.04	0.04	0.01	0.04	0.01	0.01	0.01	0.01
#Mn+2	-	0.00	-	0.00	0.01	0.00	-	0.00	0.00
#Mg+2	-	-	0.00	-	-	-	-	-	0.01
#Ca+2	2.90	2.95	3.01	2.89	2.14	2.96	3.02	2.71	2.74
#Na+1	0.95	1.05	1.08	1.12	1.71	1.07	0.96	1.29	1.24
#K	0.01	0.00	0.00	0.01	0.01	0.00	0.00	0.01	0.00
#TOTAL	19.97	20.03	20.07	20.04	19.94	20.05	20.00	20.03	20.02
#O-2	32.00	32.00	32.00	32.00	32.00	32.00	32.00	32.00	32.00

Table 3.1 (cont'd.)

	J-445			
	1a	1e	1e	Mean
SiO2	48.35	45.25	50.26	49.09
TiO2	-	0.10	0.02	0.03
Al2O3	34.53	28.72	31.11	31.69
FeO	0.32	0.13	0.08	0.16
MnO	0.02	-	-	0.01
MgO	0.10	0.11	-	0.23
CaO	8.37	12.71	13.77	14.25
Na2O	4.08	8.65	3.73	3.01
K2O	1.25	2.74	0.04	0.11
Total	97.02	98.41	99.01	98.58
Ab	0.43	0.50	0.33	0.27
Or	0.09	0.10	-	0.01
An	0.49	0.40	0.67	0.72
#Si+4	9.00	8.75	9.24	9.08
#Ti+4	-	0.01	0.00	0.00
#Al+3	7.58	6.55	6.74	6.91
#Fe+2	0.05	0.02	0.01	0.03
#Mn+2	0.00	-	-	0.00
#Mg+2	0.03	0.03	-	0.06
#Ca+2	1.67	2.63	2.71	2.82
#Na+1	1.47	3.24	1.33	1.08
#K	0.30	0.68	0.01	0.03
#TOTAL	20.10	21.92	20.05	20.01
#O-2	32.00	32.00	32.00	32.00

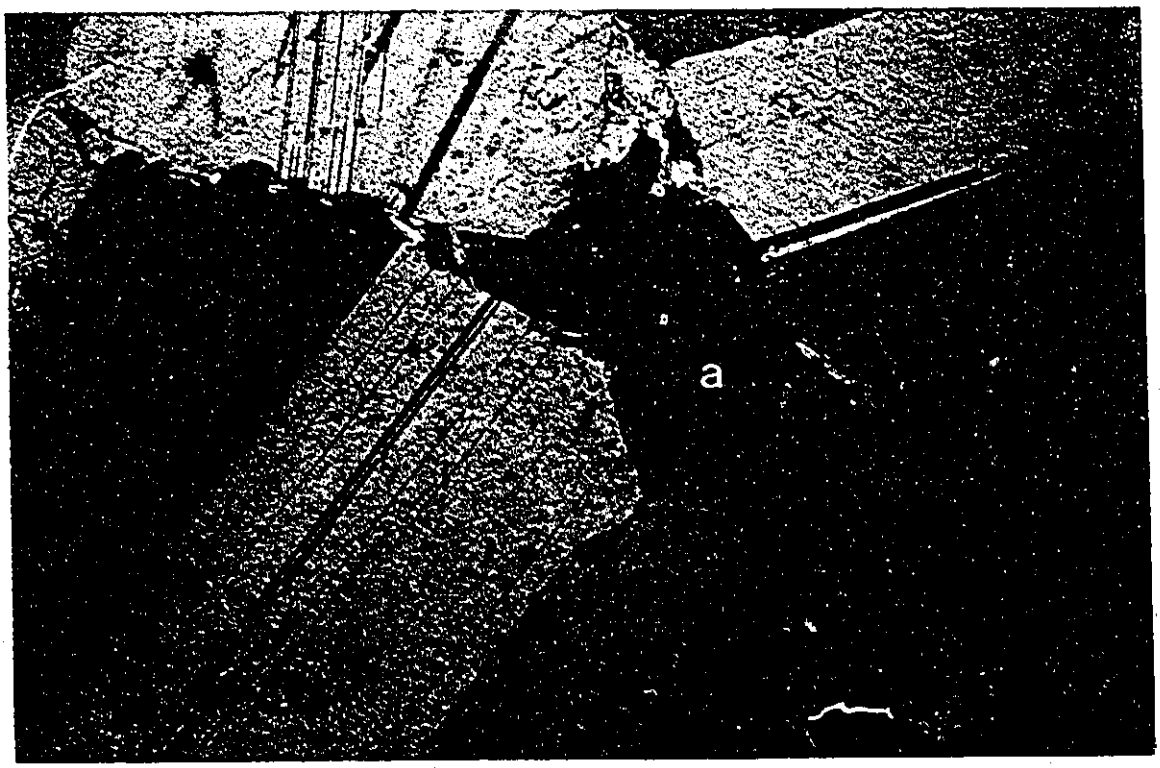

Fig. 3.6: Well preserved igneous plagioclase showing abundant Carlsbad twinning, and a well preserved portion of an amphibole oikocryst (a) (nearly at extinction). Note lack of zoning in plagioclase. Crossed polars; field of view=2 mm.

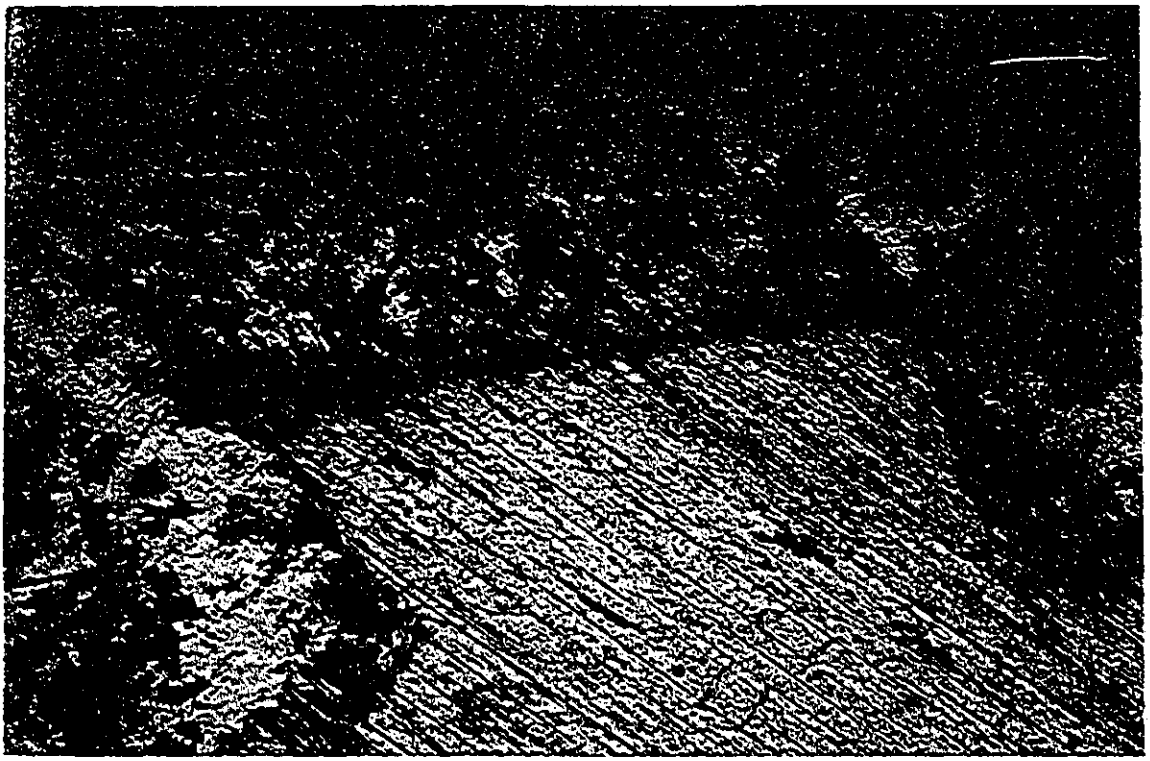

Fig. 3.7: Portion of oikocrystic amphibole grain with enclosed plagioclase altered to pseudomorphs of fine epidote and clusters of opaque grains. Note extensive overgrowth of margins of plagioclase pseudomorphs by fine amphibole prisms. Note also slight colour variation in ocarse amphibole grain, from very light green actinolitic core to slightly darker hornblendic margin. Plane polarized light; field of view=4.5 mm.

compositional homogeneity of plagioclase throughout individual samples, were not observed. Secondary plagioclase replacing other minerals is not present. Where primary textures are deformed in shear zones plagioclase is completely replaced by epidote.

Two types of replacement of plagioclase by secondary minerals have occurred. One consists of replacement of plagioclase by fine epidote. This is minor in most rocks, but in some rocks the original presence of plagioclase is indicated only by pseudomorphs consisting of fine epidote (Fig. 3.7). The second type of replacement consists of marginal overgrowths of tschermakitic amphibole (Fig. 3.7, 3.8), chlorite and titanite. Evidence of secondary effects on the composition of unreplaced plagioclase adjacent to secondary minerals was not observed.

3.3.3 Amphibole

3.3.3.1 Coarse oikocrystic amphibole

Coarse interstitial oikocrystic amphibole (Fig. 3.7, 3.8), as opposed to the fine amphibole which replaces it in many places, is the most important amphibole type. It constitutes approximately 50% of all mafic minerals of the intrusion, and approximately 25% of the intrusion as a whole. It ranges in composition from actinolite to tschermakite and occurs as grains which are commonly 10 cm in size but which range in size from 0.5 to 40 cm. The oikocrystic amphibole occasionally overgrows trellis networks of ilmenite and rutile.

Oikocrystic amphibole is dark green in hand sample and light green in thin section (Fig. 3.7, 3.8). Most grains are optically homogeneous, apart from variable recrystallization to finer amphibole.

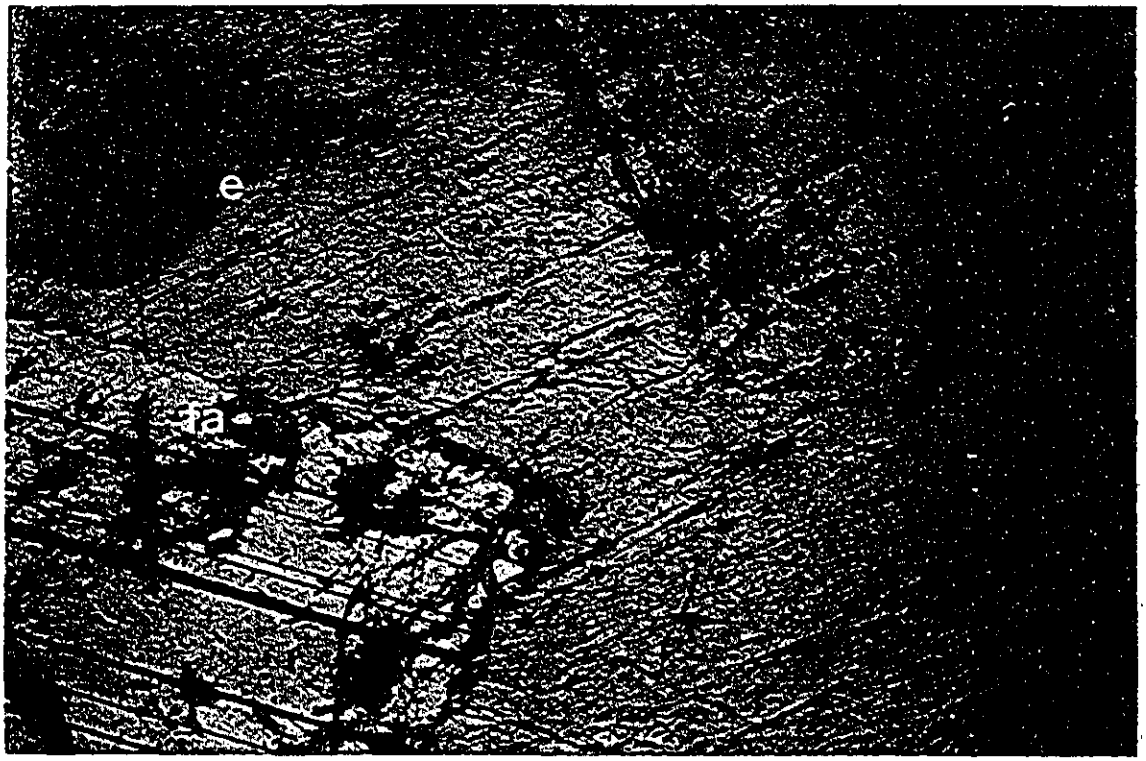

Fig. 3.8: Coarse amphibole oikocryst (light green) overgrowing margins of relatively well-preserved plagioclase. Fine amphibole grains (fa) and discrete grains of epidote (e) also overgrow margins of plagioclase grains. Crossed polars; field of view=4.5 mm.

Cores of grains tend to be lighter in colour. Twinning and internal grain boundaries are not present. The oikocrystic amphibole has the following pleochroic scheme: X=yellow green, Y=olive green, Z=dark green. Interference colours range to middle second order, and maximum extinction angles range up to 21° (Z ^ C). In rare cases, margins with neighbouring oikocrystic-appearing grains are complexely sutured. In hand specimen, reflection from cleavage planes reveals the extent of the crystals.

The chemistry of oikocrystic amphiboles and the amphiboles described below is discussed in detail in Chapter 5.

3.3.3.2 Fine amphibole

Fine amphibole, up to 2 mm in maximum diameter and fibrous to equidimensional, overgrows earlier amphibole, plagioclase grains, and minor secondary minerals. It accounts for approximately 25% of the amphibole of the intrusion. It displays a range of textures and occurs as: grains overgrowing or replacing oikocrystic amphibole and/or other primary minerals; prismatic grains extending from the margins of oikocrystic grains into neighbouring plagioclase grains; and fine amphibole overgrowing chlorite.

Grains which overgrow coarse oikocrystic amphibole may occur singly (Fig. 3.9), or grade to massive fine amphibole which completely replaces the earlier mineral. Amphibole grains overgrowing coarse amphibole oikocrysts show no preferred orientation, except in cases where the c-axes of fine amphibole grains occur parallel to that of the host oikocryst. Secondary grains replacing oikocrystic amphibole usually consist of magnesio-hornblende. In many cases masses of fine

Fig. 3.9: Fine hornblendic amphibole grains (h) replacing coarse oikocrystic amphibole. Minor fine epidote (fe) replacing plagioclase is also present. Crossed polars; field of view=3 mm.

amphibole contain optically parallel remnants of coarse oikocrystic amphibole, while in other cases no direct evidence of the precursor phase remains. Where remnants of oikocrystic amphibole grains are preserved, it is not clear whether the fine amphibole entirely replaces an oikocrystic grain, or whether it in part represents coeval topotactic and multiple non-topotactic nucleation of amphibole on pyroxene. It is not clear whether all masses of fine amphibole are of the same generation. One variant which does not appear to replace oikocrystic amphibole fills space between lamellae in opaque trellis networks. This amphibole commonly occurs with chlorite. However, coarse oikocrystic grains also overgrow some trellis networks, and relations between these amphibole types are not clear.

Fine prismatic amphibole overgrowing and replacing plagioclase occurs in all rocks. These grains extend from the margins of oikocrystic grains into neighbouring plagioclase (Fig. 3.8) or epidote pseudomorphs of plagioclase (Fig. 3.7), generally maintaining optical continuity with the oikocrystic parent. The secondary marginal grains are present around virtually all oikocrystic grains, and true original oikocryst/plagioclase boundaries are only rarely preserved. Usually there are no other mineral phases present between the secondary amphibole and the plagioclase. The plagioclase unreplaced by the amphibole shows no noticeable compositional gradient towards it. Clusters of the secondary amphibole grains extend well into some plagioclase grains, replacing large amounts of plagioclase in this manner. Strikingly similar textures are described by Kamineni (1986) from a deuterically altered anorthosite-gabbro intrusion in Ontario.

Fine prismatic amphibole also overgrows plagioclase along

fractures. This amphibole is optically and compositionally identical to the grains occurring along oikocryst/plagioclase interfaces.

Amphibole replacing chlorite is minor, but occurs throughout the intrusion. This amphibole consists of fine, typically radiating, fibres. It is actinolitic hornblende, and overgrows clusters of fine, pale, weakly pleochroic green chlorite showing grey birefringence (Fig. 3.10).

3.3.4 Evidence of altered pyroxene

Ragged cores of fibrous material are present in some coarse oikocrystic amphibole grains in sample J-445 (Fig. 3.11). The mineralogy of the material could not be identified optically, and it occurs in zones which are too fine to separate for X-ray diffraction. It has the fibrous texture of uralite as described by Buseck et al. (1980), and its composition, as revealed by electron microprobe, is close to that of clinopyroxene (Table 3.2). It is clearly replaced topotactically by optically identifiable amphibole identical to that of the abundant oikocrystic amphibole found throughout the intrusion. The uralitic pyroxene remnants are up to 0.5 cm in diameter and are scattered throughout the central parts of the oikocrystic amphibole grains. Within a single amphibole oikocryst all of the uralitic pyroxene remnants exhibit optical parallelism. In thin section this uralite is darker than the host amphibole, is non-pleochroic, and under crossed nicols has lower birefringence.

Approximately 15% of the uralite remnants consist of fine lamellae, about 20 microns wide, visible by their higher birefringence (Fig. 3.11). These lamellae mimic exsolution lamellae in pyroxene. The

Fig. 3.10: Fine hornblendic amphibole prisms (h) overgrowing chlorite (c) which is itself partially altered to amphibole. Some chlorite shows Berlin blue birefringence. Chlorite overgrows fine epidote which replaces plagioclase. Crossed polars; field of view=1.2 mm.

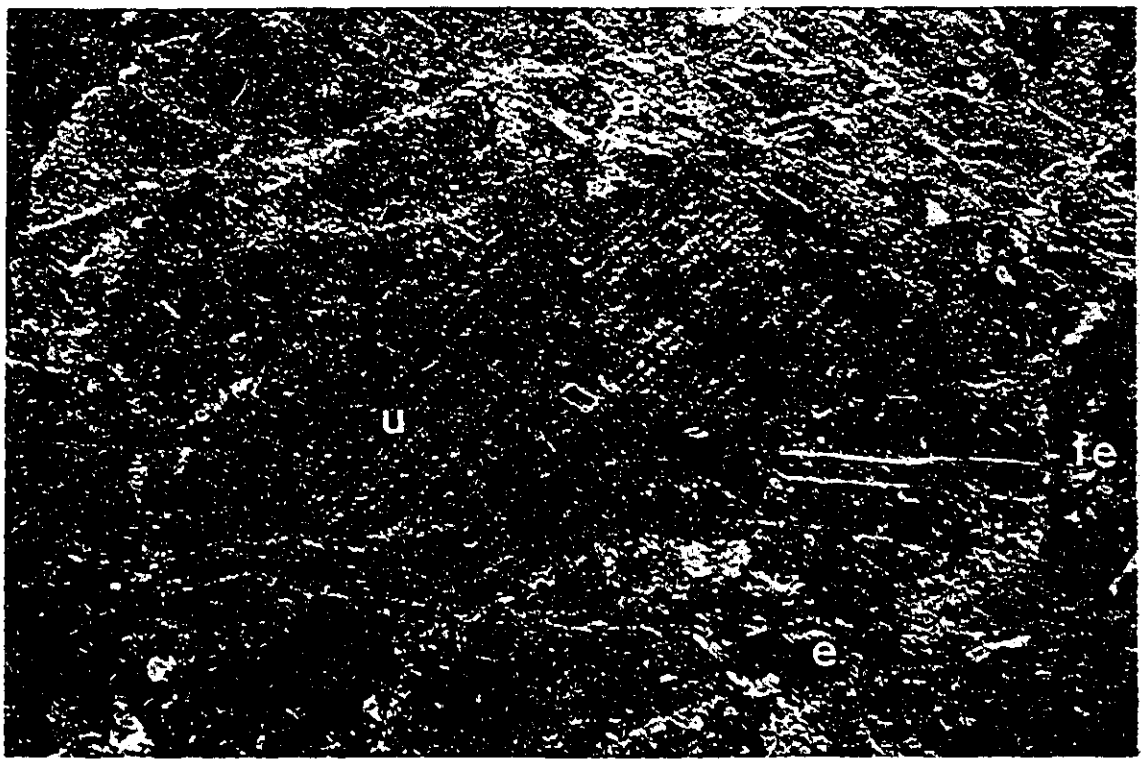

Fig. 3.11: Uralite cores (u) in oikocrystic calcic amphibole (a) grain in sample J445. Amphibole replaces uralite along uneven fronts and along fractures. Note exsolution-like lamellae in uralite. Also note abundant discrete epidote grains (e), showing yellow and blue-green birefringence, around margins of coarse amphibole grain. Plagioclase is mostly altered to fine epidote (fe). Crossed polars; field of view=3 mm.

Table 3.2: Microprobe analyses of uralite from sample J-445. Points a to d correspond to points shown in Figure 4.8b. L=lamella resembling exsolution in pyroxene. Normalization of analyses as pyroxene yields augite, Ca:Mg:Fe=0.9:0.78:0.29. Recalculated on basis of 6 oxygens.

	a	b	c	d	L	L	L	Mean
SiO2	49.75	47.74	49.15	51.09	50.29	51.49	51.63	50.16
TiO2	0.48	0.40	0.26	0.16	0.48	0.27	0.37	0.35
Al2O3	2.01	2.70	1.54	2.48	2.00	1.84	2.00	2.08
FeO	8.70	8.04	9.14	11.35	8.67	8.79	8.56	9.04
MnO	0.23	0.29	0.28	0.29	0.32	0.28	0.27	0.28
MgO	13.89	14.42	13.05	14.37	13.20	13.45	13.59	13.71
CaO	21.64	21.96	24.01	18.18	23.41	22.54	21.91	21.95
Na2O	0.23	0.15	0.22	0.29	0.25	0.22	0.19	0.22
Total	96.93	95.70	97.65	98.21	98.62	98.88	98.52	97.79
#Si IV	1.92	1.87	1.91	1.94	1.92	1.95	1.95	1.92
#Al IV	0.08	0.12	0.07	0.06	0.08	0.05	0.05	0.08
T site	2.00	2.00	1.98	2.00	2.00	2.00	2.00	2.00
#Al VI	0.01	-	-	0.05	0.01	0.03	0.04	0.02
#Ti	0.01	0.01	0.01	0.00	0.01	0.01	0.01	0.01
#Fe +2	0.28	0.26	0.30	0.36	0.28	0.28	0.27	0.29
#Mn +2	0.01	0.01	0.01	0.01	0.01	0.01	0.01	0.01
#Mg	0.80	0.84	0.75	0.81	0.75	0.76	0.77	0.78
#Ca	0.90	0.92	1.00	0.74	0.96	0.91	0.89	0.90
#Na	0.02	0.01	0.02	0.02	0.02	0.02	0.01	0.02
M1,M2	2.03	2.06	2.08	2.01	2.03	2.01	2.00	2.03
#O	6.00	6.00	6.00	6.00	6.00	6.00	6.00	6.00

microprobe analyses reveal no significant compositional differences between lamellae and matrix, suggesting that the uralitization process resulted in compositional homogenization of the original pyroxenes without completely eradicating the crystallographic angular discordance which existed (Robinson et al., 1971). Such compositional homogenization during uralitization is common (Mongkoltip and Ashworth, 1986).

The uralitic remnants are replaced by coarse, clear amphibole along ragged alteration fronts, along some of the exsolution lamellae, and along fractures. Progressive replacement along fractures results in the subdivision of the pyroxene core into smaller domains. The final product is a coarse oikocrystic amphibole grain with a mosaic of ragged uralitic inclusions. The division between matrix and uralite is not always sharp. For example, marginal parts of uralite domains, as seen under plane polarized light, appear under crossed nichols to be part of the advancing coarse amphibole grains. It is clear that the optical, and hence crystallographic, properties are gradational. This is typical of uralitic alteration in general (Buseck et al., 1980).

3.3.5 Opaque oxide minerals

3.3.5.1 Introduction

Approximately 0.25% of the Clinton-Colden intrusion consists of opaque oxide minerals. The abundance of ilmenite trellis networks indicates that oxide minerals accounted for approximately 1% of the original mineralogy of the intrusion, but have since been largely replaced by chlorite and amphibole. The opaque oxide minerals are ilmenite, rutile, hematite and minor magnetite or titanomagnetite.

Some oxide minerals occurred as oikocrysts, and although they have been degraded to skeletal outlines (Fig. 3.12) during subsequent alteration, they were originally a primary interstitial phase.

3.3.5.2 Ilmenite

Ilmenite occurs in all rocks and is the most common opaque oxide mineral in the intrusion. It is fine grained and anhedral. One textural type, common throughout the intrusion, consists of discrete rounded to irregular grains up to 3 mm in size. They typically contain 10 to 20% fine rounded to lamellar parallel exsolved blebs of rutile similar to those described by Haggerty (1976). Rectilinear twin networks also described by Haggerty (1976) occur locally. Margins of ilmenite grains show variable amounts of alteration to fine rutile. Rutile and silicate minerals fill fractures in some ilmenite grains.

A second textural type consists of oriented trellis networks of ilmenite which occur in all parts of the intrusion, often in association with the coarser discrete grains. These networks consist of discontinuous lamellae and irregular fine ilmenite grains. The maximum intersection angle observed between lamellae is 85°. Networks extend for up to 10 mm, and often define skeletal textures clearly interstitial to plagioclase. Individual grains and lamellae which make up the network show variable alteration to rutile. Networks are also outlined in part by titanite, which surrounds all ilmenite. In some cases ilmenite is almost or completely replaced by rutile and titanite. Identical trellis networks are described by Haggerty (1976), and are attributed to oxy-exsolution of titanomagnetite (see below). Trellis interstices are usually filled by finely matted to granular amphibole,

Fig. 3.12: Skeletal remains of oikocrystic magmatic opaque oxide, now consisting of trellis network of ilmenite and rutile laths with lesser anhedral ilmenite-rutile masses, which in reflected light are seen to be partially replaced by rutile. Space between laths filled with coarse calcic amphibole (a) and chlorite (c). Plagiclase grains enclosed in original oxide oikocryst are now extensively altered to fine epidote. Plane polarized light; field of view=1.2 mm.

although in some cases individual amphibole grains fill interstices. In rare cases coarse oikocrystic amphibole overgrows and infills the trellis networks. Amphibole within and near trellis networks contain greater amounts of TiO_2. Chlorite also commonly occurs in the trellis networks.

3.3.5.3 Rutile

Exsolved rutile in discrete ilmenite grains is very common. It is distributed evenly throughout ilmenite grains, and shows evidence of having formed in two generations, one of which is coarser. It also forms as an alteration rather than an exsolution product of ilmenite. This rutile is irregular in distribution and occurs both along the margins of discrete and trellis-texture ilmenite grains, and along fractures within those grains. In both cases it is associated with titanite, silicate minerals, and occasionally hematite. The rutile is usually fine and polycrystalline, and the degree of alteration of the ilmenite varies from slight to complete.

3.3.5.4 Hematite and magnetite

Hematite, a minor mineral in the Clinton-Colden intrusion, occurs in association with ilmenite. In some rocks it fills space within the ilmenite lamellae described above. In most cases it occurs as a very minor phase in fractures within ilmenite, along with rutile. Hematite also occurs as discrete grains in the neighbourhood of trellis textured ilmenite.

Anhedral grains of magnetite with minor hematite inclusions occur in some samples. Magnetite containing ilmenite lamellae were not

observed, which suggests that the magnetite observed is of a different generation than the titanomagnetite whose oxidation gave rise to the ilmenite trellis networks, as is discussed below.

3.3.5.5 The evolution of the opaque oxide minerals

Textures observed in the oxide minerals of the intrusion are identical to textures described by Haggerty (1976) and attributed to oxidation of primary oxide minerals. The original magmatic opaque oxide assemblage has been entirely replaced, but it must have been dominated by ilmenite or titanomagnetite.

The skeletal ilmenite trellis networks present in all rocks studied are most easily explained in terms of oxy-exsolution of ilmenite from titanomagnetite, as described by Haggerty (1976), followed by continued dissolution of the magnetite. The presence of rutile and combined ilmenite-rutile lamellae in trellis networks, as well as rutile rims on ilmenite grains, points to oxidation of ilmenite to rutile (Haggerty, 1976). The presence of hematite in similar relationships, along with rims of titanite on rutile and ilmenite grains, likewise points to continued oxidation, as does minor titanite occurring as rims and pseudomorphs of rutile and ilmenite laths. An almost complete absence of magnetite in the observed assemblage indicates that the oxidation/dissolution process was considerably advanced. The advanced nature of the oxidizing reactions agrees with the observation that the fine amphibole which overgrew oikocrystic amphibole was somewhat more oxidized than its predecessor (see Chapter 4), suggesting that the fO_2 buffering capacity of the titanomagnetite to ilmentite to rutile reaction diminished as reactants were consumed, resulting in production

of more oxidized late-stage amphibole. In the absence of knowledge of the composition of the parental Ti-magnetite detailed reactions cannot be written, but it is clear that postmagmatic oxidation was involved in the alteration of the intrusion.

3.3.6 Epidote

Epidote group minerals are abundant as products of plagioclase alteration. Epidote species occur as very fine material replacing plagioclase, and as discrete fine to medium grained crystals within plagioclase and between plagioclase and other phases.

Alteration of plagioclase to very fine, often optically non-resolvable, epidote is common in the intrusion (Fig. 3.7, 3.10). This type of alteration of plagioclase is irregular in distribution and intensity. In some samples plagioclase is pseudomorphically replaced by fine epidote. On a macroscopic scale distribution of epidote alteration of plagioclase is controlled by an ubiquitous fracture network. Away from the fractures this alteration declines, and is controlled by grain boundaries and intra-grain fractures. Epidotized plagioclase is white in hand sample, and is easily distinguished from the dark grey pristine plagioclase.

Coarser grains of epidote are minor but common in rocks of the intrusion. They occur as clear homogeneous grains with sharp margins, with high birefringence and lacking pleochroism. They range in size from <0.01 to 0.5 mm, are anhedral to subhedral, and occur as single grains and as granular clusters. The average composition of a grain from sample J-445 (Fig. 3.11) is

$Si_{2.98}Al_{2.38}Fe^{+3}_{0.63}Mn_{0.01}Ca_{1.97}O_{12}(OH)$.

Discrete grains of epidote replace plagioclase, mostly where that mineral lies against coarse hornblende. Some samples contain abundant epidote along plagioclase-coarse amphibole contacts, with a relative absence of very fine alteration of plagioclase. In many samples both fine epidote and coarser epidote are common, and the coarser epidote appears to overgrow the fine, amorphous, saussuritic material. The reverse is never observed.

3.3.7 Chlorite

Chlorite is a minor but widespread mineral in the intrusion, usually occurring in intergrowths with fine amphibole. It is pale green and weakly pleochroic, and shows grey birefringence. It occurs in fine clusters <0.1 mm in size. In some cases it is interstitial to rutile/ilmenite trellis networks, along with coarse or fine amphibole. In some cases, fine amphibole has overgrown chlorite (Fig. 3.10), suggesting minor prograde metamorphism. In general, chlorite constitutes less than 1% of the intrusion, but is present in trace amounts in virtually all rocks.

3.3.8 Quartz

Quartz is a very minor mineral in the Clinton-Colden intrusion. It is found as tiny blebs resolvable at 400X magnification in some amphibole pseudomorphs of clinopyroxene (Fig. 3.13). It does not occur as a late-stage granophyric product such as might be expected during closed-system fractionation of a mafic magma.

3.3.9 Zircon

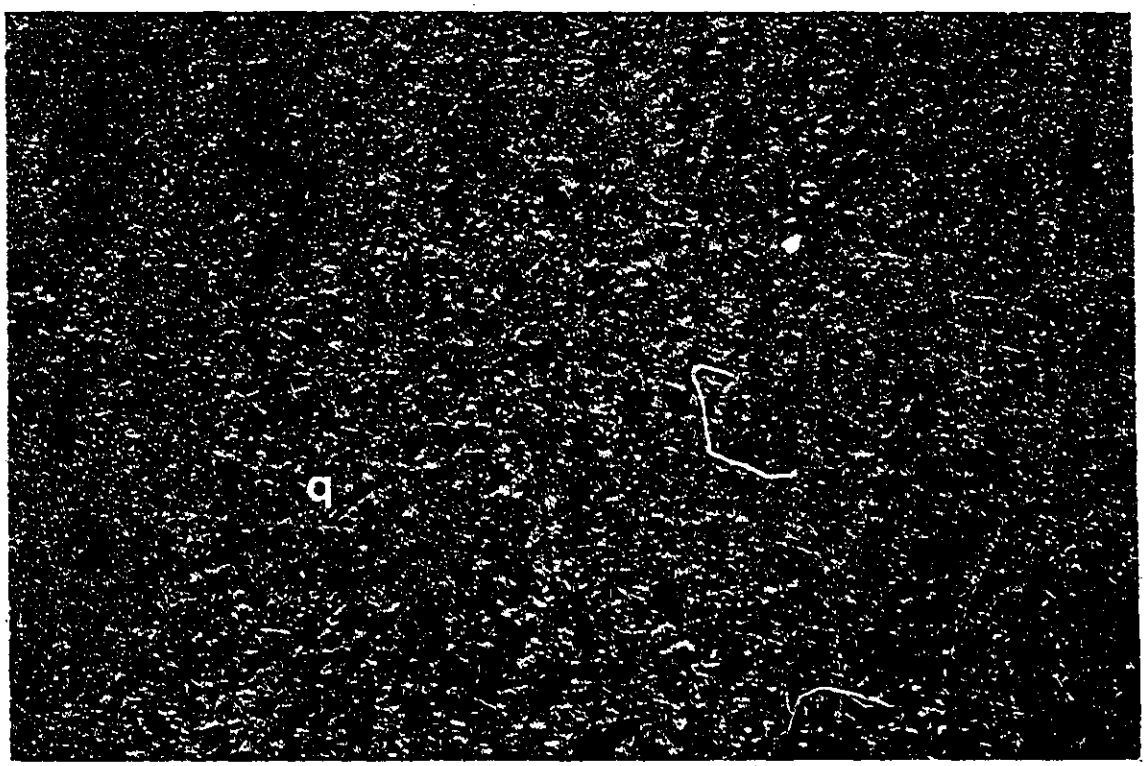

Fig. 3.13: Quartz rods and blebs (q) visible in coarse amphibole oikocryst. Plane polarized light; field of view=0.5mm.

Zircon is a minor constituent of the Clinton-Colden intrusion. It occurs as very fine interstitial anhedral grains, as expected in a mafic intrusion (van Breemen, pers. com. 1988), and as rare subhedral to euhedral grains, the latter clearly indicating a magmatic origin. Many grains are metamict, showing brownish colouration, but others are clear and colourless.

3.4 Alteration veins in the intrusion

The distribution of much of the alteration in the intrusion has been controlled by an extensive sub-rectilinear network of fractures which shown no apparent relation to regional structure, and along which alteration of plagioclase to fine epidote is most strongly developed. These fractures are hierarchical in that sets of minor fractures often terminate at major fractures, and may have developed as a result of shrinkage of the body during cooling (cf. Spry, 1966). However, evidence presented in Chapter 5 indicates that cooling of the body may have occurred at depths greater than the low-pressure near-surface environment required for development of open shrinkage-fractures (Nelson, 1979). The fractures may therefore be due to brittle failure of the body during an early compressional event.

The fractures are usually less than 1 mm in width, and are highlighted by selvages of white saussuritized plagioclase and bleached amphibole (Fig. 3.14). These selvages grade quickly to less altered material. The fractures dissect the intrusion, on a 10 cm to 1 m scale, into zones of rock having relatively pristine plagioclase, wherein overgrowth of plagioclase by amphibole is the dominant alteration effect.

Fig. 3.14: Network of fractures outlined by plagioclase altered to fine epidote, which dissects the intrusion. Alteration of plagioclase decreases away from fractures, resulting in zones of rock containing dark relatively well-preserved plagioclase. Station G-98.

The fractures appear to have conducted the H^+-bearing phase responsible for much of the hydration and alteration of the magmatic mineralogy of the body, since the effects of the the hydration are most evident along them. The gradation from rock containing highly saussuritized (i.e. epidote-altered) to relatively unsaussuritized plagioclase is striking, and points to ease of transport of fluid through open fractures, with greatly reduced mobility of fluid along grain boundaries into adjacent rock. Fractures themselves are filled with epidote, calcite, chlorite (with Berlin blue and brown anomalous birefringence) and minor quartz. Minor amounts of these minerals are present between plagioclase grains immediately adjacent to the fractures.

CHAPTER 4

THE MINERAL CHEMISTRY AND SIGNIFICANCE OF THE AMPHIBOLES OF THE CLINTON-COLDEN GABBRO-ANORTHOSITE INTRUSION

4.1 Introduction

Coarse amphibole enclosing plagioclase in a poikilitic manner is the most common type of amphibole in the intrusion. Together with clearly secondary amphibole overgrowing coarse amphibole and plagioclase and growing along coarse amphibole-plagioclase grain boundaries, it makes up essentially all of the ferromagnesian phases present. The only exceptions are minor chlorite and uralite. A pertinant question regards the timing of development of the coarse oikocrystic amphibole, which at first glance appears to be magmatic and thus the only significant primary mineral apart from plagioclase.

In mafic systems hornblende can appear on the liquidus but it generally does so after the appearance of olivine and pyroxene (Yoder and Tilley, 1962; Helz, 1973; Allen and Boettcher, 1978) (e.g. Fig. 4.1). High water pressure increases the importance of hornblende during crystallization of mafic magmas, but the presence in the Clinton-Colden intrusion of abundant plagioclase phenocrysts, which predate any other phase for which evidence is preserved, precludes high water pressure during the early stages of crystallization. Figure 4.1 indicates that in high-Al basalt, often considered as a potential parental magma to anorthosite (e.g. Emslie, 1978), plagioclase is the first phase to crystallize only at low water pressure. Even at high water pressure hornblende is never the only ferromagnesian phase to crystallize (e.g. Yoder and Tilley, 1962; Helz, 1973). Thus the

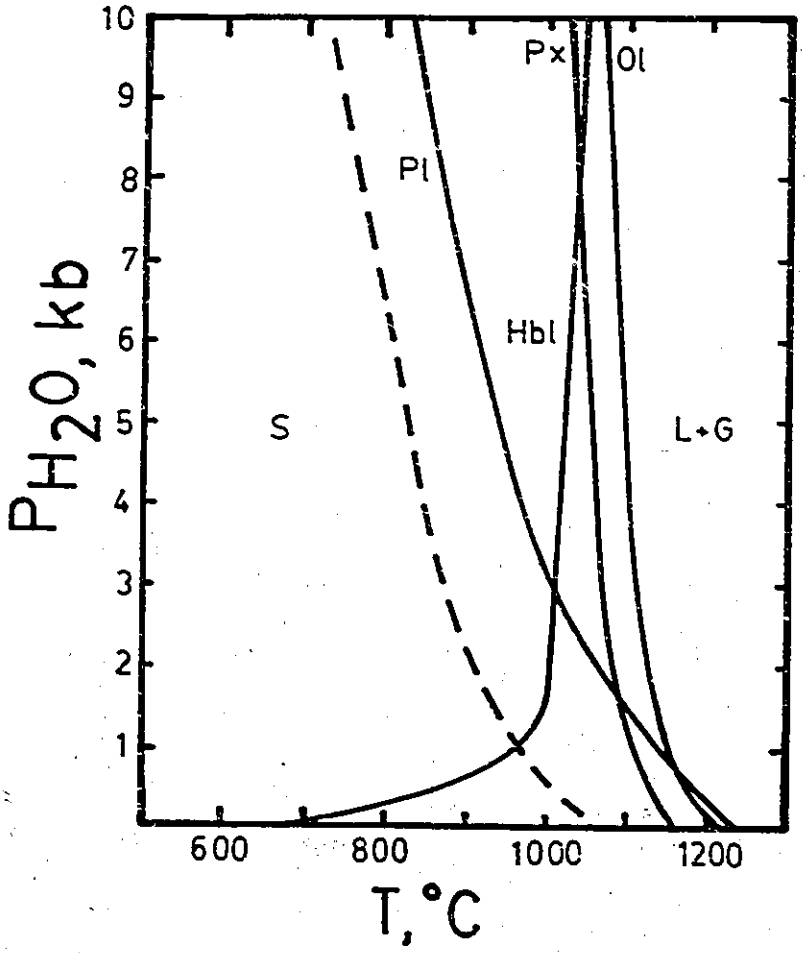

Fig. 4.1: Phase relations in the high-Al basalt system, simplified after Yoder and Tilley (1962). S=solid, Pl=plagioclase, Hbl=hornblende, Px=pyroxene, Ol=olivine, L+G=liquid + gas, dashed line=solidus.

development of hornblende-enriched gabbro by crystal fractionation, without other mafic phases present, is unlikely. In the case of the Clinton-Colden gabbro-anorthosite intrusion, either a reaction relationship between pyroxene and the melt, or subsolidus modification, must be responsible for the extreme enrichment in amphibole.

4.2 Analysis, calculation of formulae, and nomenclature of the amphiboles

A knowledge of the relative abundances of Fe^{+3} and Fe^{+2} is essential in the classification of amphiboles (Hawthorne, 1983). However, microprobe analyses do not report Fe^{+3}, so some workers (e.g. Ujike, 1982) have considered all Fe as Fe^{+2}, some have calculated Fe^{+3} values midway between possible maximum and minimum Fe^{+2} and Fe^{+3} values based on crystal-chemical constraints (Stout, 1972), and others have calculated Fe^{+3} on the basis of charge balance. To evaluate the oxidation state of iron in the amphiboles of the Clinton-Colden intrusion, separates of the two textural end-members were analysed. Material was extracted from a coarse amphibole oikocryst and a monomineralic clot of fine secondary amphibole, and FeO was determined by titration methods. Total Fe as Fe_2O_3 was determined by XRF analysis (Table 4.1). Although the separates contain approximately 0.25% ilmenite, Fe contamination from this source is minor and the Fe^{+3}/Fe^{+2} ratios obtained for the amphiboles are considered useful. The ratios for the amphibole oikocryst ($Fe^{+3}/Fe^{+2}=0.15$) and fine secondary amphibole clot ($Fe^{+3}/Fe^{+2}=0.21$) were then applied to all microprobe analyses of oikocrystic amphibole and fine secondary amphibole respectively.

Representative amphibole analyses are given in Table 4.2, and all

Table 4.1: Chemical compositions of a clot of fine secondary amphibole (G-25) and a coarse amphibole oikocryst (G-28), and $Fe^{+3}/Fe^{+3}+Fe^{+2}$ ratios. Fine amphibole clot yields compostion of tschermakite. Coarse amphibole oikocryst is hornblende. FeO determined by titration method. Other oxides determined by X-ray fluorescence. Recalculated on basis of 22 oxygens.

	G-25	G-28
Si+4	19.50	23.31
Ti+4	0.65	0.62
Al+3	7.76	3.55
Fe+3	2.02	1.30
Fe+2	9.62	8.66
Mn+2	0.14	0.14
Mg+2	6.99	8.20
Ca+2	7.34	8.96
Na+1	0.92	0.38
K+1	0.18	0.12
H+1	0.23	0.23
Total	55.35	55.47
Fe3/Fe2+Fe3	0.17	0.13
#Si IV	6.21	7.21
#Al IV	1.79	0.79
T site	8.00	8.00
#Al VI	0.79	0.36
#Fe +3	0.32	0.20
#Ti	0.12	0.11
#Mg	2.57	2.93
#Fe +2	1.19	1.35
#Mn	0	0.02
#Ca	0	0.03
M1,2,3	5.00	5.00
#Fe +2	0.35	0
#Mn	0.02	0
#Ca	1.63	1.94
#Na	0	0.06
M4 site	2.00	2.00
#Ca	0.01	0
#Na	0.36	0.08
#K	0.04	0.03
A site	0.41	0.09
#O	22.00	22.00
#OH	2.00	2.00

Table 4.2: Compositions of selected amphiboles. Numbered analyses correspond to analysed points in Fig. 5.8. Act=actinolite; ActHbl=actinolitic hornblende; Hbl=magnesio-hornblende; Ts=tschermakite; TsHbl=tschermakitic hornblende. a) oikocrystic amphibole; analyses 1-5 are of a single grain in sample J-445; analyses 6-11 are of single grain in sample T-7; b) amphibole grains overgrowing plagioclase; analysis 12 is of fine grain overgrowing plagioclase in sample T-7; other analyses are of single grains from samples as indicated; c) single fine amphibole grains replacing oikocrystic amphibole, from samples as indicated. Recalculated on a basis of 22 oxygens, OH + F + Cl=2. Fig. 5.1: Distribution of major elements and Zr versus SiO_2 for rocks of the Clinton-Colden gabbro-anorthosite intrusion. Filled square=gabbro; open square=leucogabbro; circle=anorthosite. (cont'd. next page)

a)

	1 Act	2 Act	3 ActHbl	4 ActHbl	5 ActHbl	6 Hbl	7 Hbl	8 Hbl	9 Hbl	10 Hbl	11 Hbl
SiO2	53.95	52.34	51.39	51.14	49.97	49.50	48.68	48.74	47.31	47.50	46.14
TiO2	0.08	0.08	0.12	0.14	0.20	0.28	0.36	0.35	0.27	0.39	0.52
Al2O3	2.74	2.87	4.40	4.57	5.62	7.24	6.86	7.88	7.62	8.89	10.13
Fe2O3	1.76	1.83	1.92	1.89	2.03	2.06	2.04	2.12	2.12	2.22	2.26
FeO	10.92	11.35	11.92	11.73	12.54	12.74	12.62	13.11	13.11	13.73	13.99
MnO	0.29	0.29	0.23	0.21	0.20	0.13	0.24	0.15	0.12	0.19	0.23
MgO	16.08	15.74	14.57	15.01	13.89	13.26	13.41	12.92	12.79	11.79	11.29
CaO	12.61	12.75	12.52	12.32	12.64	11.83	11.80	12.02	11.97	12.15	12.16
Na2O	0.27	0.23	0.51	0.47	0.55	0.82	0.76	0.86	0.88	1.09	0.98
K2O	0.02	0.02	0.03	0.03	0.05	0.13	0.10	0.12	0.12	0.13	0.25
H2O	2.10	1.98	2.06	2.06	1.97	2.06	2.03	2.03	1.87	2.03	2.02
F	-	0.17	-	-	0.17	-	-	0.06	0.31	-	-
Cl	0.03	0.04	0.04	0.04	0.02	0.05	0.03	0.04	0.02	0.06	0.07
O=F	-	0.07	-	-	0.07	-	-	0.03	0.13	-	-
O=Cl	0.01	0.01	0.01	0.01	0.00	0.01	0.01	0.01	0.00	0.01	0.02
Total	100.86	99.77	99.72	99.62	99.93	100.11	98.94	100.43	98.68	100.19	100.06
#Si IV	7.66	7.57	7.45	7.41	7.28	7.19	7.15	7.07	7.03	6.95	6.79
#Al IV	0.34	0.43	0.55	0.59	0.72	0.82	0.85	0.93	0.97	1.05	1.21
T site	8.00	8.00	8.00	8.00	8.00	8.00	8.00	8.00	8.00	8.00	8.00
#Al VI	0.12	0.06	0.20	0.19	0.24	0.41	0.34	0.42	0.36	0.48	0.54
#Fe +3	0.19	0.20	0.21	0.21	0.22	0.22	0.23	0.23	0.24	0.24	0.25
#Ti	0.01	0.01	0.01	0.02	0.02	0.03	0.04	0.04	0.03	0.04	0.06
#Mg	3.40	3.39	3.15	3.24	3.02	2.87	2.94	2.80	2.83	2.57	2.48
#Fe +2	1.28	1.34	1.43	1.35	1.50	1.46	1.46	1.51	1.53	1.66	1.68
M1,2,3	5.00	5.00	5.00	5.00	5.00	5.00	5.00	5.00	5.00	5.00	5.00
#Fe +2	0.02	0.03	0.01	0.07	0.03	0.08	0.09	0.08	0.09	0.02	0.05
#Mn	0.03	0.04	0.03	0.03	0.02	0.02	0.03	0.02	0.02	0.02	0.03
#Ca	1.92	1.93	1.94	1.90	1.95	1.84	1.86	1.87	1.89	1.90	1.92
#Na	0.03	-	0.01	-	-	0.07	0.02	0.03	-	0.05	0.01
M4 site	2.00	2.00	2.00	2.00	2.00	2.00	2.00	2.00	2.00	2.00	2.00
#Ca	-	0.04	-	0.01	0.03	-	-	-	0.02	-	-
#Na	0.04	0.06	0.13	0.13	0.16	0.16	0.20	0.21	0.25	0.26	0.27
#K	0.00	0.00	0.01	0.01	0.01	0.02	0.02	0.02	0.02	0.02	0.05
A site	0.05	0.11	0.13	0.15	0.19	0.19	0.22	0.23	0.29	0.28	0.32
#O	22.00	22.00	22.00	22.00	22.00	22.00	22.00	22.00	22.00	22.00	22.00
#OH	1.99	1.91	1.99	1.99	1.92	1.99	1.99	1.96	1.85	1.99	1.98
#F	-	0.08	-	-	0.08	-	-	0.03	0.15	-	-
#Cl	0.01	0.01	0.01	0.01	0.00	0.01	0.01	0.01	0.01	0.01	0.02

Table 4.2 (cont'd.) (cont'd. next page)

b)

	12 Hbl	G-95 TsHbl	G-92 Ts	G-92 Ts	T-7 Hbl	G-73 TsHbl
SiO2	45.45	42.60	40.67	41.92	44.10	45.38
TiO2	0.38	0.42	0.11	0.12	0.67	0.38
Al2O3	11.19	14.45	16.07	16.04	12.63	12.26
Fe2O3	3.15	3.41	2.98	3.08	3.23	2.70
FeO	13.57	14.67	12.83	13.22	13.98	11.62
MnO	0.17	0.19	0.22	0.20	0.19	0.20
MgO	10.84	9.61	10.04	9.63	10.04	10.98
CaO	11.82	11.34	11.43	11.49	11.68	11.12
Na2O	1.11	1.47	1.61	1.59	1.38	1.15
K2O	0.19	0.22	0.20	0.21	0.27	0.16
H2O	2.03	1.96	1.96	1.99	1.94	2.03
F	-	0.09	-	-	0.15	-
Cl	0.05	0.11	0.14	0.14	0.10	-
O=F	-	0.04	-	-	0.06	-
O=Cl	0.01	0.02	0.03	0.03	0.02	-
Total	99.96	100.60	98.29	99.66	100.44	97.98
#Si IV	6.69	6.29	6.11	6.20	6.50	6.71
#Al IV	1.31	1.71	1.89	1.80	1.50	1.29
T site	8.00	8.00	8.00	8.00	8.00	8.00
#Al VI	0.63	0.81	0.96	1.00	0.70	0.85
#Fe +3	0.35	0.38	0.34	0.34	0.36	0.30
#Ti	0.04	0.05	0.01	0.01	0.07	0.04
#Mg	2.38	2.12	2.25	2.12	2.21	2.42
#Fe +2	1.60	1.65	1.45	1.52	1.67	1.38
M1,2,3	5.00	5.00	5.00	5.00	5.00	5.00
#Fe +2	0.07	0.16	0.17	0.12	0.06	0.06
#Mn	0.02	0.02	0.03	0.03	0.02	0.03
#Ca	1.86	1.79	1.81	1.82	1.84	1.76
#Na	0.05	0.02	-	0.04	0.07	0.16
M4 site	2.00	2.00	2.00	2.00	2.00	2.00
#Ca	-	-	0.03	-	-	-
#Na	0.27	0.40	0.47	0.42	0.32	0.17
#K	0.04	0.04	0.04	0.04	0.05	0.03
A site	0.30	0.44	0.54	0.46	0.37	0.20
#O	22.00	22.00	22.00	22.00	22.00	22.00
#OH	1.99	1.93	1.96	1.96	1.91	2.00
#F	-	0.04	-	-	0.07	-
#Cl	0.01	0.03	0.04	0.04	0.02	-

Table 4.2 (cont'd.)

c)

	G-95 TsHbl	G-95 TsHbl	G-87 TsHbl	G-87 Hbl	G-87 Hbl	G-92 Hbl
SiO2	42.60	43.49	49.59	42.86	51.00	44.34
TiO2	0.42	0.19	0.66	0.38	0.34	0.36
Al2O3	14.45	13.37	6.62	14.13	5.45	12.34
Fe2O3	3.38	3.33	2.57	3.08	2.45	3.05
FeO	14.56	14.36	11.10	13.28	10.55	13.12
MnO	0.19	0.19	0.22	0.16	0.19	0.19
MgO	9.61	10.23	14.94	10.45	15.31	10.90
CaO	11.34	10.97	11.63	11.38	11.10	11.54
Na2O	1.47	1.48	0.68	1.41	0.66	1.25
K2O	0.22	0.20	0.11	0.22	0.06	0.23
H2O	1.96	1.91	2.02	1.89	2.04	2.02
F	0.09	0.19	-	0.25	0.03	-
Cl	0.11	0.09	0.24	0.06	0.08	0.04
O=F	0.04	0.08	-	0.11	0.01	-
O=Cl	0.02	0.02	0.05	0.01	0.02	0.01
Total	100.46	100.10	100.44	99.67	99.29	99.39
#Si IV	6.30	6.44	7.14	6.35	7.36	6.55
#Al IV	1.70	1.56	0.86	1.65	0.64	1.45
T site	8.00	8.00	8.00	8.00	8.00	8.00
#Al VI	0.82	0.77	0.27	0.82	0.29	0.70
#Fe +3	0.38	0.37	0.28	0.34	0.27	0.34
#Ti	0.05	0.02	0.07	0.04	0.04	0.04
#Mg	2.12	2.26	3.21	2.31	3.30	2.40
#Fe +2	1.64	1.58	1.18	1.49	1.11	1.51
M1,2,3	5.00	5.00	5.00	5.00	5.00	5.00
#Fe +2	0.16	0.20	0.16	0.15	0.16	0.11
#Mn	0.02	0.02	0.03	0.02	0.02	0.02
#Ca	1.80	1.74	1.79	1.81	1.72	1.83
#Na	0.02	0.04	0.02	0.02	0.10	0.04
M4 site	2.00	2.00	2.00	2.00	2.00	2.00
#Ca	-	-	-	-	-	-
#Na	0.40	0.38	0.17	0.39	0.09	0.32
#K	0.04	0.04	0.02	0.04	0.01	0.04
A site	0.44	0.42	0.19	0.43	0.10	0.36
#O	22.00	22.00	22.00	22.00	22.00	22.00
#OH	1.93	1.89	1.94	1.87	1.97	1.99
#F	0.04	0.09	-	0.12	0.01	-
#Cl	0.03	0.02	0.06	0.02	0.02	0.01

available amphibole analyses are given in Appendix 1.

Microprobe analyses of amphiboles were normalized on the basis of 22 oxygens, OH + F + Cl = 1, and assignment of cations to crystallographic sites was carried out following the recommendations of Leake (1978). All formulae so calculated met the criteria for acceptable amphibole formulae summarized by Robinson et al. (1982).

Nomenclature is also according to Leake (1978). All amphiboles are calcic, magnesian with $Mg/Mg+Fe^{+2}>0.5$, and have $(Na+K)_A<0.5$. They lie within the fields ranging from actinolite to tschermakite in Figure 4.2.

4.3 Coupled substitutions in the amphiboles

Amphiboles of the intrusion range in composition from actinolite to hornblende and essentially reflect a trend of decreasing Si^{+4} in tetrahedral coordination (with concomittant increase in Al^{3+}) (Fig. 4.2). This is true whether they form oikocrysts or fine-grained secondary products, or whether overgrowing uralite, amphibole or plagioclase. The major coupled substitutions responsible for this trend, as in the actinolite-hornblende solid solution series in general (Grapes, 1975; Robinson et al., 1982; Kamineni, 1986; Arai and Hirai, 1985) are the edenitic and tschermakitic ones, as presented graphically in Figures 4.3 to 4.5. These plot abundances of Al^{3+} in tetrahedral sites (Al^{IV}) of the amphibole against abundances of elements substituting into octahedral sites and A-sites in order to compensate for resulting charge imbalances. Figure 4.3 is a plot of Al^{IV} against combined A-site occupancy, octahedral Al (Al^{VI}, Fe^{+3}, and Ti in the half-unit-cell. The components on the x-axis account for the combined

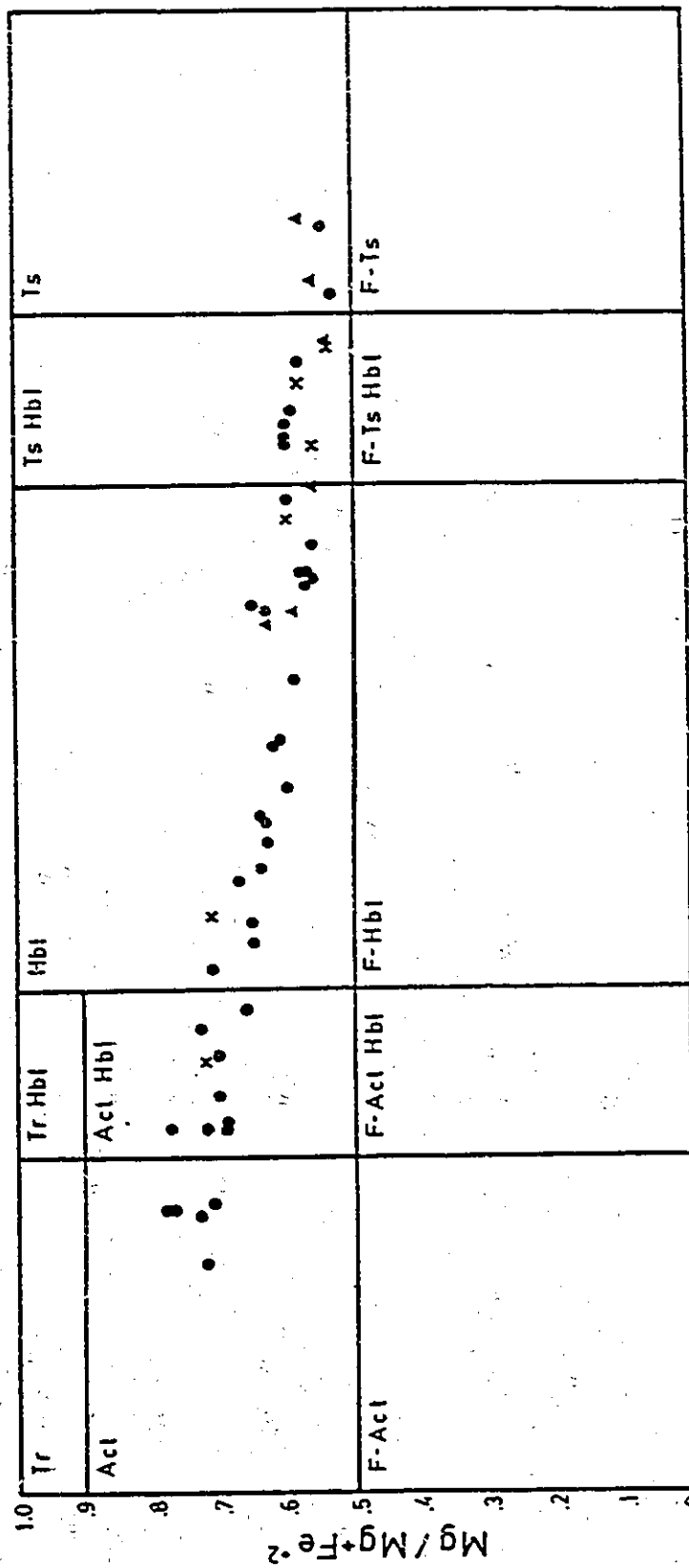

Fig. 4.2: Nomenclature of amphiboles of the Clinton-Colden Intrusion, following Leake (1978). Tr=tremolite; Tr Hbl=tremolitic hornblende; Act=actinolite; Act Hbl=actinolitic hornblende; Hbl=magnesio-hornblende; Ts=tschermaklte; Ts Hbl=tschermaklitic hornblende; F=ferro. Circles=oikocrystic amphibole; triangles=amphibole overgrowing plagioclase; x=fine amphibole overgrowing oikocrystic amphibole.

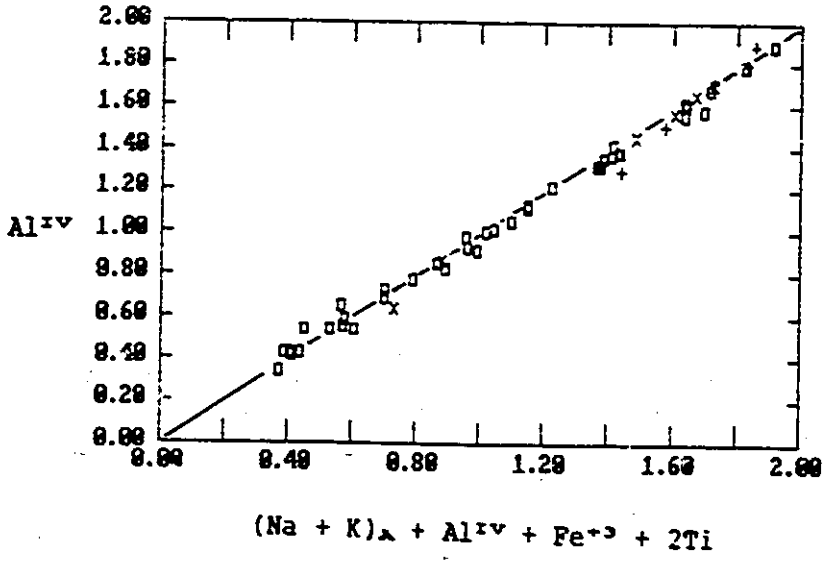

Fig. 4.3: Plot illustrating effect of combined edenite $(Na + K)_A$, tschermakite $(Al^{VI} + Fe^{3+})$ and Ti-tschermakite (2Ti) substitutions on Al^{IV} occupancy for all amphiboles analysed. Line of complete substitution, having a slope of 1, is shown for comparison. Rectangle=oikocrystic amphibole; x=amphibole overgrowing plagioclase; +=fine amphibole replacing coarse amphibole.

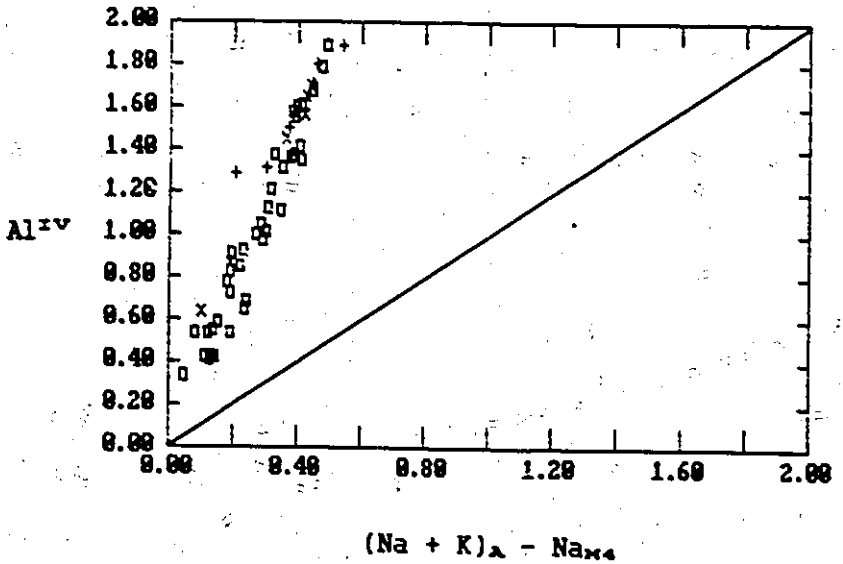

Fig. 4.4: Plot illustrating effect of tschermakite plus Fe-tschermakite substitutions on Al^{IV} occupancy for all amphiboles analysed. Line of complete substitution shown for comparison. Symbols as in Fig. 4.3.

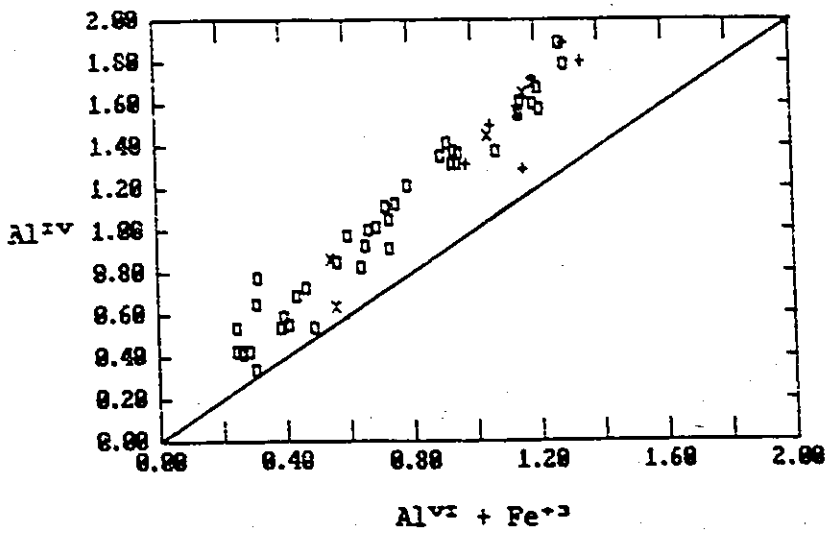

Fig. 4.5: Plot illustrating effect of edenite substitution on Al^{IV} occupancy for all amphiboles analysed. Na^{M4} subtracted from total A-site occupancy in order to remove effect of richterite substitution (Czamanske et al., 1981). Line of complete substitution shown for comparison. Symbols as in Fig. 4.3.

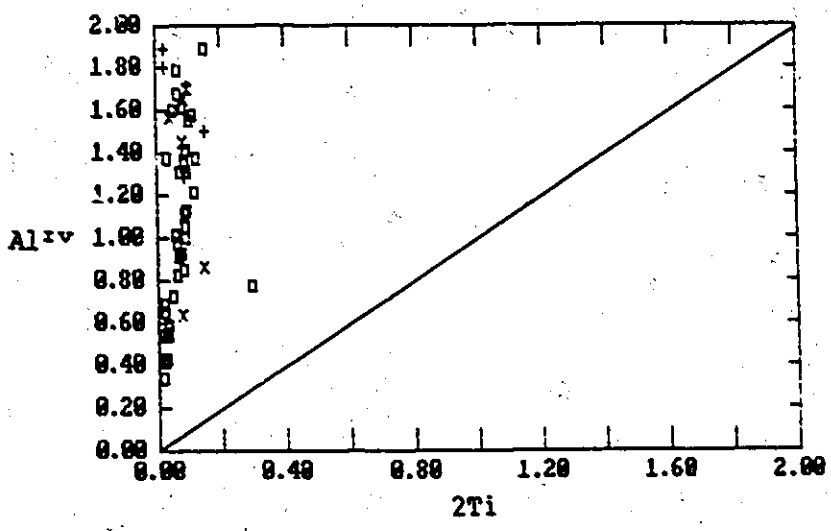

Fig. 4.6: Plot illustrating effect of Ti-tschermakite substitution on Al^{IV} occupancy for all amphibloles analysed. Line of complete substitution shown for comparison. Symbols as in Fig. 4.3.

effects of the edenitic (with a minor amount of richteritic), tschermakitic and Ti-tschermakitic substitutions (Pe-Piper, 1988; Ujike, 1982; Grapes et al., 1977). The well-defined trend has a slope of nearly one, with a correlation coefficient (r^2) of 0.997, indicating that these substitutions account for virtually all of the Al^{IV} in the amphiboles.

Figure 4.4 depicts the effect of the edenitic coupled substitution, $(Na,K)_A + Al^{IV} \quad \square_A + Si^{IV}$. The amphiboles define a trend having a slope considerably greater than that of the line of complete substitution, indicating that although significant, the edenitic substitution alone does not account for the bulk of the Al^{IV} in the amphiboles. Figure 4.5 depicts the effects of the tschermakitic substitution, $(Al,Fe^{+3})_{M1-M3} \quad (Mg,Fe^{+2})_{M1-M3} + Si^{IV}$. The slope of the trend defined by the amphiboles approaches that of the line of complete substitution, indicating that the tschermakitic substitution is of greater importance than the edenitic one. Note that $(Na + K)_A/Al^{IV} = 0.26$, somewhat less than the value of 0.3 generally observed in calcic amphiboles (Mongkoltip and Ashworth, 1986), indicating the importance of the tschermakitic substitution relative to the edenitic one.

A minor substitution which is of interest is the Ti-tschermakite one, $Ti + Al_2^{IV} \quad Mg + Si_2$, illustrated in Figure 4.6. Although only accounting for approximately 1/25 of Al^{IV} present as actinolite grades to hornblende, this substitution agrees well with the increase in Ti seen with increasing Al^{IV} (i.e. as amphibole becomes more hornblendic) in Figure 4.7. The correspondence may be attributed to increasing Ti and Al as grain boundaries are approached, a possible consequence of

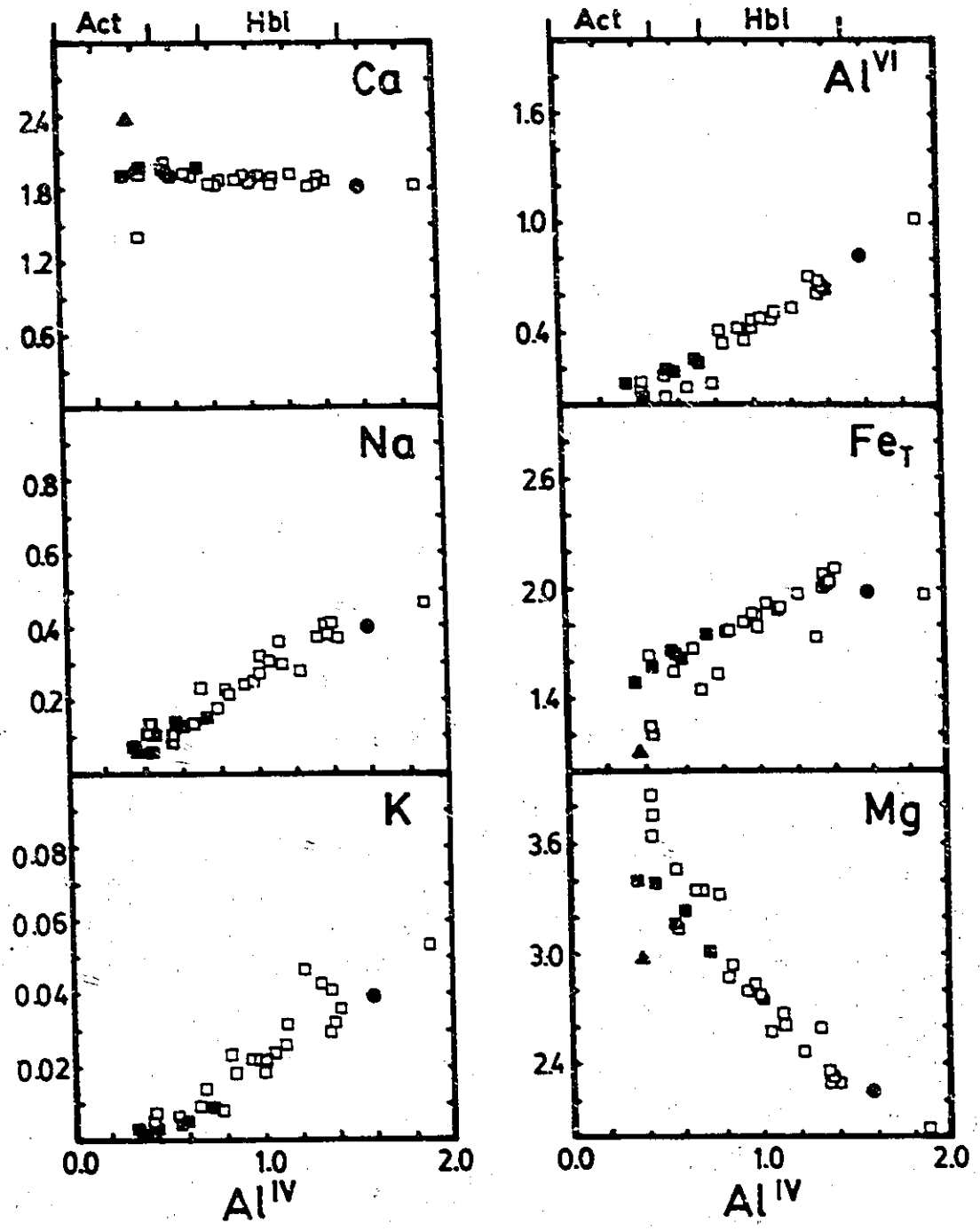

Fig. 4.7: Atoms per unit formula versus tetrahedral Al^{IV} for points analysed in amphibole oikocrysts. Open square=amphibole oikocryst; triangle=average of uralite analyses (Table 3.2) from sample J-445, recast as amphibole; filled square=points analysed in amphibole oikocryst in sample J-445; circle=average of 6 amphibole grains which overgrow plagioclase (Table 4.2); Act=actinolite; Hbl=hornblende.

(cont'd. next page)

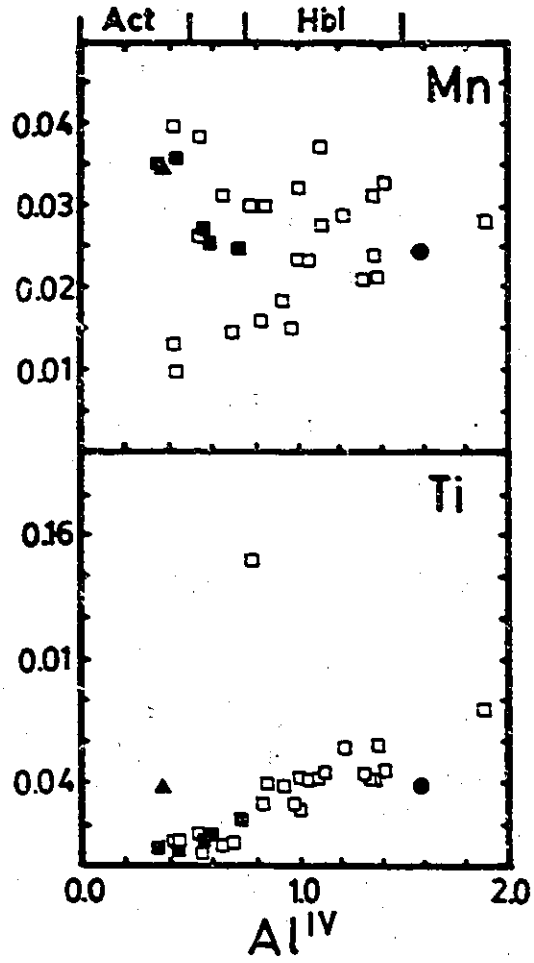

Fig. 4.7 (cont'd.)

oxidation of Fe-Ti oxides during the alteration process.

The crossite substitution, also of potential importance in calcic amphiboles (e.g. Brown, 1977), is not significant in the Clinton-Colden intrusion, as reflected in the paucity of Na_{M4} (Table 4.2). Other possible substitutions, such as the ferri-tschermakitic and the riebeckitic ones which Offler (1984) observed in Fe-rich subcalcic actinolite-hornblende series amphiboles from a metadiabase, and the cummingtonite substitution which Arai and Hirai (1985) postulated as having occurred in calcic actinolite-hornblende series amphiboles in Japanese metabasites, are similarly inoperative in the Clinton-Colden amphiboles.

4.4 The origin of the coarse amphiboles

4.4.1 The origin of the actinolite-hornblende solid solution

Single crystal microprobe traverses indicate that oikocrysts vary within the actinolite and magnesio-hornblende fields (Fig. 4.8a). The more hornblendic material occurs adjacent to enclosed plagioclase. Similar gradations within amphibole adjacent to plagioclase are described by Pe-Piper (1988), Chivas (1981), and Mongkoltip and Ashworth (1986). In contrast with this, grains overgrowing plagioclase in the Clinton-Colden intrusion are optically homogeneous and are consistently aluminous (Table 4.2).

The concentration of Al within the oikocrystic grains increases as plagioclase is approached (Fig. 4.8a,b) and adjacent to plagioclase achieves values similar to those of the homogeneous, fine aluminous amphibole which overgrows the plagioclase. This suggests that the rate of diffusion of Al from plagioclase, through the amphibole structure,

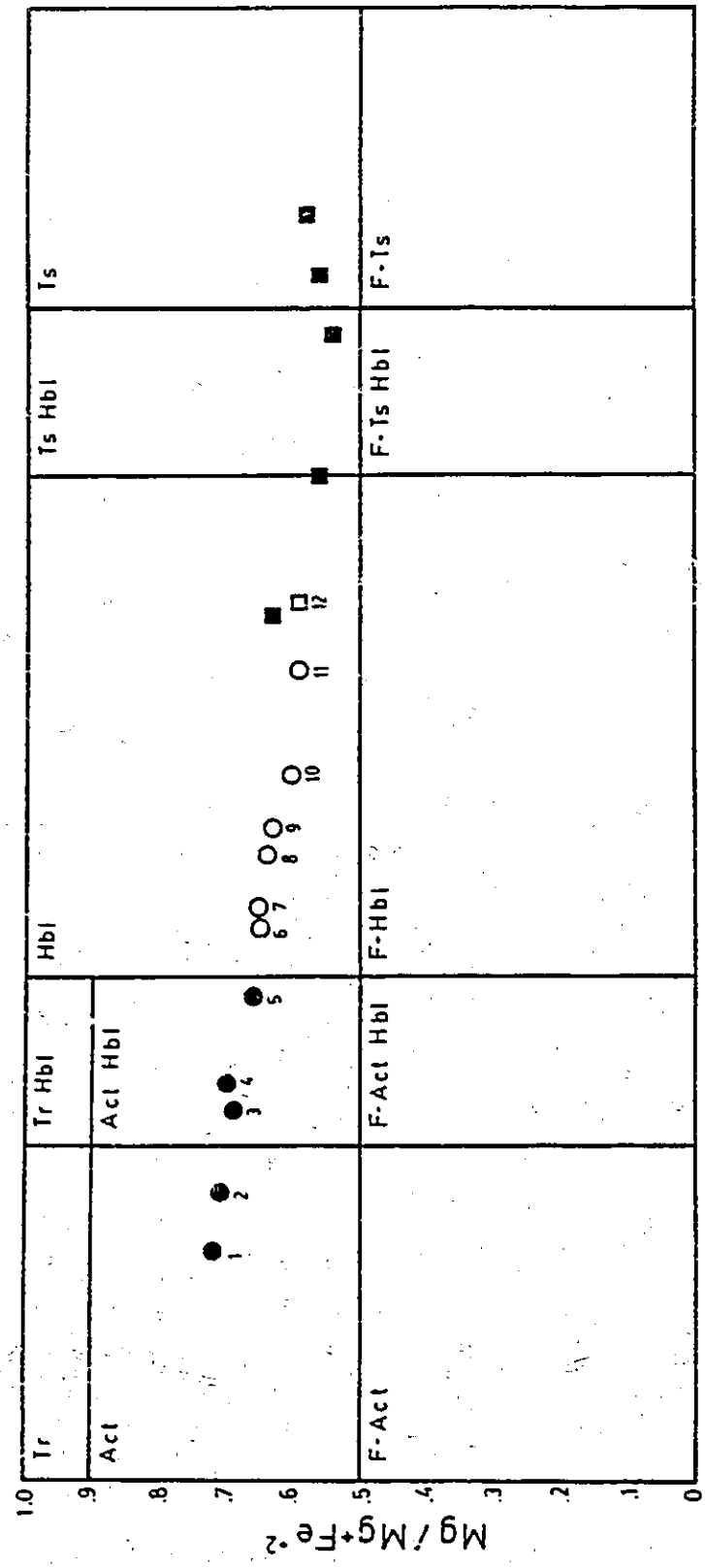

Fig. 4.8a: Nomenclature of olkocrystic amphibole from two single-crystal microprobe traverses (analyses given in Table 4.2). Filled circles from olkocryst overgrowing uralite in sample J-445, points 1 to 5 lying successively further from sample T-7, points 6 to 11 lying successively nearer to fine amphibole occurring at interface between olkocryst and altered plagioclase; point 12 lies in grain of fine amphibole overgrowing altered plagioclase.

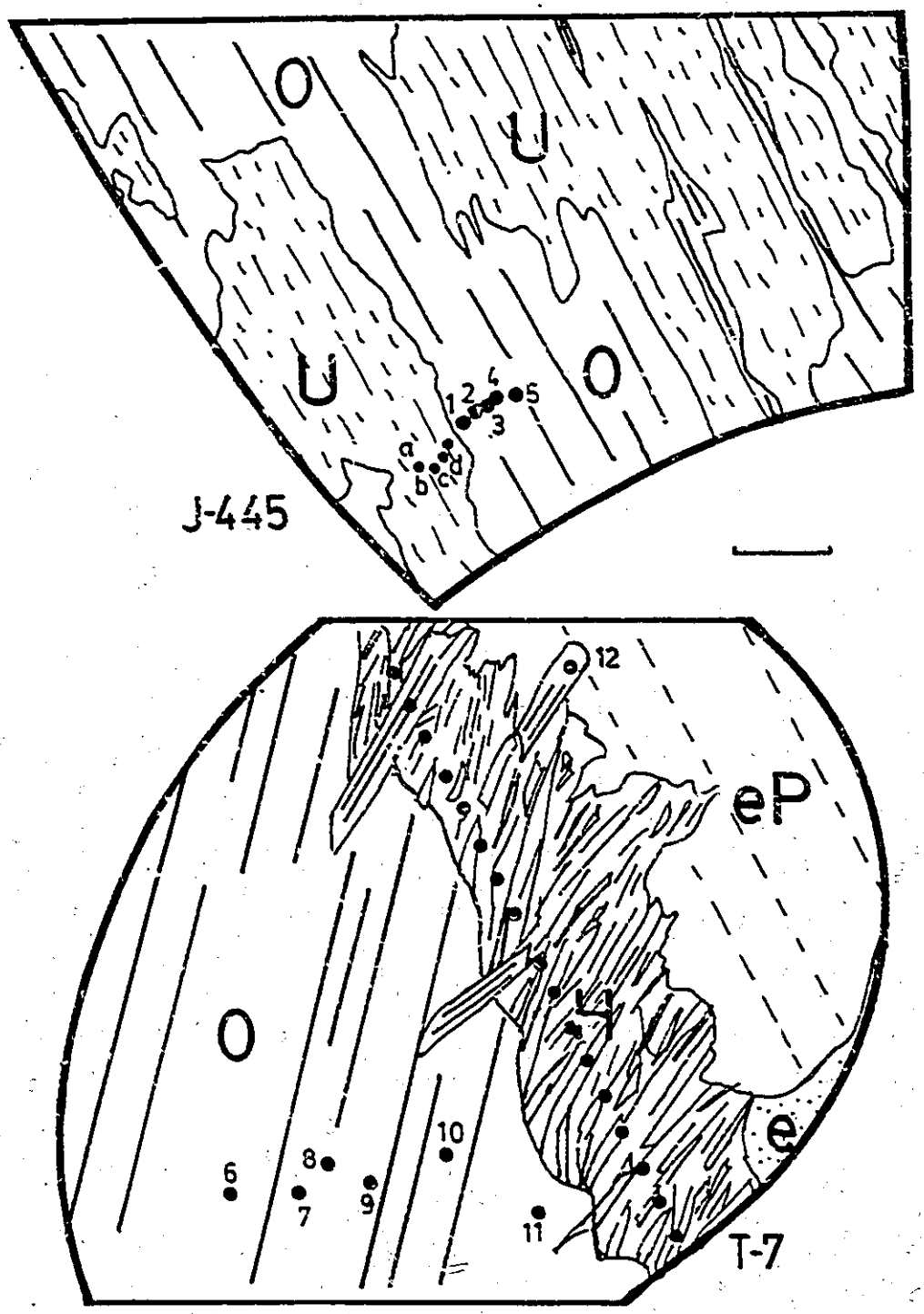

Fig. 4.8b: Sketches of two microprobe traverses. One crosses uralite (a-d) and amphibole oikocryst (1-5) in sample J-445. The second crosses amphibole oikocryst, ending with amphibole prism overgrowing plagioclase which is largely altered to fine epidote, in sample T-7. Analyses of points given in Table 3.2 (uralite) and Table 4.2 (amphibole). Amphibole compositions plotted in Figure 4.8a. O=oikocryst; H=fine hornblende and more aluminous calcic amphibole; e=fine epidote; eP=extensively epidotized plagioclase grain showing traces of albite twinning. Dotted line in fine amphibole=approximate original grain boundary. Scale bar=0.12 mm.

controlled the aluminum concentration in oikocrystic amphibole from aluminous rims to actinolitic cores. A similar process apparently took place during the deuteric alteration of the East Bull Lake anorthosite-gabbro intrusion of Ontario (Kamineni, 1986). Austreheim and Robins (1981) also studied diffusion of elements, including Al, which controlled amphibole composition during hydration of pyroxene in anorthosite-gabbro in Norway. In these studies, as in the Clinton-Colden intrusion, the most Al-rich amphiboles occurred adjacent to plagioclase. In the Clinton-Colden intrusion some amphiboles have >16% Al_2O_3 (Table 4.2), which approaches the Al_2O_3 contents of the most aluminous (17%) ones given in Leake's (1971) compilation of calcic amphibole analyses.

Fine amphibole prisms and extensions of coarse amphibole oikocrysts overgrowing plagioclase occur at most oikocryst-plagioclase grain boundaries (e.g. Figs. 3.7, 3.8). Although these amphibole grains are aluminous, they have less Al than does the host plagioclase (see reaction 4.3 below). The surplus Al represents a source for the modification of the oikocrysts. In a similar context, Mongkoltip and Ashworth (1986) observed hornblende rims on actinolite pseudomorphs of clinopyroxene in metagabbros only where the pseudomorphs abutted against plagioclase.

The compositional trend in the amphiboles of the intrusion suggests a secondary origin for the amphibole oikocrysts, since the cores of these have Al contents well below those normally seen in magmatic amphiboles, while the most aluminous amphiboles, which have Al contents within the range of igneous amphibole (Leake, 1971), are clearly secondary grains overgrowing plagioclase. A similar distribution of

Ti, with concentrations well below those seen in igneous amphiboles (e.g. Helz, 1973), likewise points to a secondary origin for the coarse amphibole. In the light of this evidence in favour of a postmagmatic origin for the coarse amphibole, a clarification of the origin of its oikocrystic texture is required.

4.4.2 Evidence of oikocrystic pyroxene and of the pyroxene to actinolite to hornblende transformation

The fine grained uralitized remnants of pyroxene within amphibole oikocrysts have compositions very similar to augite (Table 3.2). They are in optical continuity with each other, and the c-axes of the enclosing amphibole are oriented parallel to the elongation directions of the fine fibres in the uralite. Presumably the elongation direction in the uralite is parallel to the c-axis in the precursor pyroxene (cf. Buseck et al., 1980). It thus appears that coarse pyroxene oikocrysts have been replaced by optically parallel amphibole (cf. Mongkoltip and Ashworth, 1986), an intermediate state being represented by the uralitized pyroxene remnants. This intermediate state may represent an incipiently hydrated and distorted pyroxene chain structure (Velbel, 1984), interleaved amphibole and pyroxene domains (Buseck et al., 1980), or defect-riddled material resulting from the multiple nucleation of amphibole domains (Buseck et al., 1980). According to Thompson (1981), detailed analysis of uralite indicates the presence of disordered material approximating amphibole. In any case, the coarse actinolite which replaces uralite in the Clinton-Colden intrusion clearly represents the end product of a hydration and alteration process, by which abundant coarse pyroxene oikocrysts were pseudomorphically replaced by coarse actinolite. Such production of

coarse actinolitic amphibole in metaplutonic rocks is described by Rodgers (1973). Similarly, Grapes et al. (1977) document replacement of fibrous actinolitic uralite pseudomorphs (after clinopyroxene) by single actinolite crystals during progressive regional metamorphism of gabbro in Japan. In most cases, some clinopyroxene remains in evidence (e.g. Kamineni, 1986). In the case of the Clinton-Colden intrusion the process advanced sufficiently that virtually all pyroxene was replaced by actinolite, and no fresh pyroxene is preserved.

Quartz blebs occurring within many of the amphibole oikocrysts (see Chapter 3) provide further evidence that the coarse amphibole replaces pyroxene. Since calcic amphiboles are generally less SiO_2-rich than clinopyroxenes, these quartz blebs probably represent excess SiO_2 during the pyroxene to amphibole transformation (see reaction 4.1, below). Austreheim and Robins (1981) and Mongkoltip and Ashworth (1986) observed such quartz blebs within amphibole of less completely altered gabbroic rocks, and attributed to them a similar origin.

Chemical compositions of the uralitized pyroxene remnants of sample J445 are given in Table 3.2, and compositions of the overgrowing actinolite adjacent to the uralite are given in Table 4.2 (analyses 1,2). The uralite is relatively homogeneous, but this compositional homogeneity cannot be attributed to a homogeneous precursor since the pyroxene remnants show textural evidence of exsolution (Fig. 3.11). Homogeneity of uralite in similar rocks has been attributed to the alteration process (Mongkoltip and Ashworth, 1986), so it is likely that the uralite in the Clinton-Colden intrusion does not represent truly the original pyroxene composition. In the absence of pristine original pyroxene an exact pyroxene to actinolite reaction cannot be

written. However, a simplified reaction can be written based upon the average uralite composition and the composition of the immediately adjacent actinolite which overgrows it. Because the concentration of Al in the uralite is greater than that expected for magmatic pyroxene, and its original concentration is undeterminable, it is considered to be entirely derived from alteration of adjacent plagioclase. Minor components accounting for less than 0.02 atoms per unit formula are ignored.

$$4.2(Fe_{0.3}Mg_{0.8}Ca_{0.9}Si_2O_6) + 0.25Al_2O_3 + 0.34FeO + 0.05Na_2O + H2^{\circ}$$
$$Na_{0.1}Ca_2Mg_{3.4}Fe^{+2}_{1.4}Fe^{+3}_{0.2}Al_{0.1}Al_{0.4}Si_{7.6}O_{22}(OH)_2 + 0.8SiO_2 + 1.78CaO \quad (4.1)$$

This reaction assumes MgO to be constant since its concentration is similar in uralite and actinolite and no external source of MgO is apparent in the rock. SiO_2 is not considered constant since an influx of Al^{3+} into the tetrahedral sites of the amphibole has occurred, resulting in excess silica and quartz precipitation in many cases.

The above reactions, as well as those below, are approximate, but they conform with the observed mineralogy. Reaction 4.1 generates a minor excess in SiO_2 and consumes the FeO produced during the dissolution of Fe-Ti oxides. The excess CaO probably contributes to the epidote found throughout the intrusion. The source of the Al_2O_3 consumed is accounted for in reaction 4.3 below.

A second reaction can be written, using the composition of actinolite lying immediately adjacent to uralite (point 1 in Figure 4.8b) as the major reactant, and the composition of magnesiohornblende lying adjacent to plagioclase (point 11 in Figure 4.8b) as the major product, illustrating the transition from actinolite to hornblende as

Al increases towards the margin of the coarse amphibole grain. In this case Ca is assumed to be constant, based upon its similarity in concentration (a function of its approximately complete occupancy of the M4 site) across the grain:

$$Na_{0.1}Ca_2Mg_{3.4}Fe^{+2}_{1.4}Fe^{+3}_{0.2}Al_{0.1}Al_{0.4}Si_{7.6}O_{22}(OH)_2 + 0.05Na_2O + 0.2FeO + 0.65Al_2O_3$$

$$Na_{0.2}Ca_2Mg_{2.9}Fe^{+2}_{1.7}Fe^{+3}_{0.2}Al_{0.7}Al_{1.1}Si_{6.9}O_{22}(OH)_2 + 0.9MgO + 0.7SiO_2 \quad (4.2)$$

A further reaction can be written which illustrates the nature of the Al-releasing process. The mean of all plagioclase grains analysed is used as the major reactant, and the mean of all analysed amphibole grains overgrowing plagioclase is the major product.

$$2.85(Na_{0.27}Ca_{0.71}Al_{1.73}Si_{2.28}O_8) + 2.3MgO + 2.05FeO + H_2O = Na_{0.4}Ca_{1.8}Mg_{2.3}Fe^{+2}_{1.7}Fe^{+3}_{0.35}Al_{0.3}Al_{1.3}Si_{0.65}O_{22}(OH)_2 + 0.185Na_2O + 1.27Al_2O_3 + 0.22CaO \quad (4.3)$$

This reaction also supplies the Na required during reactions 4.1 and 4.2. Plagioclase thus contributes Al and Na during its replacement by amphibole without requiring modification of surviving plagioclase.

4.4.3 Diffusion of elements during the production and modification of coarse amphibole

The transformation of pyroxene to actinolite involved consumption of Al, Fe and H^+ and the release of Ca. A flux of these elements must have taken place in order to alter to actinolite the interiors of what were very coarse pyroxene oikocrysts. Indirect evidence of this flux remains in the form of element concentration gradients within pseudomorphic amphibole oikocrysts. Figure 4.7 illustrates the concentration of major cations versus number of Al^{IV} per unit formula

for all points analysed in amphibole oikocrysts. The amounts of total Fe, Na and K present in the amphibole all increase as Al^{IV} increases (i.e. as more actinolitic compositions are approached). Conversely, Mg decreases in this direction. The mean of all uralite analyses from sample J-445, recast as an amphibole for comparison, lies at the actinolite end of the compositional trends, suggesting that these trends developed as a result of diffusion of Al, Fe, Na and K towards the site of uralite replacement by amphibole, and of Mg away from it.

This suggestion is supported by an examination of compositional trens in the amphibole oikocrysts as neighbouring plagioclase, rather than uralite, is approached. Figure 4.8a shows that amphibole overgrowing plagioclase lies at one end of the compositional gradient observed in the oikocrystic amphibole analysed in sample T-7.

Reaction 4.3 (the replacement of plagioclase by aluminous amphibole) requires a source of Mg. Whereas Fe was available from sites of alteration of Fe-Ti oxides, Mg is abundant only in actinolitic amphiblole (Figure 4.7). For example, actinolite replacing uralite in sample J445 (reaction 4.1) has 3.4 atoms Mg per unit formula, quite high for calcic amphibole (cf. Robinson et al., 1982, p. 17). The source of Mg may have been the pyroxene, which could have been more Mg-rich than is indicated by the composition of its uralitic alteration product. Mg may have been liberated during the amphibolitization of calcic pyroxene, since that mineral has greater $Mg/Mg+Fe^{+2}$ than does coexisting calcic amphibole (Kretz and Jen, 1978). Mg saturation of adjacent actinolite may have resulted. As diffusion of Fe and Al into the cores of the coarse amphibole grains occurred, displacement of Mg may have produced the observed decline in the concentration of that

element, and in the $Mg/Mg+Fe^{+2}$ ratio in the coexisting amphibole (Ramberg, 1952, p. 345) at the margins of the grains. A flux of Mg outwards from the uralite-actinolite transition zone could have supplied the Mg consumed during the growth of tschermakite over plagioclase. These amphibole grains have low $Mg/Mg+Fe^{+2}$ ratios (Fig. 4.2), in part a function of the availability at grain margins of Fe from altered Fe-Ti oxides.

Consideration of the above trends suggests that diffusion of Al and Fe, from plagioclase and Fe-oxides respectively, into the actinolitic product of hydration of clinopyroxene, with concomitant outward diffusion of Ca and Mg, resulted in the observed pattern of actinolitic cores of amphibole oikocrysts being rimmed by progressively more hornblendic and less magnesian amphibole. The least diffusive component, Al, exerted the greatest control during the modification of the coarse amphiboles.

The sharp drop in the Ca content from the average uralite composition to that of the actinolite which replaces (Fig. 4.7) it is mineralogically predictable, amphibole being limited in its capacity to accept Ca (Robinson et al., 1982). Within the oikocrystic amphibole grain, however, the Ca gradient is slight, indicating that Ca diffused with relative ease away from the uralitic source. Mg, on the other hand, actually increases slightly from average uralite in sample J445 to the amphibole which overgrows it, before declining sharply in concentration as Si declines towards the margins of the oikocrystic amphibole. The calcium ion, being larger, might be expected to diffuse less readily than Mg through the amphibole structure, producing a steep Ca gradient. However, in amphiboles Ca occurs in the large M4 site

between the octahedral strip and the tetrahedral chain (Hawthorne, 1981), which may promote its diffusion through the amphibole structure. The influx of Al into the amphibole structure resulted in a decline in the $Mg/Mg+Fe^{+3}$ ratio relative to more actinolitic amphibole (Fig. 4.8a) (Ramberg, 1952), and produced a decrease in the Mg concentration from core to rim. Fe_T increases as Mg declines, probably because Al from plagioclase and Fe and Ti from opaque oxides probably competed for M2 sites (Mongkoltip and Ashworth, 1986). Therefore the Mg distribution in the oikocrystic amphibole is probably constrained by the slow diffusivity of Al.

The clinopyroxene-actinolite reaction is not a closed system one. The component required in the case of the Clinton-Colden intrusion, apart from H^+, is Al. Therefore the Al-releasing plagioclase-hornblende overgrowth reaction, which consumed Mg, was probably coeval with the alteration of clinopyroxene to actinolite. The epidotization of plagioclase probably consumed excess Ca produced by both of the amphibole-producing reactions.

4.4.4 Precursors of coarse amphibole

A clinopyroxene progenitor would account for the calcic nature of all amphibole oikocrysts. None of these oikocrysts represent primary amphibole since all have actinolitic cores. Furthermore, all amphiboles analysed, including margins of oikocrysts, have Ti concentrations well below that expected for magmatic hornblendes coexisting with Fe-Ti oxides (Otten, 1984). No minerals suggestive of alteration of other mafic phases, for instance serpentine after olivine, cummingtonite after orthopyroxene (Austreheim and Robins,

1981), or ferro-actinolite after hedenbergitic pyroxene (Ike, 1985), were observed in the Clinton-Colden intrusion. Mongkoltip and Ashworth (1986) observed complex relationships between discrete cummingtonite and hornblende grains in clinopyroxene + orthopyroxene-bearing metagabbros in Scotland. They found hornblende rims on cummingtonite grains where they were in contact with plagioclase. This is not the case in the Clinton-Colden intrusion, where the cores of the oikocrysts grains are always actinolitic. Rodgers (1973) describes actinolitic amphibole produced during alteration of bronzite, but in that study a nearby source of Ca, in the form of a magnesio-hornblende rich rock, was invoked to explain the production of calcic amphibole during alteration of orthopyroxene. In the Clinton-Colden intrusion the presence of small amounts of orthopyroxene may have been masked in secondary amphibole by the presence of excess Ca from the more abundant clinopyroxene. Abundant epidote in rocks of the intrusion indicates availability of Ca during at least part of the alteration process. It is possible that pervasive Ca metasomatism has obscured original variations in the ferromagnesian minerals.

4.4.5 The nature of the hydration process

Postmagmatic hydrothermal and regional metamorphic origins are possible for the coarse interstitial amphibole of the intrusion. A postmagmatic hydrothermal rather than regional metamorphic origin is supported by the lack of penetrative deformation and foliation and by the ubiquity of igneous plagioclase textures and compositions where that mineral has not been epidotized. The replacement of coarse clinopyroxene oikocrysts by amphibole pseudomorphs suggests a pervasive

static hydration rather than the regional metamorphism which caused extensive recrystallization and deformation of the enclosing volcanic rocks. Furthermore, the rectilinear fracture network (Fig. 3.14), which could be of a cooling-shrinkage origin and which controls epidote alteration of plagioclase, could have provided a ubiquitous system for circulation of a H^+-bearing phase. From these major fractures diffusion of hydrogen, probably in a hydrous fluid, occurred along grain boundaries and through minor fractures, resulting in pervasive hydration of pyroxene.

On the other hand, the gabbro-anorthosite intrusion must have undergone some metamorphism during the emplacement of granitoid intrusions, which are thought to have recrystallized adjacent volcanic rocks to the amphibolite facies (Henderson et al., 1987). The igneous plagioclase of the intrusion was relatively stable during this event because of its calcic composition and the absence of a phase like alkali feldspar suitable for Na-Ca exchange during metamorphic re-equilibration. Some of the hornblende rimming coarse oikocrystic amphibole may have grown during this event, and may have been involved in limited Ca-for-Na exchange with plagioclase, but the surviving plagioclase was little-affected and the effects of the amphibolite facies metamorphism appear to have been relatively slight. Nonetheless, the magnitude of its effect is difficult to evaluate. A relatively static contact metamorphic event might have significantly altered the mineralogy of the gabbro-anorthosite intrusion without deforming it. However, a discrepancy remains between the deformed, finely recrystallized and foliated volcanic rocks and the relatively well preserved intrusion. The former may have been deformed and

metamorphosed before intrusion of the gabbro-anorthosite occurred, but direct evidence of an early tectonic event is not observed.

A completely deuteric origin is unlikely, since the parental mafic magma is unlikely to have been water-rich, and there is no evidence of high-temperature hydrous phases. Evidence of igneous hornblende is not observed, nor are myrmekitic textures attributed by Dymek and Schiffries (1987) to reaction of plagioclase phenocrysts with a hydrous magmatic fluid in the St-Urbain anorthosite complex. If the alteration was deuteric the parental liquid must have been anomalously water-rich, and early high-temperature hornblende phenocrysts or reaction rims must have been destroyed or strongly modified by subsequent lower-temperature reactions.

If, on the other hand, the hydrating phase was a country rock fluid, it was of non-marine origin, despite the fact that the intrusion has been emplaced in volcanic rocks which include pillowed flows. The fluid was low in Na, as indicated by the very Na-poor mineral assemblage, and was poor in CO_2, since carbonate is rare in the intrusion. The fact that plagioclase is calcic, with nearly pristine igneous compositions even where grains are partially overgrown by amphibole, indicates that Ca-Na exchange was limited in extent, presumably because the fluid was Ca-rich. Lagache (1984, p. 272) indicates that, for example, at 500°C and 3 kb calcic plagioclase is stable with fluids containing high Ca/Na ratios, and that An contents such as are observed in the Clinton-Colden intrusion are compatible with fluid Ca/Na values greater than one. Much of the Ca in the hydrating phase may have been liberated during hydration of clinopyroxene to amphibole. However, the origin of the hydrating phase

(fluid or otherwise) remains enigmatic.

4.5 Fine amphibole overgrowing coarse amphibole

About 10% of the interstitial ferromagnesian minerals of the intrusion consist of fine (<0.5 mm) grains which overgrow the oikocrystic amphibole grains. These grains are optically similar to the actinolite-hornblende amphiboles discussed above, and consist of calcic amphibole. In some cases they almost completely replace the host grains, although it is difficult to distinguish large-scale replacement of oikocrystic amphibole from partial topotactic and partial fine-grained replacement of uralite by amphibole.

Six microprobe analyses of fine secondary amphibole from clots of such material in three samples are given in Table 4.2 and are plotted in Figure 4.2. These data fall into two groups, in the fields of actinolitic hornblende and tschermakitic hornblende. The former may represent non-topotactic replacement of uralite distal to the Al source, while the latter represent either non-topotactic uralite replacement adjacent to the Al source, or later recrystallization of margins of coarse amphibole oikocrysts. This gap could also reflect the controversial Ca-amphibole miscibility gap, sluggishness of prograde reactions in the amphiboles, or simply reflect a paucity of data.

4.6 Amphiboles of the intrusion and the Ca-amphibole miscibility gap

Compilations of large numbers of amphibole analyses from the geological literature reveal a significant compositional gap between actinolite and hornblende (e.g. Grapes and Graham, 1978). This

compositional gap could represent a miscibility gap (e.g. Miyashiro, 1973), but exsolution textures indicative of immiscibility are extremely rare (Mongkoltip and Ashworth, 1986). Although many workers postulate a miscibility gap does exist in calcic amphiboles under certain conditions (e.g. Oba, 1980; Arai and Hirai, 1985), a more generally accepted explanation of the observed compositional gap is that it represents kinetic "sluggishness" of amphibole-producing reactions at the greenschist-amphibolite facies boundary, resulting in the sudden appearance of aluminous amphiboles rather than the progressive development of succesively more Al-rich ones (Grapes and Graham, 1978).

The amphiboles of the Clinton-Colden intrusion show no compositional gap (Fig. 4.2). Compositions of points analysed even within single grains range from actinolite to hornblende (Fig. 4.8a). No internal grain boundaries or sharp compositional discontinuities suggestive of exsolution in the amphiboles were observed.

Although exsolution may have occurred on a scale too fine to observe by optical or microprobe methods (Hawthorne, 1981), the regular compositional gradients observed in amphiboles of the intrusion are incompatible with the presence of discrete Al-rich and Al-poor domains. Al was apparently free to move through the amphibole structure from one unit cell to another. Otherwise, optically discrete hornblende rims might more reasonably have developed on actinolite cores, the hornblende rims expanding as the reaction progressed, preserving the two-phase condition. While it is clear that the amphibole-modifying process was arrested before the coarse amphibole grains equilibrated, the presence of the regular compositional gradients and the absence of

exsolution lamellae within the amphibole grains indicate that amphibole compositions ranging from actinolite to tschermakitic hornblende were stable during the cooling of the Clinton-Colden intrusion.

CHAPTER 5

GEOCHEMISTRY

5.1 Introduction

Twenty four whole-rock samples of the Clinton-Colden gabbro-anorthosite intrusion and twenty-three samples of volcanic rocks (this study and Wodicka, 1987) of the area were analysed for major elements and trace elements. Eight gabbro-anorthosite and eight volcanic rocks were analysed for the rare-earth elements (REE) and additional trace elements (Table 5.1).

Meta-volcanic rocks were sampled and analysed in order to test the hypothesis that the gabbro-anorthosite intrusion was consanguinous with the contemporaneous volcanic pile which it intrudes (see Chapter 2). Due to alteration of the rocks, paucity of data on the volcanic rocks, and the lack of layering, chilled margins or other spatio-temporal organization in the intrusion, modelling of crystal fractionation did not yield useful results. Nonetheless, the chemical data for the volcanic rocks of the southern Clinton-Colden greenstone belt are presented below, with a brief discussion.

5.2 Geochemistry of the Clinton-Colden gabbro-anorthosite intrusion

Chemical compositions of samples of the intrusion are presented in Appendix 2, major element data are presented in Figure 5.1, and REE data are presented in Figure 5.2. Because rocks of the intrusion are dominated by plagioclase, variation in whole-rock chemistry is essentially a function of variation in plagioclase content. Because of the absence of layering or other regularity it has not been possible to

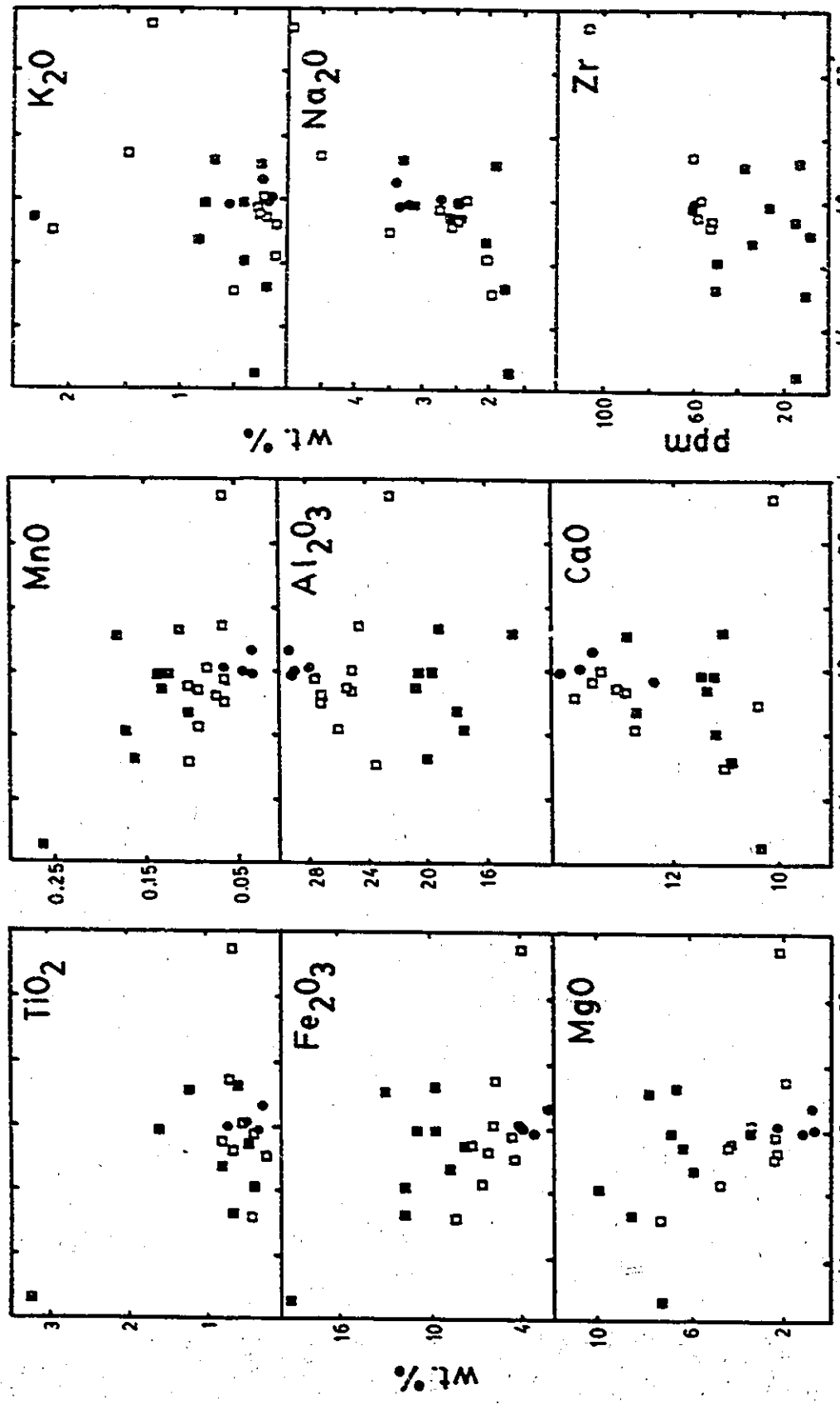

Fig. 5.1: Distributions of major oxides and Zr versus wt. % SiO_2 for rocks of the Clinton-Colden gabbro-anorthosite intrusion. Filled square=gabbro (<50% plagioclase); open square=leucogabbro (50-90% plagioclase); filled circle=anorthosite (>90% plagioclase).

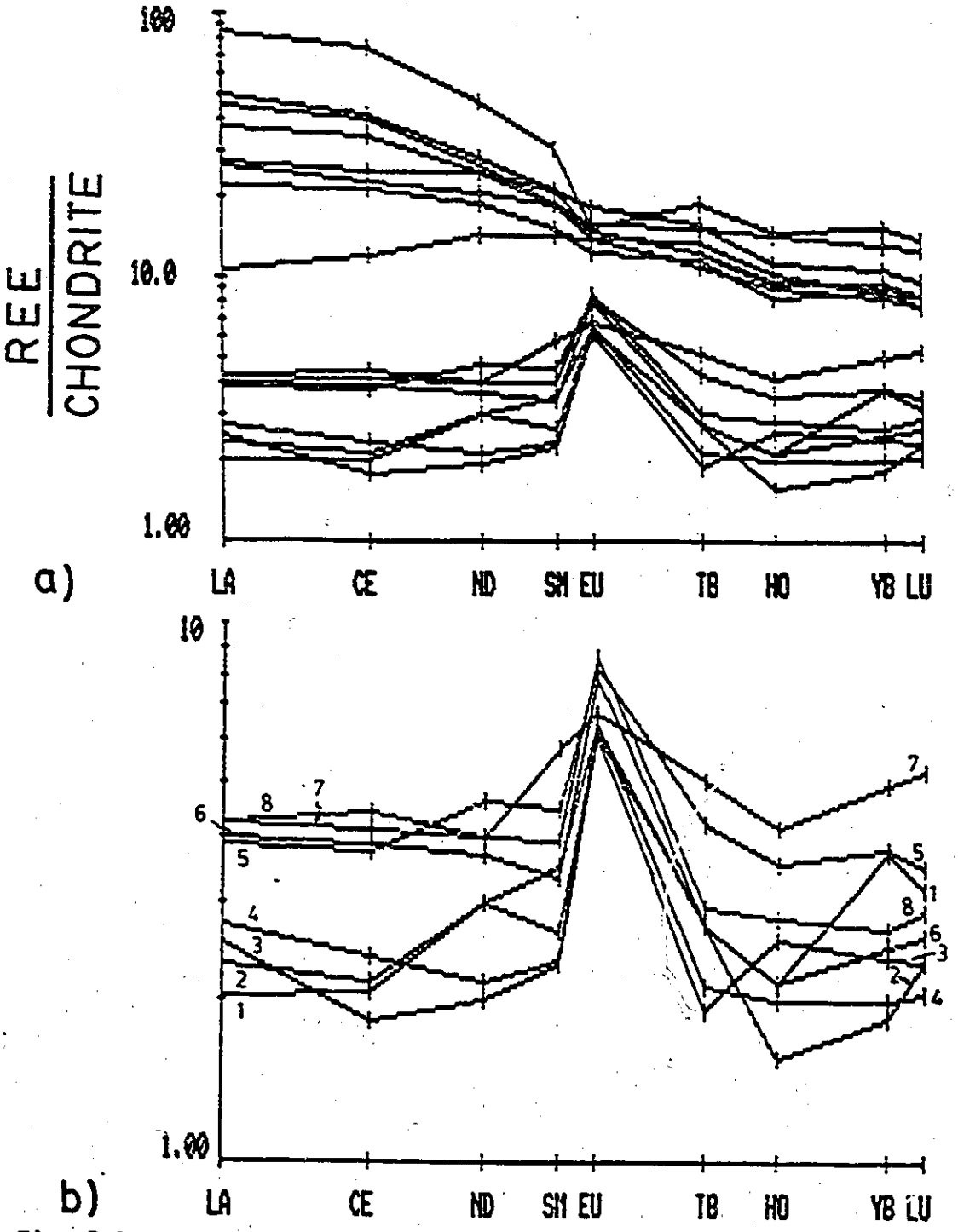

Fig. 5.2: REE spectra for rocks of the Clinton-Colden gabbro-anorthosite intrusion and volcanic rocks of the area. a) all spectra, volcanic rocks clustered between 10 and 100X chondrite, gabbro-anorthosite samples clustered at approximately 3X chondrite. b) spectra for gabbro-anorthosite samples. Note well-developed positive Eu anomaly and flat overall trends. Analyses given in Appendix 2, 1=G-73; 2=G-87; 3=G-72; 4=G-92; 5=G-85; 6=G-71; 7=G-25; 8=G-95. (cont'd. next page)

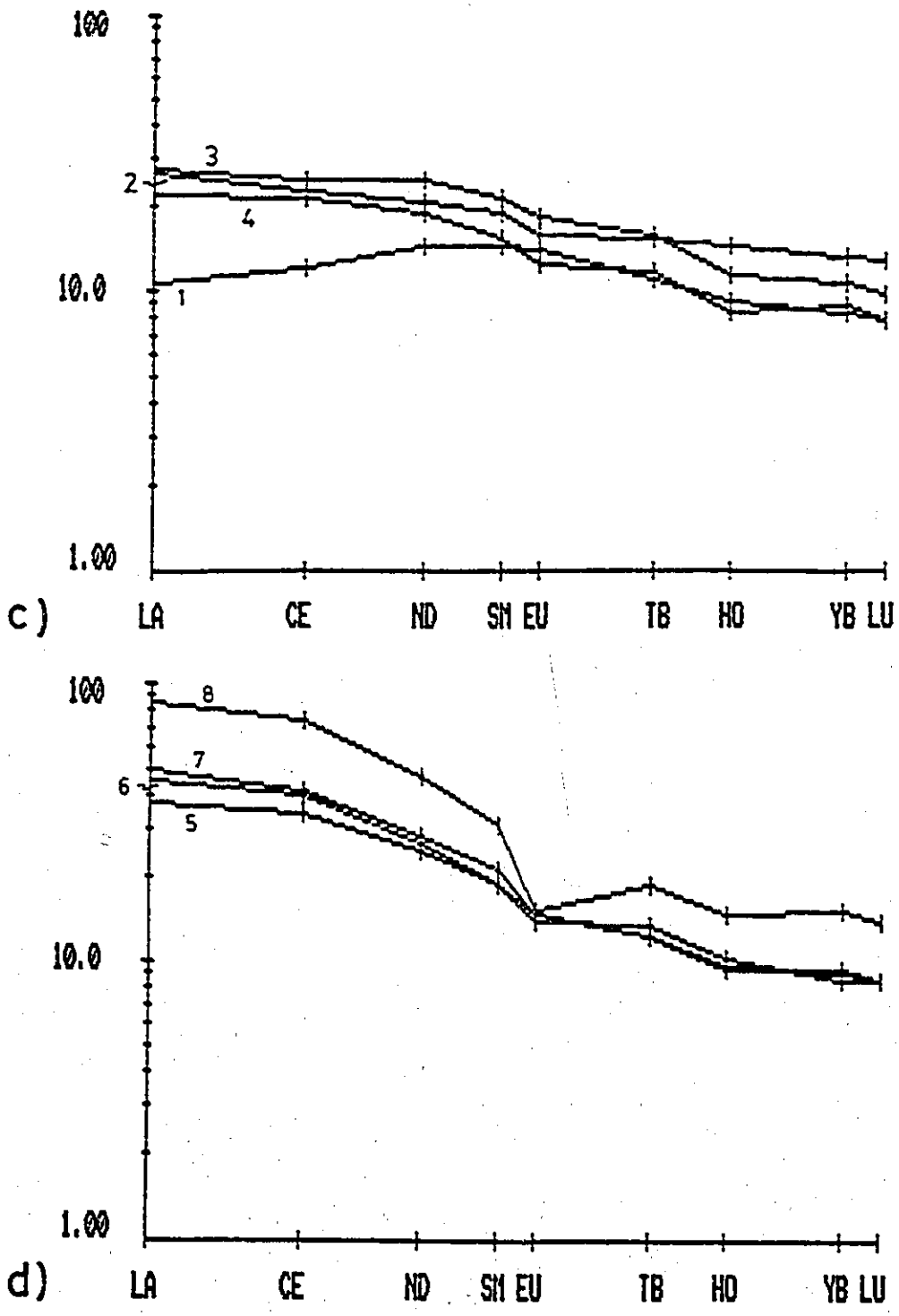

Fig. 5.2 (cont'd.) c) spectra for mafic volcanic rocks. Numbers 1 to 8 in Figures 5.2b and 5.2c correlate with increasing SiO_2. Note LREE-enriched trends. Analyses given in Appendix 2, 1=N-38; 2=N-27; 3=N-22; 4=N-25. d) Spectra for intermediate and felsic volcanic rocks. Note evolution of negative Eu anomaly with decreasing SiO_2. Analyses given in Appendix 2, 5=N-37; 6=N-43; 7=N-4A; 8=N-26.

study the crystallization history of the intrusion. Instead, it is treated as a single petrogenetic unit.

Variation in the concentration of elements relative to SiO_2 is irregular, depending upon the relative abundance of plagioclase grains in samples, a function of the physical processes occurring during emplacement of the magma. For most elements samples of anorthosite tend to cluster at the high or low end of the distribution, reflecting the concentration of each element in plagioclase. Samples of gabbro lie at the opposite extreme, while leucogabbroic samples occur between the two. This spatial distinction is most apparent in the case of Al_2O_3, the concentration of which is greatest in plagioclase. Mixing of plagioclase and (predominantly) amphibole has resulted in the variation in alumina content observed in Figure 5.1. Other elements vary in like manner. In the cases of $Fe_2O_{3(T)}$, MnO, and TiO_2, elements essentially absent from plagioclase, the whole-rock concentrations can be directly attributed to varying proportions of interstitial magma. The concentration of SiO_2 in anorthosite is approximately that of the mean plagioclase of the intrusion (cf. Table 3.1), with little variation. The SiO_2 content of more mafic samples varies widely, essentially reflecting the much greater variation in SiO_2 content in the amphiboles of the intrusion (cf. Table 4.2).

Compared to most other Archean anorthositic intrusive bodies, which have $Mg/Mg + Fe^{+2} > 0.6$, rocks of the Clinton-Colden intrusion have very low $Mg/Mg + Fe^{+2}$, averaging 0.348 (assuming $Fe^{+2}/Fe^{+2} + Fe^{+3} = 0.9$, cf. Simmons et al., 1980). The concentration of TiO_2 in gabbroic phases ranges from 0.36 to 3.23 weight percent, and in general is considerably greater than in similar rocks in the Tessiuyakh,

Piskenaesset, Shawmere and Bad Vermilion Lake complexes. The TiO_2 content of the rocks falls within the range reported by Simmons and Hanson (1978) for a number of Proterozoic anorthosite massifs of the Grenville province, and is reflected in the abundance of ilmenite and rutile in the rocks.

The intrusion has low total REE with positive Eu anomalies, as do Proterozoic massif anorthosites (Simmons and Hanson, 1978) and other Archean anorthosite occurrences (e.g. Simmons et al., 1980). This is a result of the accumulation of plagioclase, with low partition coefficients for REE other than Eu, during fractionation of a voluminous parental magma. The flat trends of the REE spectra of the intrusion probably resulted from a combination of LREE-enriched plagioclase trends and HREE-enriched clinopyroxene trends, the latter being preserved during subsequent recrystallization of clinopyroxene to form amphibole.

Like the Archean Shawmere anorthosite complex (Simmons et al., 1980), the Clinton-Colden intrusion could represent a plagioclase cumulate produced during fractionation of a magma parental to tholeiitic volcanic rocks. Indirect evidence is found in the low REE content of the tholeiitic volcanic rocks which it intrudes, and with which it is approximately coeval, being older than a rhyolite in the same greenstone belt. The chemical evidence of derivation of the mafic to felsic volcanic sequence by fractionation (see below), in particular the progressive development of a negative Eu anomaly, are compatible with the evolution of the gabbro-anorthosite during the fractionation process, as is the presence of abundant coarsely plagioclase-phyric sills within the volcanic sequence.

5.3 Geochemistry of the meta-volcanic rocks

Homogeneous, relatively non-carbonatized, non-silicified and non-mineralized rocks were selected for chemical analysis. However, compositional changes have inevitably occurred during pervasive recrystallization. It is possible to infer something about these changes from the chemical data. Relatively immobile elements such as Ti and Al show smooth trends in variation diagrams, while more mobile elements such as Na and K have highly irregular distributions. For example, samples N-4C and N-23B, which have nearly identical immobile major and trace element contents have very different K_2O contents, suggestive of mobilization of K (Fig. 5.3). Immobile elements are therefore used for the purpose of discussion of the geochemistry of the volcanic rocks. Lack of stratigraphic control made it impossible to determine whether the variation in volcanic rock types was cyclical. The volcanic rocks of the study area are therefore treated as a single petrogenetic package. Alteration and the relatively small sample population rendered an investigation of tectonic setting using empirical diagrams impossible.

Wodicka (1987) demonstrated that the volcanic rocks of the area are subalkaline and are tholeiitic (mafic flows) to calc-alkaline (intermediate and felsic flows), following the classification of Irvine and Baragar (1971). Her major element data are included in Figure 5.3 and in Appendix 2.

Wodicka (1987) concluded that the volcanic rocks of the area were compositionally bimodal, with a relative absence of intermediate compositions. However, the author's field observations and laboratory

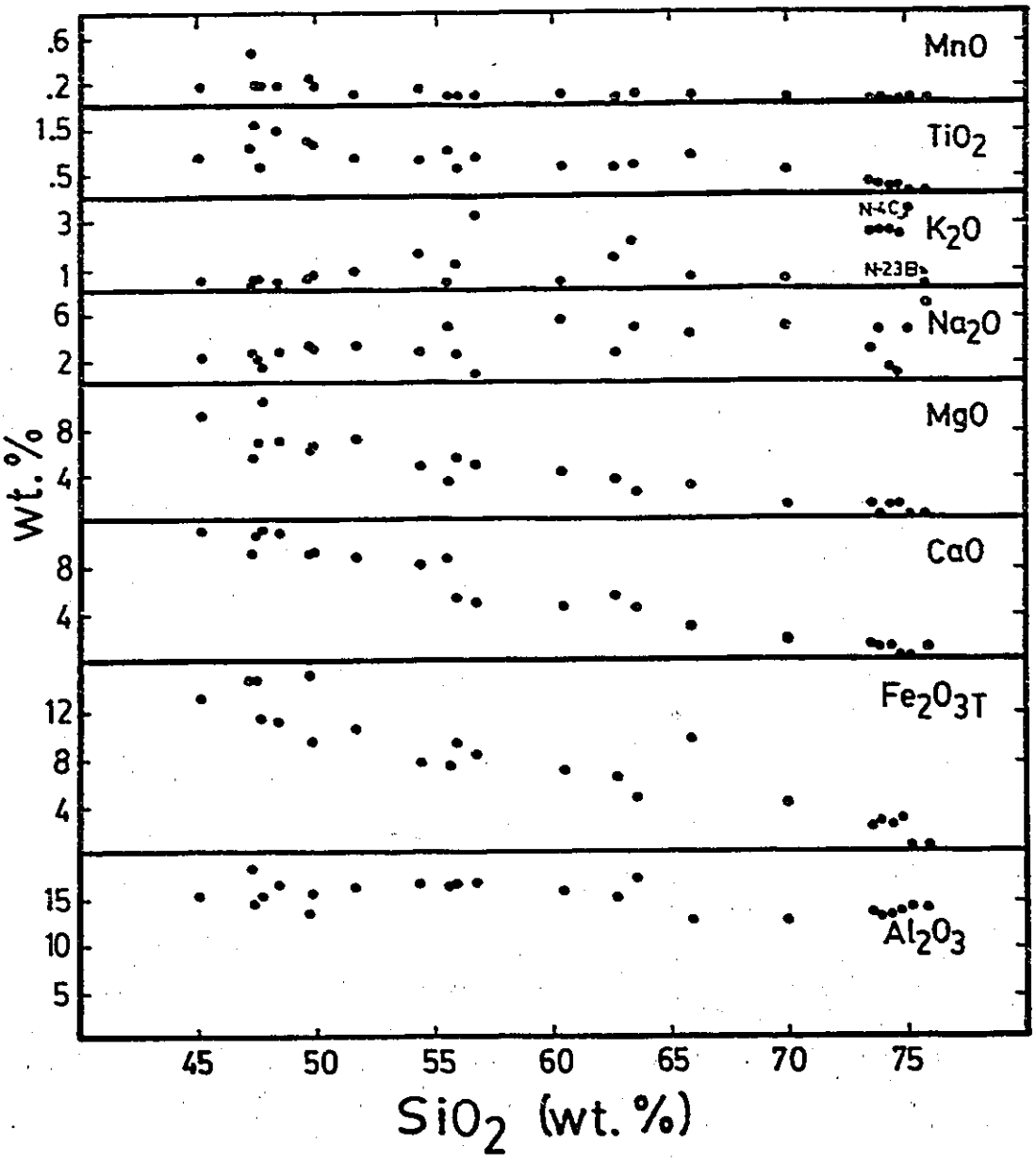

Fig. 5.3: Harker diagrams for meta-volcanic rocks of the southern Clinton-Colden greenstone belt. a) major elements; note variation in K_2O and Na_2O contents of samples N-4C and N-23B, which are otherwise similar in composition. (cont'd. next page)

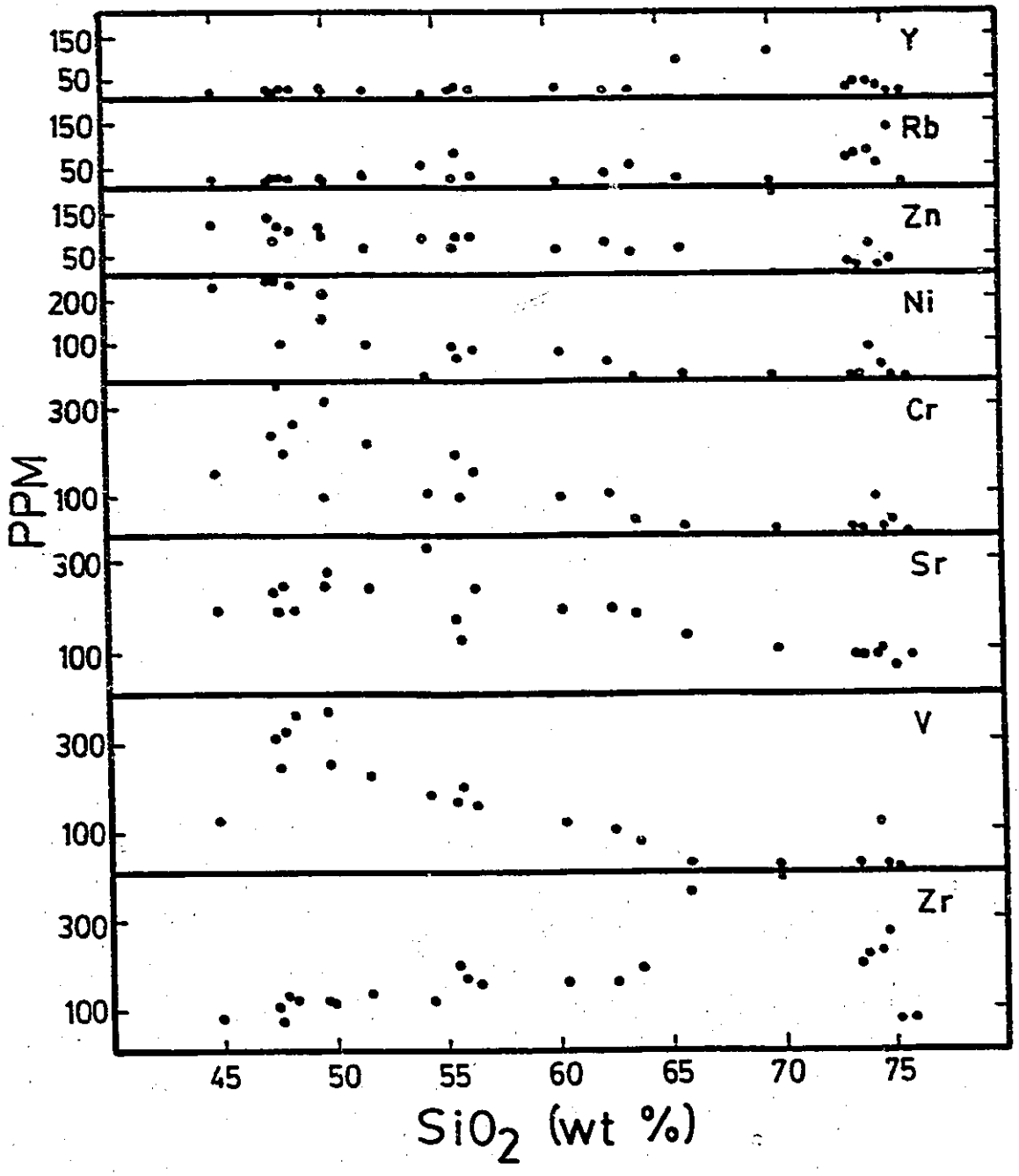

Fig. 5.3 (cont'd.): b) trace elements.

data indicate that the volcanic rocks consist predominantly of mafic volcanic rock, smaller quantities of intermediate volcanic rock, and still less felsic rock. Therefore the volcanic rocks do not seem to have a volumetric bimodal distribution. Geochemical indicators of bimodality are also inconclusive. Wodicka (1987) suggested bimodality for the volcanic rocks of the southern part of the greenstone belt as a result of 13 analyses of rocks whose composition ranged from basalt to rhyolite. She found no samples containing between 64 and 73% SiO_2, and similar gaps between mafic and felsic populations for some trace elements. Ten additional samples spanning the same compositional range (based on colour index) yielded a less pronounced gap. Nonetheless, SiO_2 variation diagrams do indicate a statistical minimum within the range of the silica gap of Wodicka (1987). The gap corresponds to a paucity of samples in the range of dacite to rhyolite rather than andesitic (the usual Daly gap (Thurston and Fryer, 1983)). This may simply reflect the small number of samples available for analysis. In any case, SiO_2 concentrations provide little evidence for or against bimodality of the volcanic sequence.

The question of bimodality may be examined from a petrogenetic, rather than purely compositional, point of view. The tectonic implications of bimodality in a volcanic sequence derive from the suggestion that felsic magmas of a bimodal suite come from a sialic source (e.g. Thurston and Fryer, 1983) rather than from fractionation of a mafic parent to produce a complete sequence. Geochemical evidence compatible with fractionation of a parental liquid resembling the mafic volcanic rocks to yield successively more silica-rich liquids represented by intermediate and felsic volcanic rocks may be observed

in variation diagrams and in REE trends (Fig. 5.2). In general, trends from mafic to felsic members of the volcanic series are smooth and no significant sharp breaks are present which could be attributed to derivation from different parental magmas. Scatter in the distribution of Rb most likely reflects the mobility of that element. Anomalously high concentrations of Y and Zr in the samples having 66 and 70% SiO_2 may be due to alteration (they have very low concentrations of K_2O and Rb), or accumulation of a mineral such as zircon (Deer et al., 1966). Such anomalies are expected given the phyric nature of the felsic volcanic rocks, and effects of metamorphism. The observed pattern of trace element distribution supports the concept of derivation by fractionation from a single parental magma perhaps resembling the mafic volcanic rocks sampled.

Evidence from REE trends is more compelling. As SiO_2 increases total REE increase, LREE increase more rapidly than HREE, and a negative Eu anomaly appears. The similarity of total HREE contents and their slopes in rocks ranging in composition from 48 to 75% SiO_2 is striking, as is the progressive and consistent development of the Eu anomaly and the smooth increase in LREE content. This pattern is consistent with the derivation of the felsic volcanic magma by fractionation of a mafic parent similar to the mafic volcanic rocks. Fractionation of plagioclase (accounting for the development of the Eu anomaly) and a ferromagnesian phase such as clinopyroxene or hornblende (accounting for the increase in LREE relative to HREE) could account for this as well (Green and Pearson, 1985; Lemarchand et al., 1987). Such a process could have yielded a body having a magmatic composition like that of the Clinton-Colden gabbro-anorthosite intrusion. However,

attempts to model fractionation processes which could link the intrusion to the volcanic pile it intrudes have proven futile, due to the altered state of the rocks, lack of data on the volcanic rocks, and lack of layering in the intrusion.

The total REE content of the volcanic rocks is low, lower for instance than the concentrations expected from partial melting of sialic sources (e.g. Cullers and Graf, 1984a,b). REE distributions in the volcanic rocks suggest that the range of volcanic compositions in the area developed by fractionation of mafic magmas from a common source.

Some other aspects of the geochemistry of meta-volcanic rocks from the area, including normative composition, are discussed by Wodicka (1987).

CHAPTER 6

DISCUSSION

6.1 The nature of the intrusion and its mode of emplacement

The Clinton-Colden gabbro-anorthosite intrusion is an altered plagioclase-rich mafic body which consists largely of magmatic plagioclase grains enclosed in coarse amphibole grains which have pseudomorphically replaced clinopyroxene oikocrysts. The intrusion was altered by hydration of clinopyroxene to produce amphibole, accompanied by some alteration of plagioclase to fine epidote. Unaltered plagioclase retains magmatic features, including abundant Carlsbad twinning. All grains are calcic. Their composition varies between grains, and there is no indication of metamorphic compositional equilibration even at hand sample scale. There is no polygonization, subgrain development, granulation, growth of plagioclase over other minerals, or other evidence of recrystallization of plagioclase. In other words, unaltered plagioclase retains its original morphology, and, insofar as can be detected, its original composition. The major alteration was restricted to areas and minerals susceptible to hydration by volatiles which circulated predominantly in the ubiquitous fracture system described.

The reason for the crystallization of very coarse pyroxene oikocrysts is not clear. Mathison (1987) documents the occurrence of coarse clinopyroxene oikocrysts enclosing plagioclase in coarse grained layered gabbroic intrusions in Australia, but in those cases enclosed plagioclase crystals are elongate and skeletal, providing additional evidence of supercooling. In those cases chamber replenishment is

believed to have resulted in supercooling of injected magma. The Clinton-Colden intrusion is not layered, shows no sign of replenishment, and contains coarse poikilitic amphibole pseudomorphs of clinopyroxene throughout. Supercooling mechanisms which might apply in this case, such as a lack of seed crystals (unlikely since plagioclase, along with possible olivine or other phases, was already on the liquidus) or reduction of temperature due to exsolution of a vapour phase, are difficult to prove. The last might have promoted coarse grain growth by promoting diffusion in the melt. It might also have been expected, however, to result in the appearance of magmatic hornblende, which is lacking.

Interstitial material included a magmatic Fe-Ti oxide phase. Other phases may have preceded plagioclase on the liquidus, but they have been obscured by reaction with the magma or by postmagmatic alteration.

The intrusion as presently exposed is a portion of a larger mafic system. No parental magma could have fractionated >50% plagioclase phenocrysts, even if it were Al-rich. Furthermore, the plagioclase of the intrusion is virtually unzoned, indicating that it was at equilibrium with a large volume of magma during most of its crystallization history.

There is no evidence that the body is extensive in the subsurface or that related bodies, including a larger parental magma chamber, lie there. No gravity anomaly (Earth Physics Branch, 1969) is centred on the intrusion, and the magnetic anomaly (Geological Survey of Canada, 1968) associated with it is minor. The available evidence indicates that the intrusion represents a single intrusive pulse of

plagioclase-rich crystal mush, detached from the bulk of the parental fractionation chamber.

The remarkably heterogeneous distribution of rock types and the complete lack of layering seen in the body are unusual for such a mafic intrusion. This is particularly true of one which contains abundant coarse sub-equidimensional plagioclase phenocrysts suggestive of slow growth (cf. Lofgren, 1971), slow enough to have permitted settling or flotation of phenocrysts in the non-viscous mafic magma, or to have resulted in in-situ development of cyclical or other layering (e.g. Huppert and Sparks, 1984). The intrusion may therefore be a remnant of a dyke or plug-like body of disrupted crystal-rich magma consisting largely of plagioclase phenocrysts originally grown in adcumulate fashion in a larger parental magma chamber. Minor interstitial late-stage fractionation products are represented only by rare zircon. Rapid diffusion of residual liquid, perhaps to an unexposed part of the system, is indicated by the abundance of oikocrystic textures, and may account for the lack of late-stage interstitial material such as granophyre (Wager et al., 1960).

Disruptive emplacement is indicated both by heterogeneous and nebulous texture and by variation in plagioclase composition suggestive of irregular mixing of the mush. For instance, although individual plagioclase grains are homogeneous and nearly unzoned (Table 3.1), grains within samples can vary somewhat in composition, in some cases by more than An_{10}. This is suggestive of mixing of previously grown phenocrysts during transport and emplacement. It may indicate disruption of earlier compositional layering developed in a parental magma.

The magma was transported from its parental magma chamber, and emplaced into the rocks of the volcanic belt. Experimental work by Campbell et al. (1978) indicates that plagioclase of composition An_{85} may be expected to float in liquids parental to mafic intrusions such as Skaergaard. The Clinton-Colden magma may have separated from its parental magma chamber as a buoyant plagioclase-rich upper cumulate phase, and been emplaced into the overlying crust. Lack of internal layering may have been caused by flow turbulence due to the relatively high viscosity of the crystal-rich mush (Marsh, 1988). The complete absence of flow-differentiation, flow-sorting or textures indicative of multiple pulses of magma (Platten and Watterson, 1987) indicates that the body was emplaced in a single event. The mush might conceivably have developed during transport of Al-rich basaltic magma from the crust-mantle interface as envisioned by Emslie (1978) in the case of Proterozoic massif anorthosite. However, the intrusion has a number of characteristics, including its small size, more calcic plagioclase, and its Archean age, which clearly distinguish it from Proterozoic massif anorthosites. Given its small size and high phenocryst content (with attendant elevated viscosity), it is unlikely that it has been transported a great distance from the site of fractionation.

Archean anorthosites usually consist of coarse equidimensional calcic (An_{80-95}) plagioclase phenocrysts in a fine-grained matrix (Ashwal et al., 1983). They generally have $Mg/Mg + Fe^{+2} > 0.6$, and are usually older than 3.0 Ga (Simmons et al., 1980). They are often associated with mafic volcanic flows containing plagioclase phenocrysts similar to those in the anorthosite (Ashwal et al., 1983). Several ideas have been advanced concerning their mode of origin. It has been

suggested that they represent segments of Archean oceanic crust, cumulate complements to enclosing gneisses, and cumulates genetically related to the volcanic rocks of the greenstone belts they often intrude (see references in Weaver et al., 1981). The Clinton-Colden intrusion is like other Archean anorthositic complexes in containing coarse calcic plagiocase, and in its relatively small size. It is also associated with plagioclase phenocryst-bearing mafic lavas with which it could be cogenetic. Unlike other Archean occurrences, however, it is unlayered, has no associated ultramafic rocks, and has a very low $Mg/Mg + Fe^{+2}$ ratio.

6.2 Physical conditions during emplacement and cooling of the intrusion

Mineral assemblages in the Clinton-Colden intrusion bear a striking resemblance to those of the East Bull Lake anorthosite-gabbro intrusion (Kamineni, 1986). Calcic plagioclase+actinolite+epidote assemblages, found elsewhere to indicate a temperature of about 600°C (Hietanen, 1974), and hydrothermal actinolite, formed at temperatures above 300°C (Mottl and Holland, 1978), indicate for both the East Bull Lake and the Clinton-Colden intrusions a postmagmatic re-equilibration temperature range of 400° to 600°C, if in fact the mineralogy of the intrusion is largely a product of cooling-related alteration. Although aluminous amphibole was stable at least in high Al parts of the system (e.g. overgrowing plagioclase), it co-existed with chlorite and epidote. Furthermore, the low Ti content of the amphiboles, averaging about 0.05 per unit formula even in most Ti-rich hornblende, indicates that they formed within the greenschist-amphibolite transition facies of Raase (1974). Therefore the hydrothermal alteration assemblage stabilized

under conditions transitional between greenschist and amphibolite facies, providing an upper limit on the temperature in the country rocks.

The pressure during intrusion and subsequent alteration must have been compatible with the greenschist-amphibolite transition described above. The very low Na_{M4} values (Appendix 1) in the amphiboles is suggestive of low pressure (Brown, 1977), although this may be due in part to a general deficiency in Na. Other evidence suggests somewhat higher pressure. Some amphiboles in the Clinton-Colden intrusion are very aluminous, containing more than 16% Al_2O_3, with high Al^{VI}/Al^{IV} ratios. Leake (1971) found that maximum Al^{VI} occurs in amphiboles from high pressure environments. The amphiboles of the intrusion fall along the boundary between high and low pressure fields in Fleet and Barnett's (1978) Al^{IV}/Al^{VI} diagram (Fig. 6.1), equivalent to approximately 5 kb pressure (Raase, 1974). The low Ti content of the amphiboles also indicates a medium or high pressure origin, based upon the work of Hynes (1982). There have been suggestions that high pressure reduces the miscibility gap in calcic amphiboles (Arai and Hirai, 1985; Pe-Piper, 1988), and no gap whatsoever occurs in the amphiboles of the Clinton-Colden intrusion, although this may be due to the arrested diffusion-controlled nature of the amphibole-modifying process, rather than an external phenomenon such as pressure. In any case, amphibole chemistry indicates that pressure during the deuteric alteration of the intrusion was somewhat elevated. However, since the pressure cannot have exceeded values compatible with transitional greenschist-amphibolite facies mineral assemblages, it is suggested that the magma intruded rocks lying in the upper pressure range of the

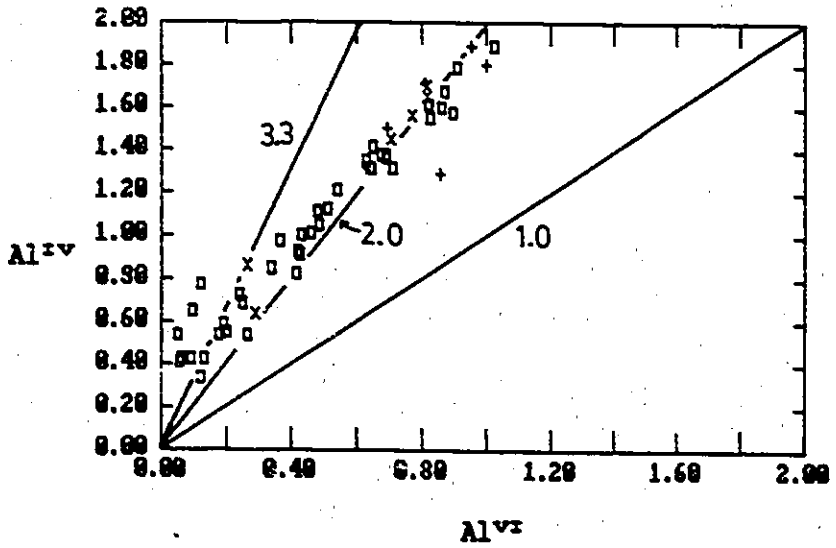

Fig. 6.1: Calcic amphiboles of the Clinton-Colden gabbro-anorthosite plotted on the Al^{IV} versus Al^{VI} diagram of Fleet and Barnett (1978). Unaltered igneous field defined by $Al^{IV}/Al^{VI}>3.3$; line of slope 2 approximates 5 kb boundary; low pressure metamorphic field defined by $Al^{IV}/Al^{VI}<2.0$. Rectangle=amphibole oikocyrst; +=fine amphibole overgrowing plagioclase; x=fine amphibole overgrowing amphibole oikocryst.

facies transition, perhaps between 5 and 9 kb, at a depth of 12 to 25 km.

6.4 Geochronological significance of the Clinton-Colden gabbro-anorthosite intrusion

The U-Pb zircon date of 2686+/-3 Ma obtained for the intrusion demonstrates that volcanism in the area had begun at least 11 million years before the rhyolite from the central part of the belt crystallized at 2671+2/-4 Ma. The former date falls between the older (2698-2687) and younger (2675-2663) of the two periods of volcanic activity in the east-central Slave province (Mortensen et al., 1988), while the latter falls within the younger episode. The date obtained for the intrusion provides a minimum age for the onset of volcanism in the Clinton-Colden belt which falls very near to the older of Mortensen et al.'s (1988) group of ages. It is thus possible that volcanism in the Clinton-Colden volcanic belt spanned both periods of volcanic activity, or was reactivated during the latter. Whereas the date obtained from the rhyolite suggested that the Clinton-Colden belt was anomalously young relative to other belts in the eastern Slave province (Mortensen et al., 1988), the early date obtained from the intrusion demonstrates that volcanism was occurring in the Clinton-Colden volcanic belt at approximately the same time as in other belts in the area.

6.5 Summary

At approximately 2.68 Ga the Clinton-Colden gabbro-anorthosite intrusion was emplaced at moderate depths into volcanic rocks of the Clinton-Colden greenstone belt, before volcanism had ceased in the

area. The crystal-rich magma which formed the intrusion was detached from a large body of Al-rich basaltic parental magma capable of crystallizing and concentrating a considerable volume of plagioclase. Following emplacement, very coarse clinopyroxene, with or without other ferromagnesian phases, crystallized, poikilitically enclosing previously formed plagioclase grains. Plagioclase appears to have left the liquidus for reasons which are not clear, although they might include an increase in P_{H_2O}.

During cooling of the body, circulation of non-marine fluids resulted in pervasive replacement of clinopyroxene by actinolite. Actinolite was variably altered to more hornblendic compositions, an effect primarily controlled by the diffusivity of Al from sites of plagioclase overgrowth by tschermakitic amphibole.

After crystallization and cooling of the body, minor prograde metamorphism occurred, probably associated with late granitoid intrusion. One or more metamorphic events, probably resulting during intrusion of granitoid bodies to the east and west, produced biotite in Thelon-trend shear zones cutting volcanic rocks, and within the intrusion, led to minor replacement of chlorite by hornblende.

Deformation of the intrusion, restricted to thin, discrete anastomosing shear zones, is related to activity along the Thelon tectonic zone. Evidence exists that movement along the zone was protracted, producing shear zones and fabrics which both pre- and post-date possible 2.4 Ga Mackay dykes.

REFERENCES

Abbey, S., 1983: Studies in "standard samples" of silicate rocks and minerals 1969-1982; Geol. Surv. Can. Paper 83-15, 114p.

Allen, J.C. and Boettcher, A.C., 1978: Amphiboles in andesite and basalt: II. Stability as a function of P-T-H_2O-O_2; Amer. Mineral. 63, 1074-1087.

Arai, S. and Hirai, H, 1985: Compositional variation of calcic amphiboles in Mineoka metabasites, central Japan, and its bearing on the actinolite-hornblende miscibility relationship; Lithos 18, 187-199.

Ashwal, L.D., Morrison, D.A., Phinney, W.C. and Wood, J., 1983: Origin of Archean anorthosites: Evidence from the Bad Vermilion Lake anorthosite complex, Ontario; Contrib. Mineral. Petrol. 82, 259-273.

Austreheim, H. and Robins, B., 1981: Reactions involving hydration of orthopyroxene in anorthosite-gabbro; Lithos 14, 275-281.

Ayre, J.A., Macfie, R.I. and Buck, S., 1987: Geology of the Chisholm Island Area, Lake of the Woods, District of Kenora; Ont. Geol. Surv. Misc. Pub. 137, 28-38.

Brown, E.H., 1977: The crossite content of Ca-amphibole as a guide to pressure of metamorphism; J. Petrology 18, 53-72.

Buseck, P.R, Nord, G.L. Jr. and Veblen, D.R., 1980: Subsolidus phenomena in pyroxenes; in Pyroxenes, C.T. Prewitt ed., Mineral. Soc. Am. Rev. Mineral. 7, 117-211.

Campbell, I.H., Roeder, P.L. and Dixon, J.M., 1978: Plagioclase buoyancy in basaltic liquids as determined with a centrifuge furnace; Contrib. Mineral. Petrology 67, 369-377.

Chivas, A.R., 1981: Geochemical evidence for magmatic fluids in porphyry copper mineralization. Part I. Mafic silicates from the Koluala igneous complex; Contrib. Mineral. Petrology 78, 389-403.

Cullers, R.L. and Graf, J.L., 1984a: Rare earth elements in igneous rocks of the continental crust: Basic and ultrabasic rocks; in Rare Earth Geochemistry, P. Henderson ed., Elsevier, Amsterdam, 237-274.

Cullers, R.L. and Graf, J.L., 1984b: Rare earth elements in igneous rocks of the continental crust: Intermediate and silicic rocks - ore petrogenesis; in Rare Earth Geochemistry, P. Henderson ed., Elsevier, Amsterdam, 275-316.

Deer, W.A., Howie, R.A. and Zussman, J., 1966: *An Introduction to the Rock Forming Minerals*, Longman Group Limited, Harlow, 528p.

Drury, S.A., 1977: Structures induced by granite diapirs in the Archaean greenstone belt at Yellowknife, Canada: Implications for

Archaean geotectonics; J. Geol. 85, 345-358.

Dymek, R.F. and Schiffries, C. M., 1987: Calcic myrmekite: Possible evidence for the involvement of water during the evolution of andesine anorthosite from St-Urbain, Quebec; Can. Mineral. 25, 291-319.

Earth Physics Branch, 1969: Artillery Lake, Northwest Territories; Gravity Map Series No. 89.

Easton, R.M., 1985: The nature and significance of pre-Yellowknife Supergroup rocks in the Point Lake Area, Slave Structural Province, Canada; in Evolution of Archean Supracrustal Sequences, L.D. Ayres, P.C. Thurston, K.D. Card and W. Weber eds., Geol. Assoc. Can. Spec. Pap. 28, 153-167.

Emslie, R.F., 1978: Anorthosite massifs, rapakivi granites, and late Proterozoic rifting of North America; Precambrian Res. 7, 61-98.

Fahrig, W. and West, T., 1986: Diabase dyke swarms of the Canadian Shield; Geol. Surv. Can. Map 1627A.

Fleet, M.E. and Barnett, R.L., 1978: Al^{iv}/Al^{vi} partitioning in calciferous amphiboles from the Frood Mine, Sudbury, Ontario; Can. Mineral. 16, 527-532.

Folinsbee, R.E., Baadsgaard, H., Cumming, G.L. and Green, G.L., 1968: A very ancient island arc; Amer. Geophys. Union, Geophys. Monograph 12, 441-448.

Fyson, W.K. and Helmstaedt, H., 1988: Structural patterns and tectonic evolution of supracrustal domains in the Archean Slave Province, Canada; Can. J. Earth Sci. 25, 301-315.

Geological Survey of Canada, 1968: Artillery Lake, District of Mackenzie, Northwest Territories; Geological Survey of Canada, Aeromagnetic Series, Map 7192G, Geophysics Paper 7192.

Grapes, R.H., 1975: Actinolite-hornblende pairs in metamorphosed gabbros; Contrib. Mineral. Petrology. 49, 125-140.

Grapes, R.H. and Graham, C.M., 1978: The actinolite-hornblende series in metabasites and the so-called miscibility gap: A review; Lithos 11, 85-97.

Grapes, R.H., Hashimoto, Seiji and Miyashita, Sumio, 1977: Amphiboles of a metagabbro-amphibolite sequence, Hidaka metamorphic belt, Hokkaido; J. Petrology 18, 285-318.

Green, T.H. and Pearson, N.J., 1985: Experimental determination of REE partition coefficients between amphibole and basaltic liquids at high pressure; Geochim. Cosmochim. Acta 49, 1465-1468.

Haggerty, 1976: Oxidation of opaque mineral oxides in basalts. in Oxide Minerals, D. Rumble ed., Mineral. Soc. Amer. Rev. Mineral. 3,

Hg1-Hg100.

Hawthorne, F.C., 1981: Crystal chemistry of the amphiboles; *in* Amphiboles and other hydrous pyriboles - mineralogy, D.R. Veblen ed., Mineral. Soc. Amer Rev. Mineral. 9A, 1-139.

Hawthorne, F.C., 1983: The crystal chemistry of the amphiboles; Can. Mineral. 21, 173-480.

Heaman, L.M and LeCheminant, A.N., 1988: U-Pb baddeleyite ages of the Muskox intrusion and Mackenzie dyke swarm, N.W.T., Canada; Geol. Assoc. Can. Prog. Abs. 13, A53.

Helz, R.T., 1973: Phase relations of basalts in their melting range at P_{H_2O}=5 kb as a function of oxygen fugacity. Part I. Mafic phases; J. Petrology 14, 249-302.

Henderson, J.B., 1981: Archean basin evolution in the Slave Province, Canada; *in* Precambrian Plate Tectonics, A. Krøner ed., Elsevier, Amsterdam, 213-235.

Henderson, J.B., 1985: Geology of the Yellowknife-Hearne Lake area, District of Mackenzie: Segment across an Archean basin; Geol. Surv. Can. Mem. 414, 135p.

Henderson, J.B., in press: Geology of the Artillery Lake Map Area, 75 O; Geol. Surv. Can. Open File.

Henderson, J.B. and Macfie, R.I, 1985: The northern Artillery Lake map area: a transect across the Thelon Front, District of Mackenzie; *in* Current Research, Part A, Geol. Surv. Can. Pap. 85-1A, 441-448.

Henderson, J.B. and Macfie, R.I., 1986: Artillery Lake map area, District of Mackenzie: a transect across the Thelon Front; *in* Current Research, Part A, Geol. Surv. Can. Pap. 86-1A, 411-416.

Henderson, J.B., McGrath, P.H., James, D.T. and Macfie, R.I., 1987: The Artillery Lake map area and the Thelon Tectonic Zone - an integrated study; *in* Current Research, Part A, Geol. Surv. Can. Pap. 87-1A, 803-814.

Henderson, J.B., Thompson, P.H. and James, D.T., 1982: The Healey Lake map area and the Thelon Front problem, District of Mackenzie; *in* Current Research, Part A, Geol. Surv. Can. Pap. 82-1A, 191-195.

Hietanen, A., 1974: Amphibole pairs, epidote minerals, chlorite, and plagioclase in metamorphic rocks, northern Sierra Nevada, California; Amer. Mineral. 59, 22-40.

Hoffman, P.F., 1980: Wopmay Orogen: a Wilson cycle of early Proterozoic age in the northwest of the Canadian Shield; *in* The Continental Crust and Its Mineral Deposits, D.W. Strangway ed., Geol. Assoc. Can. Spec. Pap. 20, 523-549.

Hoffman, P.F., 1986: Crustal accretion in a 2.7 Ga

"granite-greenstone" terrane, Slave Province, NWT: a prograding trench-arc system; Geol. Assoc. Can. Prog. Abs. 11, 82.

Huppert, H.E. and Sparks, R.S.J., 1984: Double-diffusive convection due to crystallization in magmas; Ann. Rev. Earth Sci. 12, 11-37.

Hynes, A., 1982: A comparison of amphiboles from medium- and low-pressure metabasites; Contrib. Mineral. Petrology 81, 119-125.

Ike, E.C., Bowden, P. and Martin, R.F., 1985: Amphibole in the porphyries of the Tibchi anorogenic ring-complex, Nigeria: product of deuteric adjustments; Can. Mineral. 23, 447-456.

Irvine, T.N. and Baragar, W.R.A., 1971: A guide to the chemical classification of the common volcanic rocks; Can. J. Earth. Sci. 8, 523-548.

James, D.T., 1985: Geology of the Moraine Lake area and the Thelon Front, District of Mackenzie; in Current Research, Part A, Geol. Surv. Can. Pap. 85-1A, 449-454.

Kamineni, C., 1986: A petrochemical study of calcic amphiboles from the East Bull Lake anorthosite-gabbro layered complex, District of Algoma, Ontario; Contrib. Mineral. Petrology 93, 471-481.

Kretz, R. and Jen, L.S., 1978: Effect of temperature on the distribution of Mg and Fe^{3+} between calcic pyroxene and hornblende; Can. Mineral. 16, 533-537.

Kusky, T.M., 1989: Accretion of the Archean Slave province; Geology 17, 63-67.

Lalonde, A.E., 1986: The intrusive rocks of the Hepburn metamorphic-plutonic zone of the central Wopmay orogen, N.W.T.; unpub. Ph.D. thesis, McGill University, 258p.

Lagache, M., 1984: The exchange equilibrium distribution of alkali and alkaline-earth elements between feldspars and hydrothermal solutions; *in* Feldspars and Feldspathoids -Structures, Properties and Occurrences, W. Brown ed., Nato A.S.I. Ser. C, vol. 137, D. Reidel Pub. Co.

Leake, B.E., 1971: On aluminous and edenitic hornblendes; Mineral Mag. 38, 390-407.

Leake, B.E., 1978: Nomenclature of amphiboles; Amer. Mineral. 63, 1023-1052.

Lemarchand, F., Villemant, B. and Calas, G., 1987: Trace element distribution coefficients in alkalic series; Geochim. Cosmochim. Acta 51, 1071-1081.

Lofgren, G., 1974: An experimental study of plagioclase crystal morphology: Isothermal crystallization; Amer. J. Sci. 274, 243-273.

Lougheed, P.G., 1986: Geological and geochemical investigation of the Clinton-Colden Lake greenstone belt, MacKenzie Mining District, N.W.T. Unpublished M.Sc. Thesis, University of Western Ontario, 148 p.

Macfie, R.I., 1987: The Clinton-Colden hornblende gabbro-anorthosite intrusion, Artillery Lake map area, District of Mackenzie; *in* Current Research, Part A, Geol. Surv. Can. Pap. 87-1A, 681-687.

Macfie, R.I., van Breemen, O., and Loveridge, W., in press: U-Pb zircon age of the Clinton-Colden gabbro-anorthosite intrusion, eastern Slave Province, N.W.T.; Radiogenic Age and Isotopic Studies, Geol. Surv. Can. Pap.

Marsh, B.D., 1988: Crystal capture, sorting, and retention in convecting magma; Geol. Soc. Amer. Bull. 100, 1720-1737.

Mathison, C.I., 1987: Pyroxene oikocrysts in troctolitic cumulates - evidence for supercooled crystallisation and postcumulus modification; Contrib. Mineral. Petrology 97: 228-236.

Mongkoltip, P. and Ashworth, J.R., 1986: Amphibolitization of metagabbros in the Scottish Highlands; J. Metamorphic Geol. 4, 261-283.

Mortensen, J.K., Thorpe, R.I., Padgham, W.A., King, J.E. and Davis, W.J., 1988: U-Pb zircon ages for felsic volcanism in Slave Province, N.W.T.; *in* Radiogenic Age and Isotopic Studies: Report 2, Geol. Surv. Can. Pap. 88-2, 85-95.

Mottl, M.J. and Holland, H.D., 1978: Chemical exchange during hydrothermal alteration of basalt by seawater. I. Experimental results for major and minor components of seawater; Geochim. Cosmochim. Acta 42, 1103-1116.

Miyashiro, A., 1973: *Metamorphism and Metamorphic Belts*, Wiley, New York, 492p.

Nelson, R.A., 1979: Natural fracture systems: description and classification; Amer. Assoc. Petroleum Geol. Bull. 63, 2214-2232.

Oba, T., 1980: Phase relations on the tremolite-pargasite join; Contrib. Mineral. Petrology 78, 230-239.

Offler, R., 1984: Subcalcic, Fe-rich amphiboles in meta-dolerites, Glenrock Station, NSW, Australia; Mineral. Mag. 48, 47-52.

Otten, M.T., 1984: The origin of brown hornblende in the Artfjallet gabbro and dolerites; Contrib. Mineral. Petrology 86, 189-199.

Padgham, W.A., 1985: Observations and speculations on supracrustal successions in the Slave Structural Province; *in* Evolution of Supracrustal Sequences, L.D. Ayres, P.C. Thurston, K.D. Card and W. Weber eds., Geol. Assoc. Can. Spec. Pap. 28, 133-151.

Pe-Piper, G., 1988: Calcic amphiboles of mafic rocks of the Jeffers Brook plutonic complex, Nova Scotia, Canada; Amer. Mineral. 73, 993-1006.

Platten, I.M. and Watterson, J., 1987: Magma flow and crystallization in dyke fissures; *in* Mafic Dyke Swarms, H.C. Halls and W.F. Fahrig eds., Geol. Assoc. Can. Spec. Pap. 34, 65-73.

Raase, P., 1974: Al and Ti contents of hornblende, indicators of pressure and temperature of regional metamorphism; Contrib. Mineral. Petrology 45, 231-236.

Ramberg, H., 1952: Chemical bonds and the distribution of cations in silicates; J. Geol. 60, 331-335.

Robinson, P., Spear, F.C., Schumacher, J., Laird, J., Klein, C. Evans, B. and Doolan, B., 1982: Phase relations of metamorphic amphiboles: natural occurrences and theory; *in* Amphiboles: Petrology and Experimental Phase Relations; D. Veblen and P. Ribbe eds., Min. Soc. Am. Rev. Min. 9B, 1-227.

Robinson, P., Jaffe, H.W. and Klein, C. Jr., 1971: Orientation of exsolution lamellae in clinopyroxenes and amphiboles: considerations of optimal phase boundaries; Amer. Mineral. 56, 909-939.

Rodgers, K.A., 1973: Uralites and uralitization in the ultramafic belt of southern New Caledonia; Geol. Mag. 110; 125-131.

Simmons, E.C. and Hanson, G.N., 1978: Geochemistry and origin of massif-type anorthosites; Contrib. Mineral. Petrology 66, 119-135.

Simmons, E.C., Hanson, G.N. and Lumbers, S.B., 1980: Geochemistry of the Shawmere anorthosite complex, Kapuskasing structural zone, Ontario; Precambrian Res. 11, 43-71.

Spry, A., 1966: The origin of columnar jointing, particularly in basalt flows; J. Geol. Soc. Australia 8, Pt. 2, 191-216.

Stout, J.H., 1972: Phase petrology and mineral chemistry of coexisting amphiboles from Telemark, Norway; J. Petrology 13, 99-145.

Streckeisen, A., 1976: To each plutonic rock its proper name; Earth Sci. Rev. 12, 1-33.

Thompson, J.B. Jr., 1981: An introduction to the mineralogy and petrology of the biopyriboles; *in* Amphiboles and other hydrous pyriboles, D.R. Veblen ed., Mineral. Soc. Amer. Rev. Mineral. 9A, 141-186.

Thurston, P.C. and Fryer, B.J., 1983: The geochemistry of repetitive cyclical volcanism from basalt through rhyolite in the Uchi-Confederation Greenstone Belt, Canada. Contrib. Mineral. Petrol. 83, 204-226.

Ujike, O., 1982: Microprobe mineralogy of plagioclase, clinopyroxene

and amphibole as records of cooling rate in the Shirotori Hiketa dike swarm, northeastern Shikoku, Japan; Lithos, 281-293

van Breemen, O. and Henderson, J.B., 1988: U-Pb zircon and monazite ages from the eastern Slave Province and Thelon Tectonic Zone, Artillery Lake area, N.W.T.; Geol. Surv. Can. Radiogenic and Isotope Studies: Report 2, Paper 88-2, 73-83.

van Breemen, O., Henderson, J.B., Loveridge, W.D. and Thompson, P., 1987a: U-Pb zircon and monazite geochronology and zircon morphology of granulites and granite from the Thelon Tectonic Zone, Healey Lake and Artillery Lake areas, N.W.T.; Geol. Surv. Can. Paper 87-1A, 783-801.

van Breemen, O., Henderson, J.B., Sullivan, R.W. and Thompson, P.H., 1987b: U-Pb, zircon and monazite ages from the eastern Slave Province, Healey Lake Area, N.W.T.; Geol. Surv. Can. Paper 87-2, 101-110.

Velbel, M.A., 1984: Weathering processes of rock forming minerals; in Short Course in Environmental Geochemistry, M. Fleet ed., Mineral. Assoc. Can. Short Course Handbook 10, 67-111.

Veblen, D.R., 1981: Non-classical pyroboles and polysomatic reactions in biopyriboles; in Amphiboles and Other Hydrous Pyroboles - Mineralogy, D.R. Veblen ed., Min. Soc. Am. Rev. Mineral. 9A, 189-236.

Wager, L.R., Brown, G.M. and Wadsworth, W.J., 1960: Types of igneous cumulates; J. Petrology 1, 73-85.

Weaver, B.L., Tarney, J. and Windley, B., 1981: Geochemistry and petrogenesis of the Fiskenaesset anorthosite complex, southern west Greenland: Nature of the parent magma; Geochim. Cosmochim. Acta 45, 711-725.

Wiener, R.W., 1981: Tectonic setting, rock chemistry, and metamorphism of an Archean gabbro-anorthosite complex, Tessiuyakh Bay, Labrador; Can. J. Earth Sci. 18, 1409-1421.

Wodicka, N., 1987: Geology and Geochemistry of Part of the Clinton-Colden Greenstone Belt, N.W.T.; unpublished B.Sc. thesis, University of Ottawa, 82p.

Wright, G.M., 1957: Geological notes on eastern District of Mackenzie, Northwest Territories; Geol. Surv. Can. Paper 56-10.

Wright, G.M., 1967: Geology of the southeastern barren grounds, parts of the District of Mackenzie and Keewatin (Operations Keewatin, Baker, Thelon); Geol. Surv. Can. Memoir 350.

Yoder, H.S. and Tilley, C.E., 1962: Origin of basalt magmas: An experimental study of natural and synthetic rock systems; J. Petrology 3, 342-532.

APPENDIX 1

MICROPROBE ANALYSES OF AMPHIBOLE OF THE CLINTON-COLDEN INTRUSION

Microprobe analyses were obtained with the CAMEBAX electron microprobe of the McGill University microprobe laboratory. Typical operating conditions were 15kV for beam accelerating potential with a sample current automatically maintained at 8 nA. All data were acquired in wavelength-dispersive mode and processed using the ONQUANT resident software of CAMECA.

The analyses are presented on the basis of sample number and type of grain, and grain number within each sample. The symbol "-" means less than 0.005, rounds to 0.00.

a=amphibole oikocryst b=amphibole grain overgrowing plagioclase
c=amphibole grain replacing amphibole oikocryst

a=amphibole oikocryst b=amphibole grain overgrowing plagioclase
c=amphibole grain replacing amphibole oikocryst

	G73 a	G73 b	G87 a	G87 a	G87 a	G87 a	G87 a	G87 c	G87 c	G87 c
Grain	1	2	1	1	1	1	1	2	3	4
SiO2	52.68	45.38	43.49	43.76	43.36	43.05	49.26	49.59	42.86	51.00
TiO2	0.14	0.38	0.49	0.45	0.36	0.29	0.31	0.66	0.38	0.34
Al2O3	4.82	12.26	14.17	13.70	13.98	14.74	7.90	6.62	14.13	5.45
Fe2O3	2.11	2.70	2.83	2.92	2.97	3.05	2.83	2.57	3.08	2.45
FeO	9.10	11.62	12.19	12.56	12.79	13.12	12.20	11.10	13.28	10.55
MnO	0.20	0.20	0.14	0.13	0.26	0.21	0.28	0.22	0.16	0.19
MgO	16.66	10.98	10.15	10.63	10.44	10.33	13.59	14.94	10.45	15.31
CaO	11.92	11.12	11.74	11.57	11.89	11.64	11.29	11.63	11.38	11.10
Na2O	0.51	1.15	1.57	1.49	1.37	1.52	0.93	0.68	1.41	0.66
K2O	0.04	0.16	0.26	0.24	0.24	0.23	0.07	0.11	0.22	0.06
H2O	2.12	2.03	2.01	2.03	2.02	2.04	2.06	2.02	1.89	2.04
F	-	-	-	-	-	-	0.03	-	0.25	0.03
Cl	-	-	0.06	0.04	0.05	0.01	0.05	0.24	0.06	0.08
O=F	-	-	-	-	-	-	0.01	-	0.11	0.01
O=Cl	-	-	0.01	0.01	0.01	0.00	0.01	0.05	0.01	0.02
Total	100.30	97.98	99.12	99.52	99.74	100.23	100.82	100.44	99.67	99.29
#Si IV	7.46	6.71	6.43	6.44	6.39	6.32	7.09	7.14	6.35	7.36
#Al IV	0.54	1.29	1.57	1.56	1.61	1.68	0.91	0.86	1.65	0.64
T site	8.00	8.00	8.00	8.00	8.00	8.00	8.00	8.00	8.00	8.00
#Al VI	0.27	0.85	0.89	0.82	0.82	0.87	0.43	0.27	0.82	0.29
#Fe +3	0.22	0.30	0.31	0.32	0.33	0.34	0.31	0.28	0.34	0.27
#Ti	0.01	0.04	0.05	0.05	0.04	0.03	0.03	0.07	0.04	0.04
#Mg	3.52	2.42	2.24	2.33	2.29	2.26	2.91	3.21	2.31	3.30
#Fe +2	0.98	1.38	1.50	1.47	1.52	1.50	1.32	1.18	1.49	1.11
M1,2,3	5.00	5.00	5.00	5.00	5.00	5.00	5.00	5.00	5.00	5.00
#Fe +2	0.10	0.06	0.00	0.08	0.06	0.11	0.15	0.16	0.15	0.16
#Mn	0.02	0.03	0.02	0.02	0.03	0.03	0.03	0.03	0.02	0.02
#Ca	1.81	1.76	1.86	1.83	1.88	1.83	1.74	1.79	1.81	1.72
#Na	0.07	0.16	0.12	0.08	0.03	0.03	0.08	0.02	0.02	0.10
M4 site	2.00	2.00	2.00	2.00	2.00	2.00	2.00	2.00	2.00	2.00
#Ca	-	-	-	-	-	-	-	-	-	-
#Na	0.07	0.17	0.33	0.34	0.36	0.40	0.18	0.17	0.39	0.09
#K	0.01	0.03	0.05	0.05	0.05	0.04	0.01	0.02	0.04	0.01
A site	0.08	0.20	0.38	0.39	0.41	0.44	0.19	0.19	0.43	0.10
#O	22.00	22.00	22.00	22.00	22.00	22.00	22.00	22.00	22.00	22.00
#OH	2.00	2.00	1.98	1.99	1.99	2.00	1.97	1.94	1.87	1.97
#F	-	-	-	-	-	-	0.01	-	0.12	0.01
#Cl	-	-	0.02	0.01	0.01	0.00	0.01	0.06	0.02	0.02

a=amphibole oikocryst b=amphibole grain overgrowing plagioclase
c=amphibole grain replacing amphibole oikocryst

Grain	G92 a 1	G92 a 1	G92 a 1	G92 a 2	G92 a 3	G92 a 3	G92 a 3	G92 a 3	G92 b 4	G92 b 5
SiO2	52.48	45.70	49.72	40.49	44.31	44.97	44.64	45.07	40.67	41.92
TiO2	0.10	0.41	1.35	0.67	0.41	0.38	0.53	0.38	0.11	0.12
Al2O3	2.76	11.70	5.25	16.31	11.75	11.40	11.70	11.85	16.07	16.04
Fe2O3	1.90	2.00	1.78	2.20	2.40	2.36	2.32	2.32	2.98	3.08
FeO	11.80	12.35	11.04	13.61	14.80	14.61	14.30	14.36	12.83	13.22
MnO	0.32	0.17	0.25	0.22	0.26	0.25	0.17	0.19	0.22	0.20
MgO	17.93	11.90	15.38	9.09	10.38	10.75	10.50	10.46	10.04	9.63
CaO	9.06	11.63	11.75	11.24	11.67	11.55	11.46	11.90	11.43	11.49
Na2O	0.41	1.32	0.63	1.61	1.30	1.43	1.44	1.33	1.61	1.59
K2O	0.01	0.23	0.05	0.28	0.19	0.16	0.17	0.22	0.20	0.21
H2O	2.07	2.04	2.06	1.97	2.01	2.00	2.01	1.99	1.96	1.99
F	-	-	-	-	-	0.03	-	0.06	-	-
Cl	-	0.02	-	0.07	0.04	0.04	0.05	0.07	0.14	0.14
O=F	-	-	-	-	-	0.01	-	0.03	-	-
O=Cl	-	0.00	-	0.02	0.01	0.01	0.01	0.02	0.03	0.03
Total	98.85	99.48	99.26	97.77	99.53	99.96	99.30	100.24	98.29	99.66
#Si IV	7.59	6.69	7.22	6.12	6.59	6.65	6.63	6.64	6.11	6.20
#Al IV	0.41	1.31	0.78	1.88	1.41	1.35	1.37	1.36	1.89	1.80
T site	8.00	8.00	8.00	8.00	8.00	8.00	8.00	8.00	8.00	8.00
#Al VI	0.06	0.71	0.12	1.02	0.65	0.63	0.67	0.69	0.96	1.00
#Fe +3	0.21	0.22	0.19	0.25	0.27	0.26	0.26	0.26	0.34	0.34
#Ti	0.01	0.05	0.15	0.08	0.05	0.04	0.06	0.04	0.01	0.01
#Mg	3.86	2.60	3.33	2.05	2.30	2.37	2.32	2.30	2.25	2.12
#Fe +2	0.86	1.42	1.21	1.60	1.74	1.70	1.68	1.71	1.45	1.52
M1,2,3	5.00	5.00	5.00	5.00	5.00	5.00	5.00	5.00	5.00	5.00
#Fe +2	0.56	0.09	0.13	0.12	0.10	0.11	0.09	0.05	0.17	0.12
#Mn	0.04	0.02	0.03	0.03	0.03	0.03	0.02	0.02	0.03	0.03
#Ca	1.40	1.82	1.83	1.82	1.86	1.83	1.82	1.88	1.81	1.82
#Na	-	0.07	0.01	0.03	0.00	0.03	0.06	0.04	-	0.04
M4 site	2.00	2.00	2.00	2.00	2.00	2.00	2.00	2.00	2.00	2.00
#Ca	0.01	-	-	-	-	-	-	-	0.03	-
#Na	0.11	0.31	0.17	0.44	0.37	0.38	0.35	0.34	0.47	0.42
#K	0.00	0.04	0.01	0.05	0.04	0.03	0.03	0.04	0.04	0.04
A site	0.12	0.35	0.18	0.49	0.41	0.41	0.38	0.38	0.54	0.46
#O	22.00	22.00	22.00	22.00	22.00	22.00	22.00	22.00	22.00	22.00
#OH	2.00	2.00	2.00	1.98	1.99	1.98	1.99	1.95	1.96	1.96
#F	-	-	-	-	-	0.01	-	0.03	-	-
#Cl	-	0.00	-	0.02	0.01	0.01	0.01	0.02	0.04	0.04

a=amphibole oikocryst b=amphibole grain overgrowing plagioclase
c=amphibole grain replacing amphibole oikocryst

Grain	G92 a 6	G92 a 6	G92 a 6	G92 c 7	G95 a 1	G95 a 1	G95 b 2	G95 c 3	G95 c 4	J445 a 1
SiO2	45.93	44.90	43.47	44.34	41.85	44.78	42.60	42.60	43.49	51.14
TiO2	0.31	0.16	0.23	0.36	0.28	0.13	0.42	0.42	0.19	0.14
Al2O3	11.43	13.55	14.14	12.34	15.40	11.81	14.45	14.45	13.37	4.57
Fe2O3	2.76	2.93	2.97	3.05	3.38	3.43	3.41	3.38	3.33	1.89
FeO	11.86	12.60	12.80	13.12	14.56	14.76	14.67	14.56	14.36	11.73
MnO	0.20	0.20	0.26	0.19	0.22	0.30	0.19	0.19	0.19	0.21
MgO	12.42	10.75	10.76	10.90	9.12	11.22	9.61	9.61	10.23	15.01
CaO	11.59	11.74	11.18	11.54	11.18	9.55	11.34	11.34	10.97	12.32
Na2O	1.30	1.59	1.41	1.25	1.61	1.23	1.47	1.47	1.48	0.47
K2O	0.17	0.22	0.20	0.23	0.29	0.16	0.22	0.22	0.20	0.03
H2O	2.03	2.05	2.01	2.02	1.99	2.00	1.96	1.96	1.91	2.06
F	0.03	-	-	-	-	-	0.09	0.09	0.19	-
Cl	0.06	0.05	0.10	0.04	0.10	0.10	0.11	0.11	0.09	0.04
O=F	0.01	-	-	-	-	-	0.04	0.04	0.08	-
O=Cl	0.01	0.01	0.02	0.01	0.02	0.02	0.02	0.02	0.02	0.01
Total	100.12	100.75	99.55	99.39	100.01	99.49	100.60	100.46	100.10	99.62
#Si IV	6.68	6.52	6.41	6.55	6.22	6.63	6.29	6.30	6.44	7.41
#Al IV	1.32	1.48	1.59	1.45	1.78	1.37	1.71	1.70	1.56	0.59
T site	8.00	8.00	8.00	8.00	8.00	8.00	8.00	8.00	8.00	8.00
#Al VI	0.64	0.84	0.86	0.70	0.91	0.69	0.81	0.82	0.77	0.19
#Fe +3	0.30	0.32	0.33	0.34	0.38	0.38	0.38	0.38	0.37	0.21
#Ti	0.03	0.02	0.03	0.04	0.03	0.01	0.05	0.05	0.02	0.02
#Mg	2.69	2.33	2.36	2.40	2.02	2.48	2.12	2.12	2.26	3.24
#Fe +2	1.32	1.49	1.42	1.51	1.66	1.44	1.65	1.64	1.58	1.35
M1,2,3	5.00	5.00	5.00	5.00	5.00	5.00	5.00	5.00	5.00	5.00
#Fe +2	0.12	0.04	0.16	0.11	0.15	0.39	0.15	0.16	0.20	0.07
#Mn	0.02	0.02	0.03	0.02	0.03	0.04	0.02	0.02	0.02	0.03
#Ca	1.81	1.83	1.77	1.83	1.78	1.51	1.79	1.80	1.74	1.90
#Na	0.05	0.11	0.04	0.04	0.04	0.06	0.02	0.02	0.04	-
M4 site	2.00	2.00	2.00	2.00	2.00	2.00	2.00	2.00	2.00	2.00
#Ca	-	-	-	-	-	-	-	-	-	0.01
#Na	0.32	0.34	0.36	0.32	0.42	0.30	0.40	0.40	0.38	0.13
#K	0.03	0.04	0.04	0.04	0.05	0.03	0.04	0.04	0.04	0.01
A site	0.35	0.38	0.40	0.36	0.47	0.33	0.44	0.44	0.42	0.15
#O	22.00	22.00	22.00	22.00	22.00	22.00	22.00	22.00	22.00	22.00
#OH	1.97	1.99	1.98	1.99	1.97	1.97	1.93	1.93	1.89	1.99
#F	0.01	-	-	-	-	-	0.04	0.04	0.09	-
#Cl	0.01	0.01	0.02	0.01	0.03	0.03	0.03	0.03	0.02	0.01

a=amphibole oikocryst b=amphibole grain overgrowing plagioclase
c=amphibole grain replacing amphibole oikocryst

	J445 a 1	J445 a 1	J445 a 1	J445 a 1	J445 a 1	J445 a 1	J445 a 1	T7 a 1	T7 a 1	T7 a 1
Grain										
SiO2	51.39	53.95	52.34	51.12	51.07	49.97	49.76	49.50	48.74	46.14
TiO2	0.12	0.08	0.08	0.06	0.12	0.20	0.09	0.28	0.35	0.52
Al2O3	4.40	2.74	2.87	3.44	4.15	5.62	4.29	7.24	7.88	10.13
Fe2O3	1.92	1.76	1.83	1.79	1.92	2.03	1.92	2.06	2.12	2.26
FeO	11.92	10.92	11.35	11.11	11.86	12.54	11.86	12.74	13.11	13.99
MnO	0.23	0.29	0.29	0.22	0.31	0.20	0.25	0.13	0.15	0.23
MgO	14.57	16.08	15.74	15.95	14.50	13.89	15.22	13.26	12.92	11.29
CaO	12.52	12.61	12.75	12.76	12.52	12.64	12.15	11.83	12.02	12.16
Na2O	0.51	0.27	0.23	0.31	0.37	0.55	0.48	0.82	0.86	0.98
K2O	0.03	0.02	0.02	0.04	0.04	0.05	0.05	0.13	0.12	0.25
H2O	2.06	2.10	1.98	2.04	2.03	1.97	2.02	2.06	2.03	2.02
F	-	-	0.17	-	0.03	0.17	-	-	0.06	-
Cl	0.04	0.03	0.04	0.05	0.05	0.02	0.06	0.05	0.04	0.07
O=F	-	-	0.07	-	0.01	0.07	-	-	0.03	-
O=Cl	0.01	0.01	0.01	0.01	0.01	0.00	0.01	0.01	0.01	0.02
Total	99.72	100.86	99.77	98.90	98.99	99.93	98.16	100.11	100.43	100.06
#Si IV	7.45	7.66	7.57	7.46	7.46	7.28	7.35	7.18	7.07	6.79
#Al IV	0.55	0.34	0.43	0.54	0.54	0.72	0.65	0.82	0.93	1.21
T site	8.00	8.00	8.00	8.00	8.00	8.00	8.00	8.00	8.00	8.00
#Al VI	0.20	0.12	0.06	0.05	0.18	0.24	0.10	0.41	0.42	0.54
#Fe +3	0.21	0.19	0.20	0.20	0.21	0.22	0.21	0.22	0.23	0.25
#Ti	0.01	0.01	0.01	0.01	0.01	0.02	0.01	0.03	0.04	0.06
#Mg	3.15	3.40	3.39	3.47	3.16	3.02	3.35	2.87	2.80	2.48
#Fe +2	1.43	1.28	1.34	1.28	1.44	1.50	1.33	1.46	1.51	1.68
M1,2,3	5.00	5.00	5.00	5.00	5.00	5.00	5.00	5.00	5.00	5.00
#Fe +2	0.01	0.02	0.03	0.07	0.01	0.03	0.13	0.08	0.08	0.05
#Mn	0.03	0.03	0.04	0.03	0.04	0.02	0.03	0.02	0.02	0.03
#Ca	1.94	1.92	1.93	1.90	1.95	1.95	1.83	1.84	1.87	1.92
#Na	0.01	0.03	-	-	-	-	-	0.07	0.03	0.01
M4 site	2.00	2.00	2.00	2.00	2.00	2.00	2.00	2.00	2.00	2.00
#Ca	-	-	0.04	0.10	0.01	0.03	0.09	-	-	-
#Na	0.13	0.04	0.06	0.09	0.10	0.16	0.14	0.16	0.21	0.27
#K	0.01	0.00	0.00	0.01	0.01	0.01	0.01	0.02	0.02	0.05
A site	0.13	0.05	0.11	0.19	0.12	0.19	0.23	0.19	0.23	0.32
#O	22.00	22.00	22.00	22.00	22.00	22.00	22.00	22.00	22.00	22.00
#OH	1.99	1.99	1.91	1.99	1.97	1.92	1.98	1.99	1.96	1.98
#F	-	-	0.08	-	0.01	0.08	-	-	0.03	-
#Cl	0.01	0.01	0.01	0.01	0.01	0.00	0.02	0.01	0.01	0.02

a=amphibole oikocryst b=amphibole grain overgrowing plagioclase
c=amphibole grain replacing amphibole oikocryst

	T7 a	T7 a	T7 a	T7 a	T7 a	T7 a	T7 a	T7 b	T7 b	T9 a
Grain	1	1	1	1	1	1	1	2	3	1
SiO2	47.50	47.31	48.68	48.10	46.88	48.05	47.22	44.10	45.45	51.10
TiO2	0.39	0.27	0.36	0.39	0.41	0.25	0.39	0.67	0.38	0.10
Al2O3	8.89	7.62	6.86	8.33	9.43	8.56	9.24	12.63	11.19	5.59
Fe2O3	2.22	2.12	2.04	2.14	2.18	2.09	2.17	3.23	3.15	1.71
FeO	13.73	13.11	12.62	13.23	13.51	12.95	13.44	13.98	13.57	10.58
MnO	0.19	0.12	0.24	0.19	0.22	0.26	0.30	0.19	0.17	0.12
MgO	11.79	12.79	13.41	12.80	11.96	12.76	12.30	10.04	10.84	15.69
CaO	12.15	11.97	11.80	11.90	11.91	11.98	11.78	11.68	11.82	12.53
Na2O	1.09	0.88	0.76	0.97	1.06	1.12	1.28	1.38	1.11	0.85
K2O	0.13	0.12	0.10	0.10	0.17	0.12	0.14	0.27	0.19	0.08
H2O	2.03	1.87	2.03	2.04	2.01	1.98	2.01	1.94	2.03	2.10
F	-	0.31	-	0.03	0.03	0.16	-	0.15	-	-
Cl	0.06	0.02	0.03	0.04	0.06	0.03	0.17	0.10	0.05	-
O=F	-	0.13	-	0.01	0.01	0.07	-	0.06	-	-
O=Cl	0.01	0.00	0.01	0.01	0.01	0.01	0.04	0.02	0.01	-
Total	100.19	98.64	98.94	100.28	99.86	100.38	100.48	100.44	99.96	100.45
#Si IV	6.95	7.03	7.15	7.00	6.88	6.99	6.89	6.50	6.69	7.31
#Al IV	1.05	0.97	0.85	1.00	1.12	1.01	1.11	1.50	1.31	0.69
T site	8.00	8.00	8.00	8.00	8.00	8.00	8.00	8.00	8.00	8.00
#Al VI	0.48	0.36	0.34	0.43	0.51	0.46	0.48	0.70	0.63	0.25
#Fe +3	0.24	0.24	0.23	0.23	0.24	0.23	0.24	0.36	0.35	0.18
#Ti	0.04	0.03	0.04	0.04	0.05	0.03	0.04	0.07	0.04	0.01
#Mg	2.57	2.83	2.94	2.78	2.62	2.77	2.68	2.21	2.38	3.35
#Fe +2	1.66	1.53	1.46	1.51	1.59	1.51	1.56	1.67	1.60	1.21
M1,2,3	5.00	5.00	5.00	5.00	5.00	5.00	5.00	5.00	5.00	5.00
#Fe +2	0.02	0.09	0.09	0.10	0.07	0.06	0.08	0.06	0.07	0.06
#Mn	0.02	0.02	0.03	0.02	0.03	0.03	0.04	0.02	0.02	0.01
#Ca	1.90	1.89	1.86	1.86	1.87	1.87	1.84	1.84	1.86	1.92
#Na	0.05	-	0.02	0.02	0.03	0.04	0.04	0.07	0.05	0.01
M4 site	2.00	2.00	2.00	2.00	2.00	2.00	2.00	2.00	2.00	2.00
#Ca	-	0.02	-	-	-	-	-	-	-	-
#Na	0.26	0.25	0.20	0.25	0.27	0.28	0.32	0.32	0.27	0.23
#K	0.02	0.02	0.02	0.02	0.03	0.02	0.03	0.05	0.04	0.01
A site	0.28	0.29	0.22	0.27	0.31	0.30	0.35	0.37	0.30	0.24
#O	22.00	22.00	22.00	22.00	22.00	22.00	22.00	22.00	22.00	22.00
#OH	1.99	1.85	1.99	1.98	1.97	1.92	1.96	1.91	1.99	2.00
#F	-	0.15	-	0.01	0.01	0.07	-	0.07	-	-
#Cl	0.01	0.01	0.01	0.01	0.01	0.01	0.04	0.02	0.01	-

a=amphibole oikocryst b=amphibole grain overgrowing plagioclase
c=amphibole grain replacing amphibole oikocryst

	T9 a	T9 a
Grain	1	1
SiO2	53.36	53.25
TiO2	0.11	0.08
Al2O3	3.06	3.29
Fe2O3	1.45	1.47
FeO	8.95	9.09
MnO	0.08	0.11
MgO	17.73	17.17
CaO	12.74	12.82
Na2O	0.41	0.49
K2O	0.04	0.03
H2O	2.11	2.05
F	-	0.09
Cl	-	0.06
O=F	-	0.04
O=Cl	-	0.01
Total	100.04	100.05
#Si IV	7.58	7.58
#Al IV	0.42	0.42
T site	8.00	8.00
#Al VI	0.09	0.13
#Fe +3	0.15	0.16
#Ti	0.01	0.01
#Mg	3.75	3.64
#Fe +2	0.99	1.06
M1,2,3	5.00	5.00
#Fe +2	0.07	0.02
#Mn	0.01	0.01
#Ca	1.92	1.95
#Na	-	0.01
M4 site	2.00	2.00
#Ca	0.02	-
#Na	0.11	0.12
#K	0.01	0.01
A site	0.14	0.13
#O	22.00	22.00
#OH	2.00	1.95
#F	-	0.04
#Cl	-	0.01

APPENDIX 2

WHOLE ROCK GEOCHEMISTRY

A2.1 Introduction

Most whole-rock samples were analysed for major elements and Ba, Cr, Zn, Ni and V at the University of Ottawa X-ray fluorescence laboratory. Samples N-4A, N-4B, N-4C, N-22, N026,N-27, N-36, N-37, N-40A, N-40B, N-42C, N-43, and N-46B were analysed and originally reported by Wodicka (1987). Samples N-12B, N-21C, N-23B, N-30, N-31D, N-39A, and N-41B were analysed by the inductively coupled plasma technique at the Geological Survey of Canada ICP emission spectrometry laboratory. Nb, Zr, Y, Sr and Rb determinations were carried out by X-ray fluorescence at the Geochemical Laboratories of McGill University. REE and Co, Sc, Hf, Ta and U were analysed by instrumental neutron activation INAA at Ecole Polytechnique (Université de Montréal).

A2.2 Procedures, precision and accuracy

Samples consisting of at least 5 kg of rock, with weathered surface and alteration veins removed, were prepared. They were broken in a jaw crusher to approximately 1 cm, and the fragments were homogenized and systematically split to provide fractions suitable for powdering in a tungsten carbide ringmill. Samples were crushed to <200 mesh.

X-ray fluorescence analyses carried out at the University of Ottawa XRF facility were performed on 1.3 g of sample fused with 0.433 g $LiCO_3$ and 3.900 g $Li_2B_4O_7$. An international standard, DR-N (diorite), was used to determine the accuracy of the analytical technique. Precision

of 8 analyses of DR-N is given below in terms of the first standard deviation, and the accuracy relative to the standard DR-N given in Abbey (1983) is shown in terms of percent error, (B-A)/B. Also given is an example of percent of error between two analyses of a sample of the Clinton-Colden gabbro-anorthosite intrusion.

Element	A DR-N U.O. wt. %	B DR-N (Abbey, 1983) wt. %	% error (B-A)/B X 100
SiO_2	52.78+/-0.21(1s)	52.98	0.38
TiO_2	1.04+/-0.02	1.09	4.59
Al_2O_3	17.58+/-0.11	17.56	0.11
Fe_2O_{3T}	9.69+/-0.043	9.72	0.31
MnO	0.22+/-0.0	0.22	0.0
MgO	4.09+/-0.16	4.41	7.26
CaO	6.96+/-0.046	7.07	1.56
Na_2O	2.92+/-0.20	3.00	2.67
K_2O	1.71+/-0.011	1.70	0.58
P_2O_5	0.19+/-0.019	0.25	24.00
	ppm	ppm	
Ba	401+/-25	390	2.74
Cr	41+/-4.5	42	2.38
Zn	133+/-5.4	145	8.28
Ni	12+/-6.0	16	25.00
V	225+/-12	230	2.71

	A G-49 wt. %	B G-49 duplicate wt. %	(B-A)/B X 100
SiO_2	46.21	46.04	0.36
TiO_2	0.31	0.30	3.33
Al_2O_3	26.01	25.99	0.08
Fe_2O_{3T}	6.67	6.61	0.90
MnO	0.09	0.09	0.00
MgO	4.48	4.90	1.22
CaO	12.65	12.72	0.01
Na_2O	2.02	1.88	1.98
K_2O	0.12	0.13	7.69
P_2O_5	0.00	0.00	0.00
	ppm	ppm	
Ba	73	89	17.98
Cr	300	299	0.00
Zn	80	91	0.12
Ni	117	114	2.56
V	101	100	0.01

Samples submitted to the Geological Survey of Canada ICP emission spectrometry laboratory were analysed by ICP. Data for major elements were obtained on 0.5 g of sample fused with $Li_2B_4O_7$, dissolved in 5%

HNO_3 and diluted to 250 ml. Reported estimates of validity of results are as follows:

Element	+/-	Absolute	+	Relative
SiO_2	+/-	0.4%	+	2% of conc.
TiO_2	+/-	0.02	+	2% of conc.
Al_2O_3	+/-	0.2	+	2% of conc.
Fe_2O_{3T}	+/-	0.2	+	2% of conc.
MnO	+/-	0.01	+	2% of conc.
MgO	+/-	0.1	+	2% of conc.
CaO	+/-	0.1	+	2% of conc.
Na_2O	+/-	0.1	+	2% of conc.
K_2C	+/-	0.1	+	2% of conc.
P_2O_5	+/-	0.02	+	2% of conc.

Data for trace elements were obtained on 1.0 g of sample (acid + fusion residue) dissolved in 10% HCL and diluted to 100 ml. Reported estimated validity of results are as follows:

Element	+/-	Absolute	+	Relative
Ba	+/-	20 ppm	+	5% of conc.
Cr	+/-	10	+	5% of conc.
Zn	+/-	5	+	5% of conc.
Ni	+/-	10	+	5% of conc.
V	+/-	5	+	5% of conc.

Nb, Zr, Y, Sr and Rb determinations were carried out by pressed powder pellets by XRF analysis on the fully automated Philips PW1400 spectrometer at McGill University, with a reported detection limit of 5 ppm.

REE, Co, Sc, Hf, Ta and U determinations were carried out by INAA at Ecole Polytechnique. The accuracy of the technique was determined by Lalonde (1986) as follows:

REE	error %
La	3
Ce	12
Nd	17
Sm	7
Eu	4
Tb	23
Ho	5
Yb	19
Lu	5
Trace Elements	
Co	<1
Sc	3
Hf	16
Ta	21
U	28

In the following tables "na" means not analysed.

A2.3 Whole rock analyses of meta-volcanic rocks of the south-eastern Clinton-Colden greenstone belt

	N-4A	N-4B	N-4C	N-12B	N-21	N-22	N-23B	N-25	N-26	N-27
SiO_2	63.79	47.80	75.28	60.50	66.00	49.79	75.90	47.95	74.84	51.74
TiO_2	0.67	0.61	0.04	0.70	0.96	1.26	0.04	1.60	0.22	0.89
Al_2O_3	17.10	15.15	14.85	16.00	12.80	13.64	13.80	14.37	13.59	16.76
Fe_2O_3	4.82	11.44	0.58	7.25	9.70	14.74	0.36	15.36	2.90	10.50
MnO	0.10	0.19	0.04	0.10	0.08	0.23	0.02	0.23	0.03	0.16
MgO	2.17	10.43	0.20	4.36	3.12	6.02	0.13	6.78	1.32	7.31
CaO	4.19	11.32	0.33	4.50	3.05	8.96	1.02	10.90	2.32	8.79
Na_2O	4.54	1.42	4.75	5.84	4.34	3.40	6.92	2.31	1.34	3.50
K_2O	2.15	0.56	3.65	0.30	0.59	0.60	0.27	0.50	2.42	0.77
P_2O_5	0.12	0.0	0.04	0.14	0.28	0.0	0.03	0.0	0.0	0.03
Total	99.65	98.92	99.76	99.69	100.9	98.64	98.49	100.0	98.98	100.4
Nb	12	7	22	11	21	11	22	12	15	9
Zr	173	67	69	150	352	111	67	126	268	121
Y	18	8	13	11	85	24	12	20	28	16
Sr	175	177	61	186	128	235	81	241	98	231
Rb	50	18	136	11	19	20	9	16	49	21
Ba	323	108	133	120	100	202	50	156	521	133
Cr	38	348	31	82	13	95	3	181	16	212
Zn	53	77	34	65	57	109	0	97	16	62
Ni	58	243	10	79	15	143	4	84	40	91
V	71	237	4	110	16	369	0	319	13	216
Co	43	na	na	52	49	53	48	88	39	58
Sc	13	na	na	na	na	52	na	43	7	34
La	16.1	na	na	na	na	8.8	na	9.1	27.9	7.4
Ce	36	na	na	na	na	20.3	na	22	64	18.8
Nd	16.9	na	na	na	na	12.5	na	15	27.8	11.6
Sm	3.9	na	na	na	na	3.4	na	3.9	5.6	2.8
Eu	1.02	na	na	na	na	1.08	na	1.27	1.06	0.85
Tb	0.58	na	na	na	na	0.72	na	0.75	0.9	0.55
Ho	0.68	na	na	na	na	1.01	na	0.79	1.05	0.58
Yb	1.8	na	na	na	na	2.6	na	2.1	3.1	1.77
Lu	0.29	na	na	na	na	0.44	na	0.33	0.48	0.27
Hf	4.5	na	na	na	na	2.1	na	2.4	8.1	2.5
Ta	2.04	na	na	na	na	0.63	na	1.84	2.68	1.34
Th	2.5	na	na	na	na	1.21	na	0.85	7	0.73
U	0.74	na	na	na	na	0.33	na	0.22	1.74	0.24

	N-30	N-31D	N-36	N-37	N-38	N-39A	N-40A	N-40B	N-41B	N-42C
SiO_2	70.00	45.10	55.97	56.60	47.58	48.30	55.74	73.89	74.40	73.52
TiO_2	0.61	0.89	01.01	0.84	1.16	1.49	1.07	0.25	0.25	0.35
Al_2O_3	12.60	15.30	16.48	16.77	18.06	16.60	16.00	13.29	13.40	13.66
Fe_2O_3	4.02	13.00	09.30	8.25	14.26	11.00	7.59	3.06	2.60	2.07
MnO	0.06	0.19	0.08	0.12	0.46	0.18	0.17	0.03	0.05	0.03
MgO	1.43	9.30	5.97	5.09	5.70	6.90	3.70	0.67	1.88	1.54
CaO	1.96	10.80	5.59	5.10	8.98	10.80	8.50	1.24	1.76	1.60
Na_2O	4.84	2.16	2.48	0.64	2.88	2.88	5.19	4.76	1.65	3.13
K_2O	0.51	0.49	1.06	3.26	0.27	0.35	0.34	2.59	2.68	2.47
P_2O_5	0.16	0.08	0.08	0.21	0.0	0.17	0.15	0.04	0.05	0.04
Total	96.19	97.31	98.02	96.88	99.35	98.67	98.45	99.82	98.72	98.41
Nb	29	8	10	12	7	10	13	16	16	15
Zr	475	79	164	148	100	116	146	213	219	191
Y	104	10	23	17	15	19	23	35	35	25
Sr	99	185	118	229	229	190	165	80	80	88
Rb	10	10	75	25	8	12	14	73	76	61
Ba	50	50	227	289	114	40	76	406	120	233
Cr	10	140	86	145	223	250	181	9	82	21
Zn	170	110	92	83	133	96	63	26	65	34
Ni	8	220	59	77	239	220	77	13	79	12
V	4	220	195	154	306	350	156	0	110	24
Co	69	84	na	38	82	81	na	na	52	na
Sc	na	na	na	22.6	39	na	na	na	na	na
La	na	na	na	12.4	3.5	na	na	na	na	na
Ce	na	na	na	30	10.6	na	na	na	na	na
Nd	na	na	na	15.1	8.6	na	na	na	na	na
Sm	na	na	na	3.5	2.6	na	na	na	na	na
Eu	na	na	na	0.98	0.98	na	na	na	na	na
Tb	na	na	na	0.64	0.51	na	na	na	na	na
Ho	na	na	na	0.73	0.64	na	na	na	na	na
Yb	na	na	na	1.7	1.65	na	na	na	na	na
Lu	na	na	na	0.29	0.27	na	na	na	na	na
Hf	na	na	na	3.7	1.70	na	na	na	na	na
Ta	na	na	na	1.1	1.19	na	na	na	na	na
Th	na	na	na	1.7	0.37	na	na	na	na	na
U	na	na	na	0.41	0.16	na	na	na	na	na

	N-43	N-46B	G-45B
SiO_2	62.68	54.44	49.90
TiO_2	0.68	0.84	1.19
Al_2O_3	15.12	16.73	16.30
Fe_2O_3	6.54	7.95	9.60
MnO	0.12	0.15	0.18
MgO	3.98	4.78	6.57
CaO	5.68	8.01	9.29
Na_2O	2.72	2.87	3.23
K_2O	1.46	1.55	0.60
P_2O_5	0.12	0.17	0.12
Total	99.10	97.49	96.98
Nb	12	8	10
Zr	154	114	104
Y	18	15	13
Sr	187	323	267
Rb	31	49	18
Ba	198	181	110
Cr	99	92	300
Zn	70	84	85
Ni	46	5	200
V	92	173	240
Co	51	na	82
Sc	15.3	na	na
La	15	na	na
Ce	35	na	na
Nd	16	na	na
Sm	3.5	na	na
Eu	1.04	na	na
Tb	0.58	na	na
Ho	0.66	na	na
Yb	1.9	na	na
Lu	0.29	na	na
Hf	4	na	na
Ta	2.3	na	na
Th	2.8	na	na
U	1.1	na	na

A2.4 Whole rock analyses of rocks of the Clinton-Colden gabbro-anorthosite intrusion

gab=gabbro (<50% plagioclase); lcgb=leucogabbro (50-90% plagioclase); anor=anorthosite (>90% plagioclase)

	G-25 gab	G-28 gab	G-33 lcgb	G-39 gab	G-49 lcgb	G-51 anor	G-59 gab	G-71 anor	G-72 gab	G-73 gab
SiO_2	47.84	46.70	49.40	47.85	46.21	48.60	47.40	47.93	45.23	45.09
TiO_2	0.69	0.80	0.67	1.57	0.31	0.22	0.44	0.68	0.65	0.36
Al_2O_3	19.69	18.04	24.70	20.70	26.01	29.30	20.79	28.92	20.06	17.56
Fe_2O_3	9.77	8.84	5.83	10.97	6.67	2.30	7.85	3.87	11.72	11.72
MnO	0.12	0.10	0.06	0.13	0.09	0.03	0.13	0.04	0.16	0.17
MgO	6.96	6.03	2.03	3.57	4.84	0.88	6.43	0.84	8.80	10.16
CaO	11.17	12.60	9.12	11.39	12.65	13.40	11.32	13.98	10.87	11.14
Na_2O	2.46	2.05	4.49	3.12	2.02	3.40	2.57	3.22	1.77	1.11
K_2O	0.77	0.84	1.48	0.41	0.12	0.24	2.32	0.19	0.20	0.41
P_2O_5	0.0	0.06	0.08	0.0	0.0	0.13	0.0	0.0	0.0	0.0
Total	99.47	98.10	97.86	99.72	98.92	98.27	99.25	99.67	99.46	98.72
Nb	7	na	na	na	na	na	na	7	6	5
Zr	60	34	60	26	0	na	15	60	50	49
Y	8	13	14	19	0.0	197	12	0.0	0.0	5
Sr	156	180	320	185	155	na	156	209	132	148
Rb	26	na	na	na	na	na	112	10	7	13
Ba	138	90	130	34	73	20	426	104	136	97
Cr	333	310	22	17	300	7	313	151	294	408
Zn	44	61	66	64	80	17	62	16	70	78
Ni	116	92	25	44	117	24	127	5	180	212
V	229	340	120	489	101	30	147	134	209	119
Co	62	64	42	na	na	57	na	45	73	74
Sc	29	na	na	na	na	na	na	7.3	12.3	27
La	1.39	na	na	na	na	na	na	1.32	0.84	0.67
Ce	3.9	na	na	na	na	na	na	3.4	1.6	1.8
Nd	2.4	na	na	na	na	na	na	2.2	1.19	1.8
Sm	1.05	na	na	na	na	na	na	0.61	0.42	0.64
Eu	0.47	na	na	na	na	na	na	0.55	0.42	0.44
Tb	0.24	na	na	na	na	na	na	0.13	0.09	0.13
Ho	0.29	na	na	na	na	na	na	0.15	0.18	0.15
Yb	1	na	na	na	na	na	na	0.5	0.48	0.75
Lu	0.18	na	na	na	na	na	na	0.09	0.08	0.11
Hf	0.59	na	na	na	na	na	na	0.46	0.23	0.22
Ta	1.37	na	na	na	na	na	na	1.28	1.05	0.77
Th	0.2	na	na	na	na	na	na	0.18	0.16	na
U	0.12	na	na	na	na	na	na	0.15	0.09	0.08

	G-84 gab	G-85 lcgb	G-87 lcgb	G-92 lcgb	G-95 lcgb	G-97 anor	G-98 anor	T-2B lcgb	T-3 lcgb	T-5 lcgb
SiO_2	49.07	48.04	47.39	47.48	47.48	47.19	48.07	47.82	46.99	45.11
TiO_2	1.19	0.50	0.44	0.77	0.61	0.43	0.27	0.18	0.39	0.35
Al_2O_3	14.29	25.12	25.01	25.48	27.17	27.87	29.05	27.27	23.53	27.64
Fe_2O_3	13.06	6.00	7.45	7.76	6.29	4.34	3.34	4.51	8.44	4.72
MnO	0.18	0.08	0.09	0.10	0.07	0.06	0.03	0.06	0.10	0.06
MgO	7.99	3.51	4.46	4.39	2.45	2.42	1.34	2.51	7.39	2.52
CaO	12.73	13.27	12.79	13.77	13.60	12.28	10.35	10.98	13.42	13.52
Na_2O	1.90	2.33	2.46	2.45	2.55	2.74	3.35	3.47	1.94	2.73
K_2C	0.25	0.23	0.21	0.26	0.12	0.15	0.55	2.15	0.51	0.27
P_2O_5	0.0	0.0	0.0	0.0	0.0	0.0	0.0	0.0	0.0	0.0
Total	100.7	99.08	100.3	101.7	100.2	99.68	98.10	97.49	98.39	99.41
Nb	na	7	6	6	5	na	na	na	na	na
Zr	37	56	51	58	52	0	0	8	10	0
Y	27	5	0	0	na	10	0	7	0	0
Sr	101	180	165	181	170	170	197	254	182	176
Rb	0	8	8	8	11	0	0	70	0	0
Ba	71	115	68	120	60	59	87	369	80	94
Cr	295	272	361	307	120	143	30	54	415	157
Zn	67	47	44	42	42	27	12	19	48	10
Ni	93	46	79	98	45	22	0	46	212	33
V	465	165	156	251	142	77	71	88	92	123
Co	na	57	45	52	46	na	na	na	na	na
Sc	na	17.7	11.8	11.3	6	na	na	na	na	na
La	na	1.28	0.77	0.91	1.4	na	na	na	na	na
Ce	na	3.3	1.9	2.1	3.6	na	na	na	na	na
Nd	na	2.8	1.8	1.29	2.4	na	na	na	na	na
Sm	na	0.82	0.48	0.43	0.71	na	na	na	na	na
Eu	na	0.57	0.43	0.45	0.6	na	na	na	na	na
Tb	na	0.2	0.13	0.1	0.14	na	na	na	na	na
Ho	na	0.25	0.11	0.14	0.2	na	na	na	na	na
Yb	na	0.76	0.37	0.4	0.54	na	na	na	na	na
Lu	na	0.12	0.08	0.07	0.1	na	na	na	na	na
Hf	na	0.31	0.29	0.2	0.53	na	na	na	na	na
Ta	na	1.44	0.79	0.95	1.45	na	na	na	na	na
Th	na	0.13	0	0	0.16	na	na	na	na	na
U	na	0	0.05	0.08	0.12	na	na	na	na	na

	T-6 lcgb	T-7 gab	T-8 gab
SiO_2	53.45	49.23	42.56
TiO_2	0.64	0.58	3.23
Al_2O_3	22.55	19.19	12.82
Fe_2O_3	4.08	9.79	19.92
MnO	0.06	0.11	0.26
MgO	2.24	6.73	7.39
CaO	10.07	11.01	10.25
Na_2O	4.92	3.28	1.71
K_2O	1.28	0.69	0.31
P_2O_5	0.0	0.0	0.0
Total	99.29	100.6	98.45
Nb	na	na	na
Zr	106	13	15
Y	17	18	16
Sr	288	168	69
Rb	46	10	na
Ba	324	145	18
Cr	41	350	28
Zn	16	51	123
Ni	22	48	64
V	144	245	1027
Co	na	na	na
Sc	na	na	na
La	na	na	na
Ce	na	na	na
Nd	na	na	na
Sm	na	na	na
Eu	na	na	na
Tb	na	na	na
Ho	na	na	na
Yb	na	na	na
Lu	na	na	na
Hf	na	na	na
Ta	na	na	na
Th	na	na	na
U	na	na	na

APPENDIX 3

MICROPROBE ANALYSES OF EPIDOTE FROM THE CLINTON-COLDEN INTRUSION AND OF GARNET FROM HORNFELS ADJACENT TO THE INTRUSION

Epidote analyses are of two fine (0.1 mm) epidote grains from sample J-445 (see Figure 3.11).

	1	2	Mean
SiO2	38.12	38.03	38.07
TiO2	0.09	0.04	0.06
Al2O3	25.71	26.41	26.06
Fe2O3	11.17	10.32	10.75
FeO	0.04	0.04	0.04
MnO	0.13	0.10	0.11
CaO	23.36	23.53	23.45
Na2O	0.01	0.01	0.01
H2O	1.91	1.91	1.91
TOTAL	100.55	100.40	100.47
#Si IV	2.98	2.97	2.98
#Al IV	0.02	0.03	0.02
Z site	3.00	3.00	3.00
#Al VI	2.36	2.41	2.38
#Fe +3	0.66	0.61	0.63
#Ti	0.01	0.00	0.00
Y site	3.03	3.02	3.03
#Ca	1.96	1.97	1.97
X site	1.97	1.98	1.97
#O	12.00	12.00	12.00
#OH	1.00	1.00	1.00

Garnet analyses are of 3 garnet crystals in sample N-7, from the metamorphic aureole around the Clinton-Colden intrusion. This garnet has been deformed (fractured) in biotite-grade minor shear zones attributed to movement along the Thelon tectonic zone.

Analyses 1 and 2 are single analyses of separate grains. Analyses 3 to 5 are from a short microprobe traverse from the centre to the rim of a third grain.

		1	2	3	4	5	Mean
	SiO2	37.39	37.10	37.34	37.24	36.98	37.21
	TiO2	0.09	0.03	0.10	0.02	0.04	0.06
	Al2O3	20.43	20.62	20.23	20.41	20.44	20.43
	FeO	26.49	26.26	26.22	26.86	25.64	26.29
	MnO	8.93	10.03	9.02	8.96	9.96	9.38
	MgO	0.87	0.78	0.84	0.84	0.74	0.81
	CaO	5.03	4.99	5.37	5.20	5.27	5.17
	Na2O	0.03	0.05	0.04	0.07	0.05	0.05
	K2O	0.02	0.02	-	-	0.01	0.01
	TOTAL	99.28	99.88	99.16	99.60	99.13	99.41
T	#Si+4	6.08	6.03	6.09	6.06	6.04	6.06
O	#Ti+4	0.01	0.00	0.01	0.00	0.00	0.01
	#Al+3	3.92	3.95	3.89	3.91	3.94	3.92
	#Fe+2	3.61	3.57	3.57	3.65	3.50	3.58
	#Mn+2	1.23	1.38	1.25	1.23	1.38	1.29
	#Mg+2	0.21	0.19	0.20	0.20	0.18	0.20
A	#Ca+2	0.88	0.87	0.94	0.91	0.92	0.90
	#Na+1	0.01	0.02	0.01	0.02	0.02	0.02
	#K	0.00	0.00	-	-	0.00	0.00
	#TOTAL	15.95	16.00	15.96	15.99	15.99	15.98
	#O-2	24.00	24.00	24.00	24.00	24.00	24.00

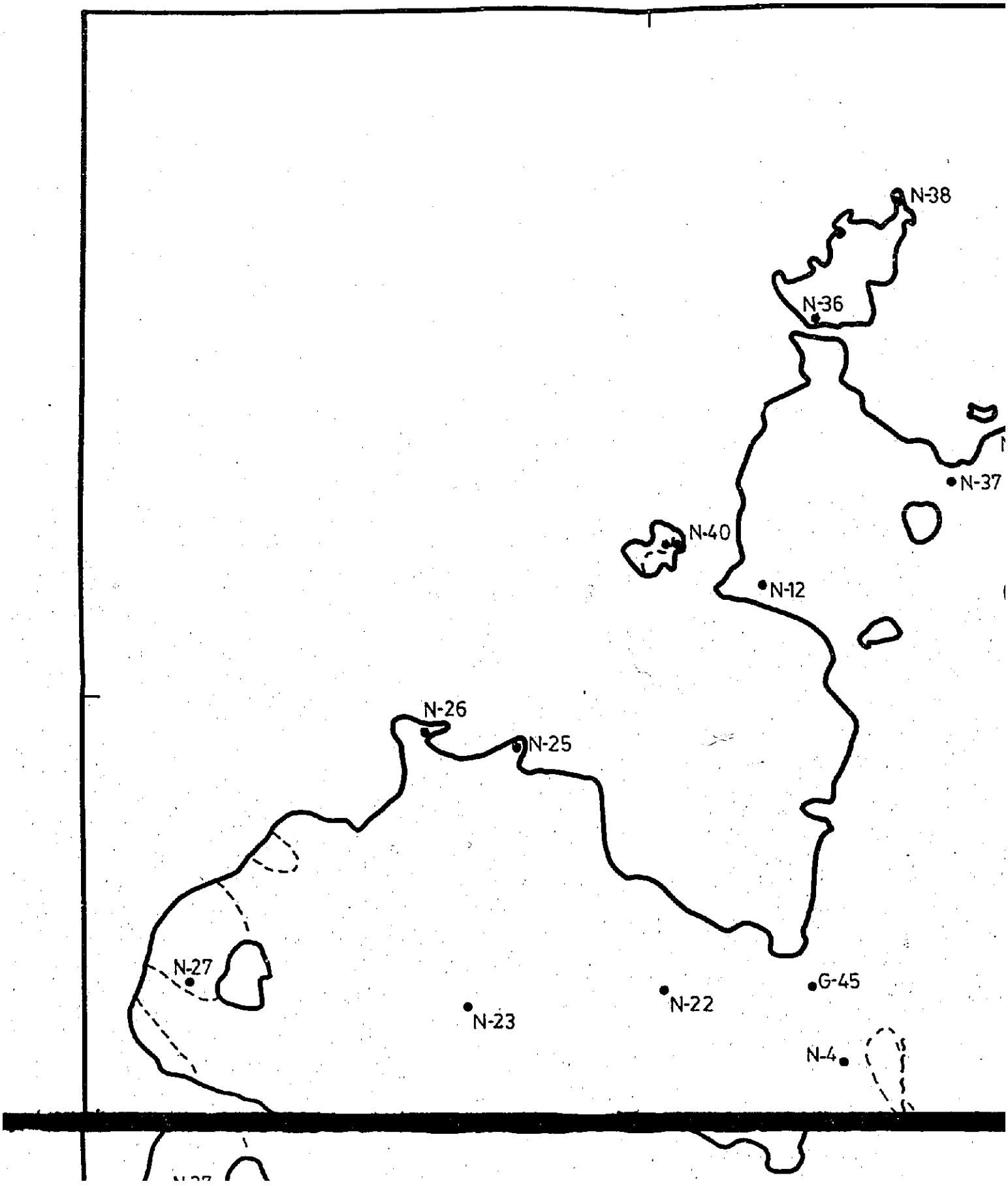
N-38
N-36
N-37
N-40
N-12
N-26
N-25
N-27
N-23
N-22
G-45
N-4

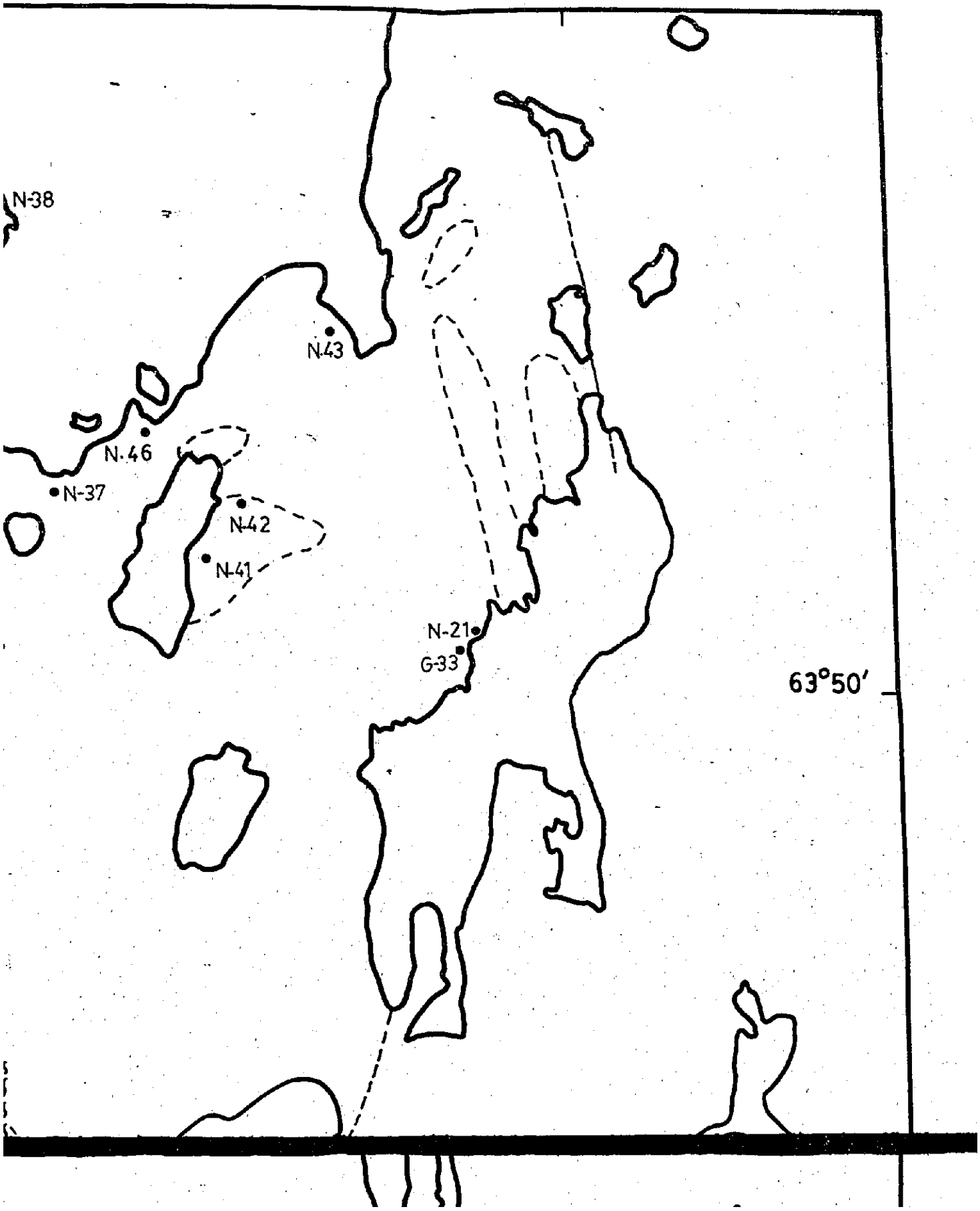
N-38
N-43
N-46
N-37
N-42
N-41
N-21
G-33
63°50'

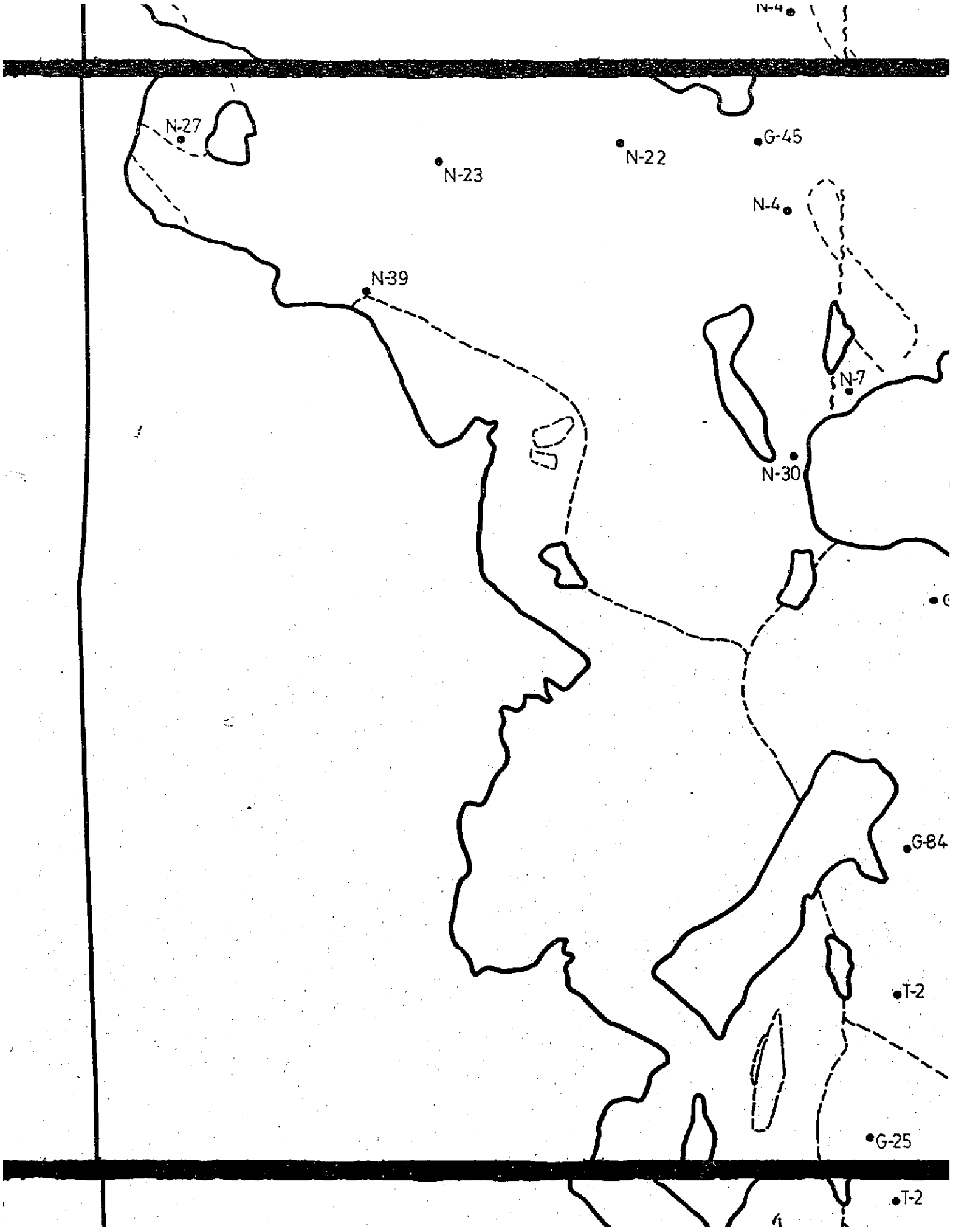
N-4
N-27
G-45
N-22
N-23
N-4
N-39
N-7
N-30
G-84
T-2
G-25
T-2

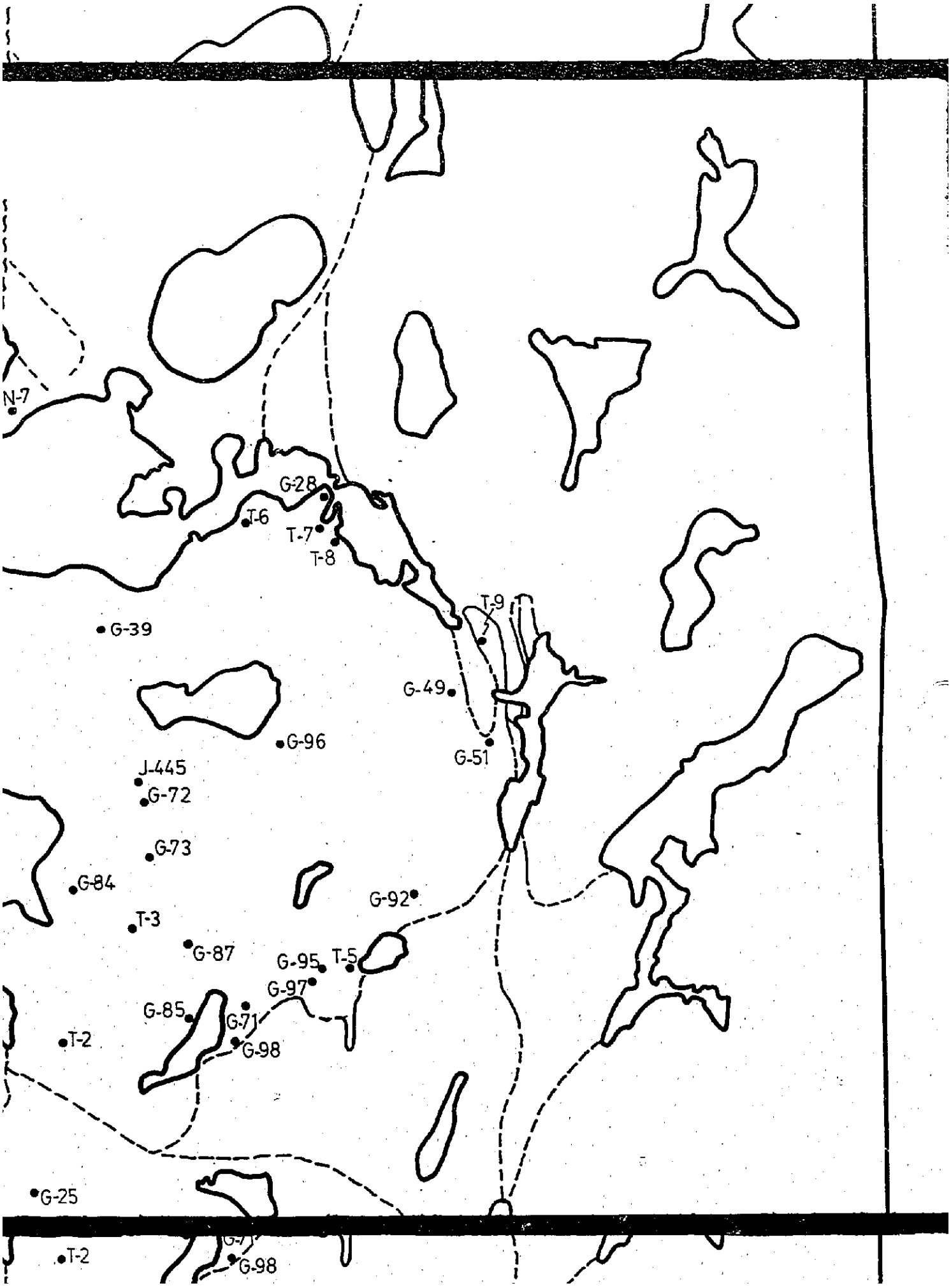
N-7
G-28
T-6
T-7
T-8
T-9
G-39
G-49
G-96
G-51
J-445
G-72
G-73
G-84
G-92
T-3
G-87
G-95
T-5
G-97
G-85
G-71
T-2
G-98
G-25
T-2
G-98

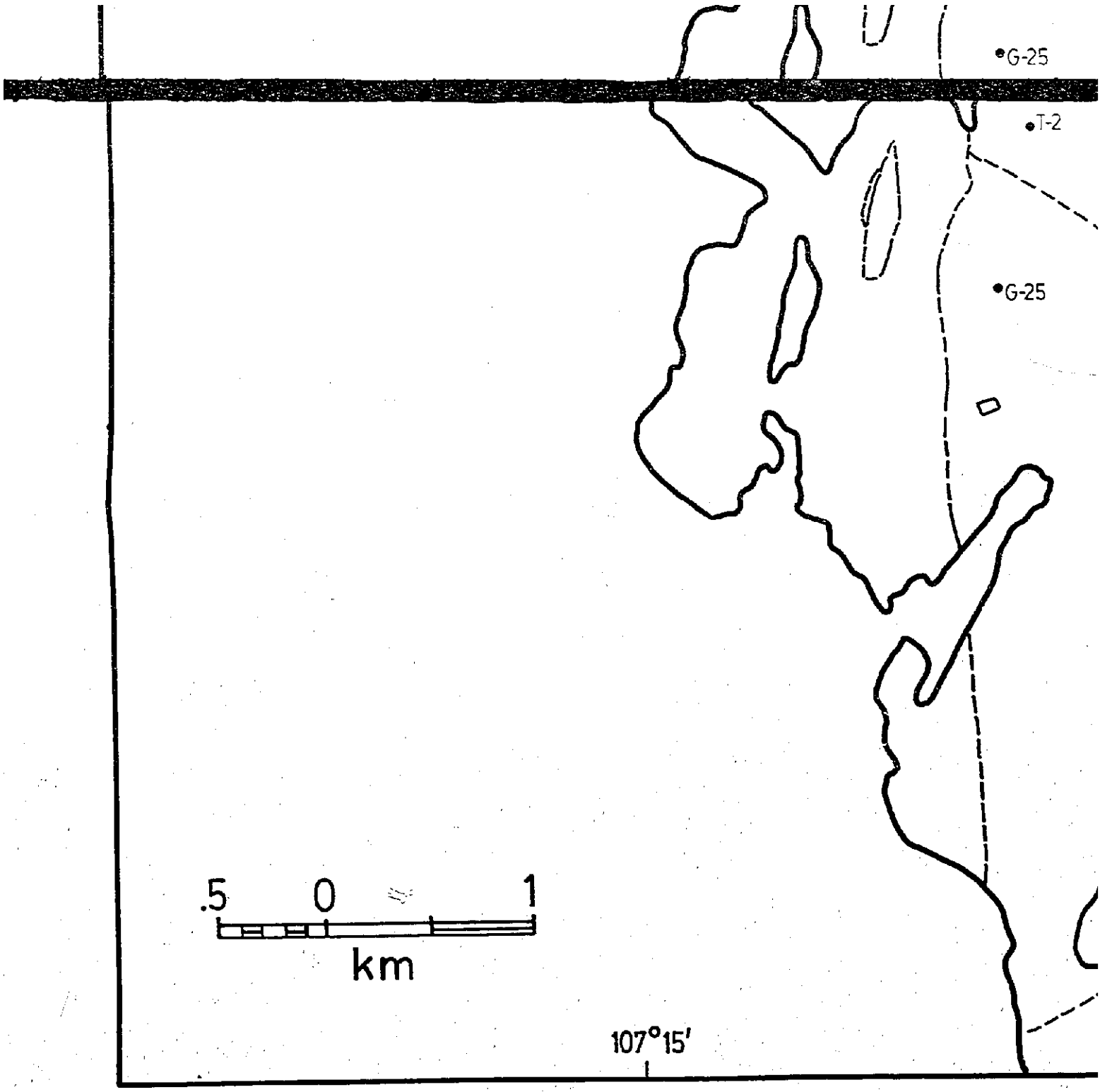

Fig. 2.2: Sample locations an

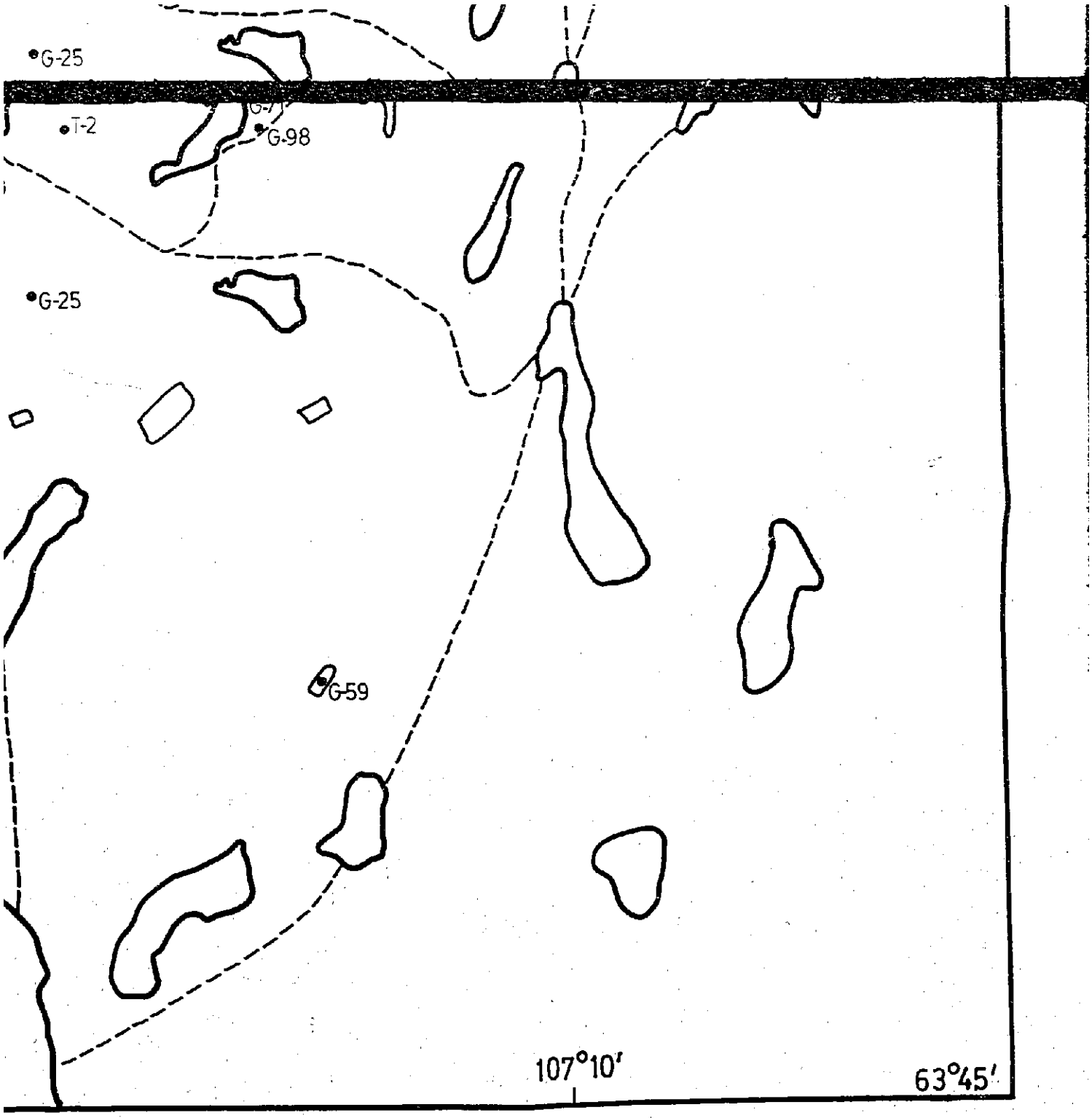

e locations and other stations mentioned in text.

LEGEND

PROTEROZOIC

7 Mackenzie diabase; 1.2 Ga

ARCHEAN

6 Mackay? diabase; 2.65 Ga

5 Tonalite to granodiorite, minor diorite; a, tonalite; b, granodiorite; c, diorite; d, hornblende-bearing; e, coarse-grained. ca. 2.62 Ga.

4 Quartz diorite to diorite; a, quartz diorite; b, diorite.

3 Clinton-Colden gabbro-anorthosite intrusion; a, predominantly 80-100% plagioclase; b, 50-100% plagioclase; c, 25-50% plagioclase; e, inclusion in younger rock. 2686±3 Ma.

2 Felsic meta-volcanic rocks, mostly tuff, banded rhyolite.

1 Mafic and intermediate meta-volcanic rocks; a, mafic; b, undivided mafic to intermediate; c, heterogeneous fine-grained amphibolite of possible volcanic origin.

Geology of the volcanic rocks from Wodicka (1987).

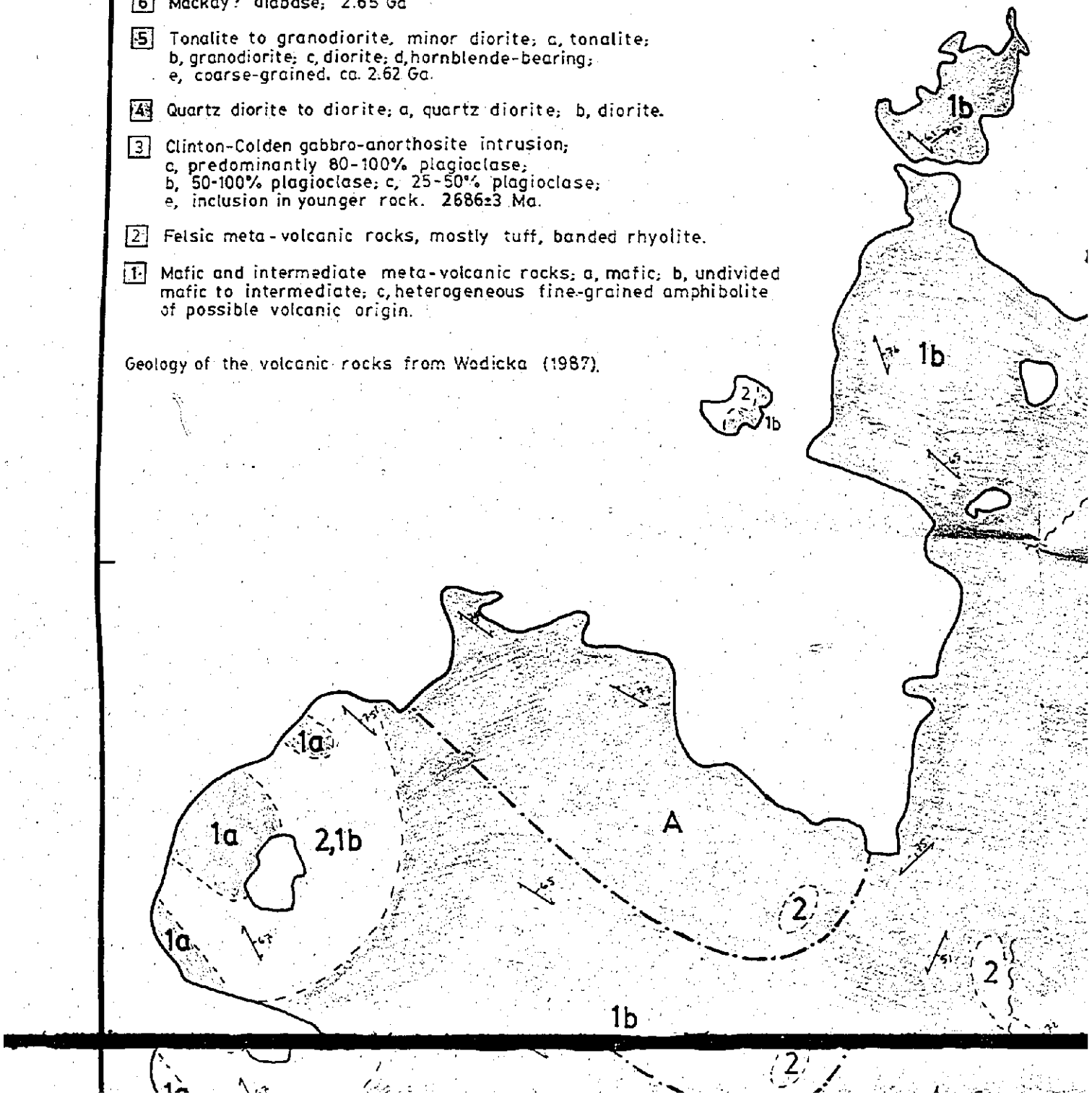

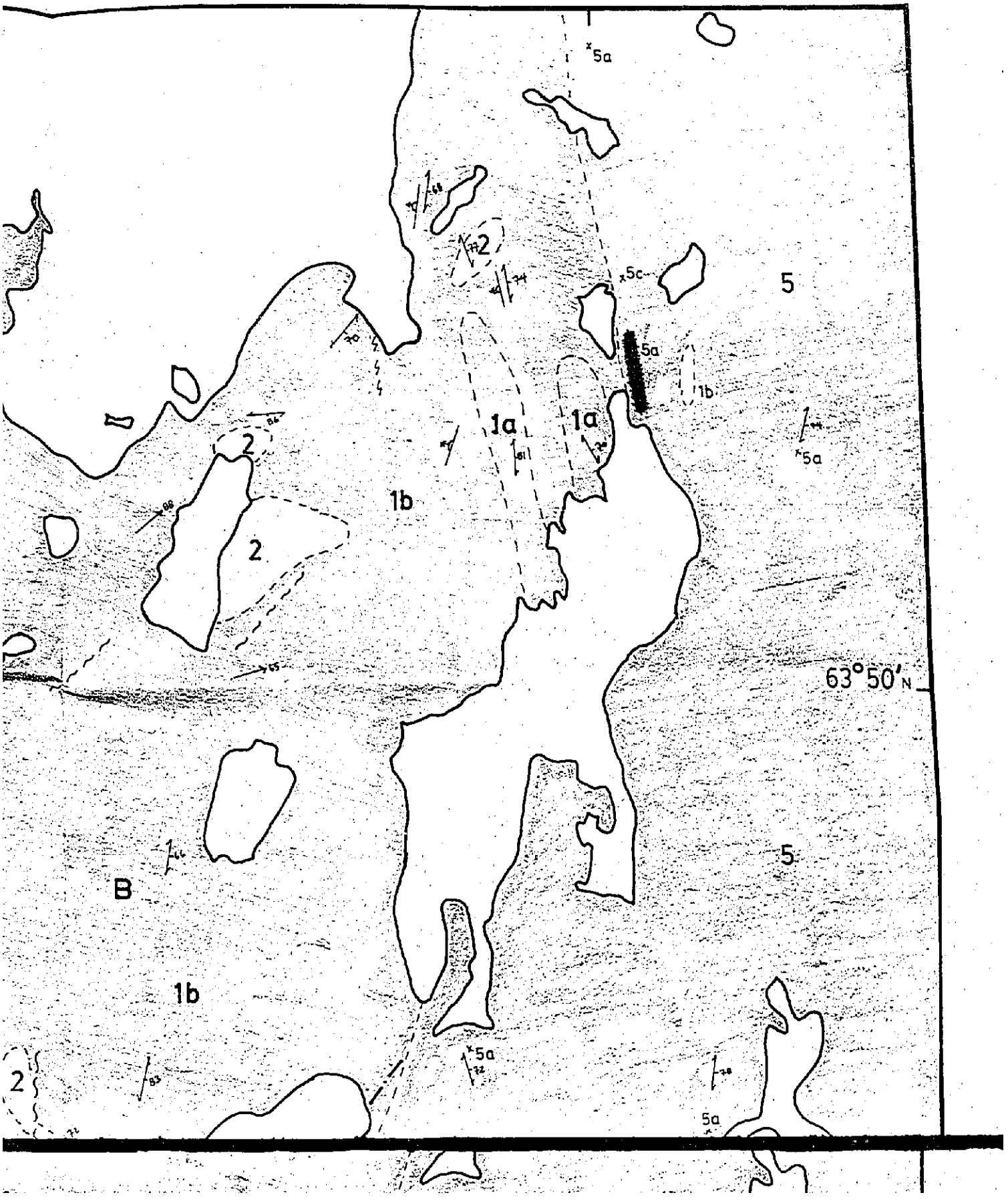
5a
5c
5
1a
1a
1b
2
2
1b
63°50'N
B
5
1b
2
5a
5a

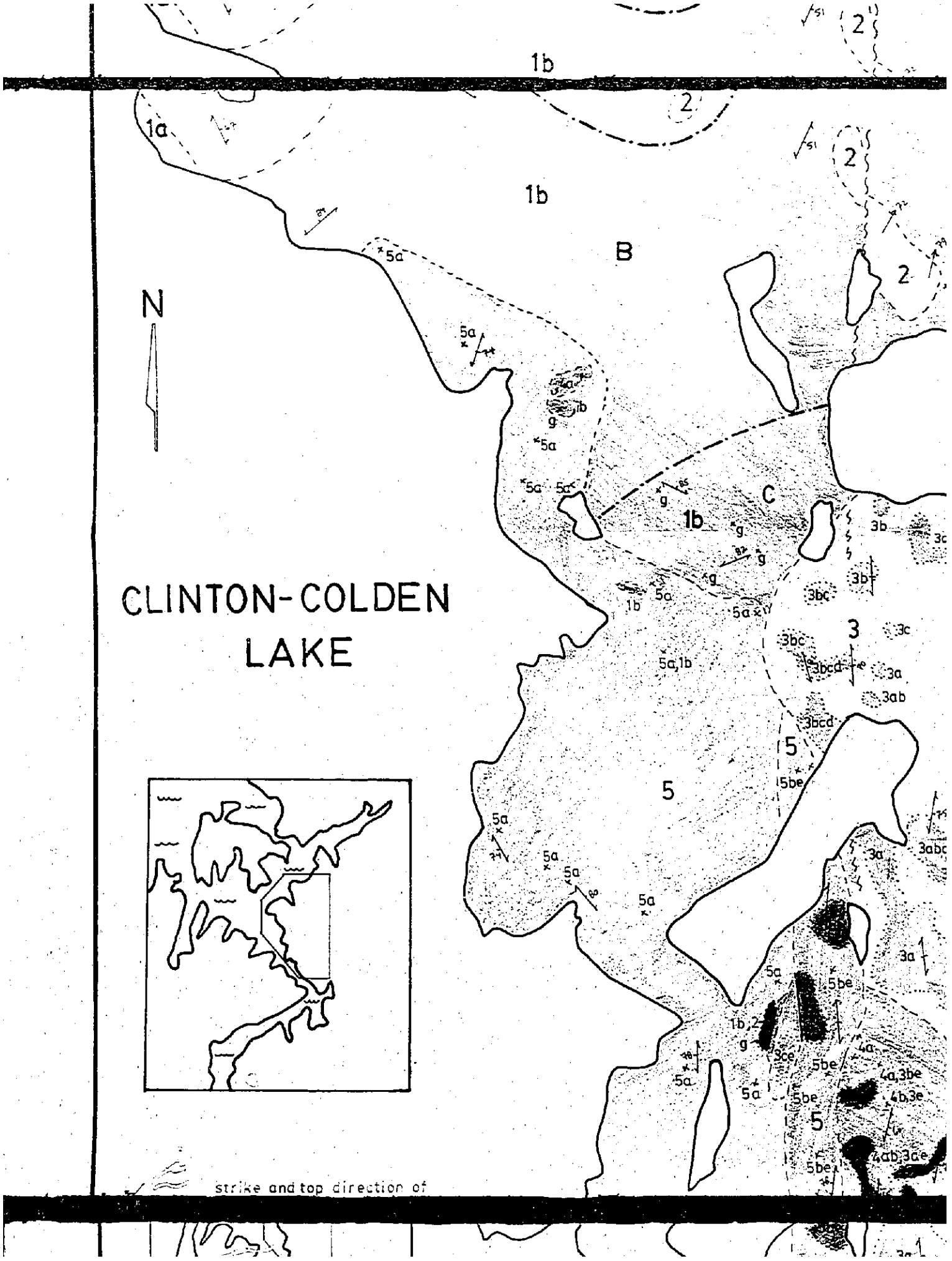
CLINTON-COLDEN LAKE
N
B
C
1a
1b
2
3
5
5a
5be
g
3a
3b
3c
3bc
3bcd
3ab
3abc
4a
4a,3be
4b,3e
4ab,3ce
strike and top direction of

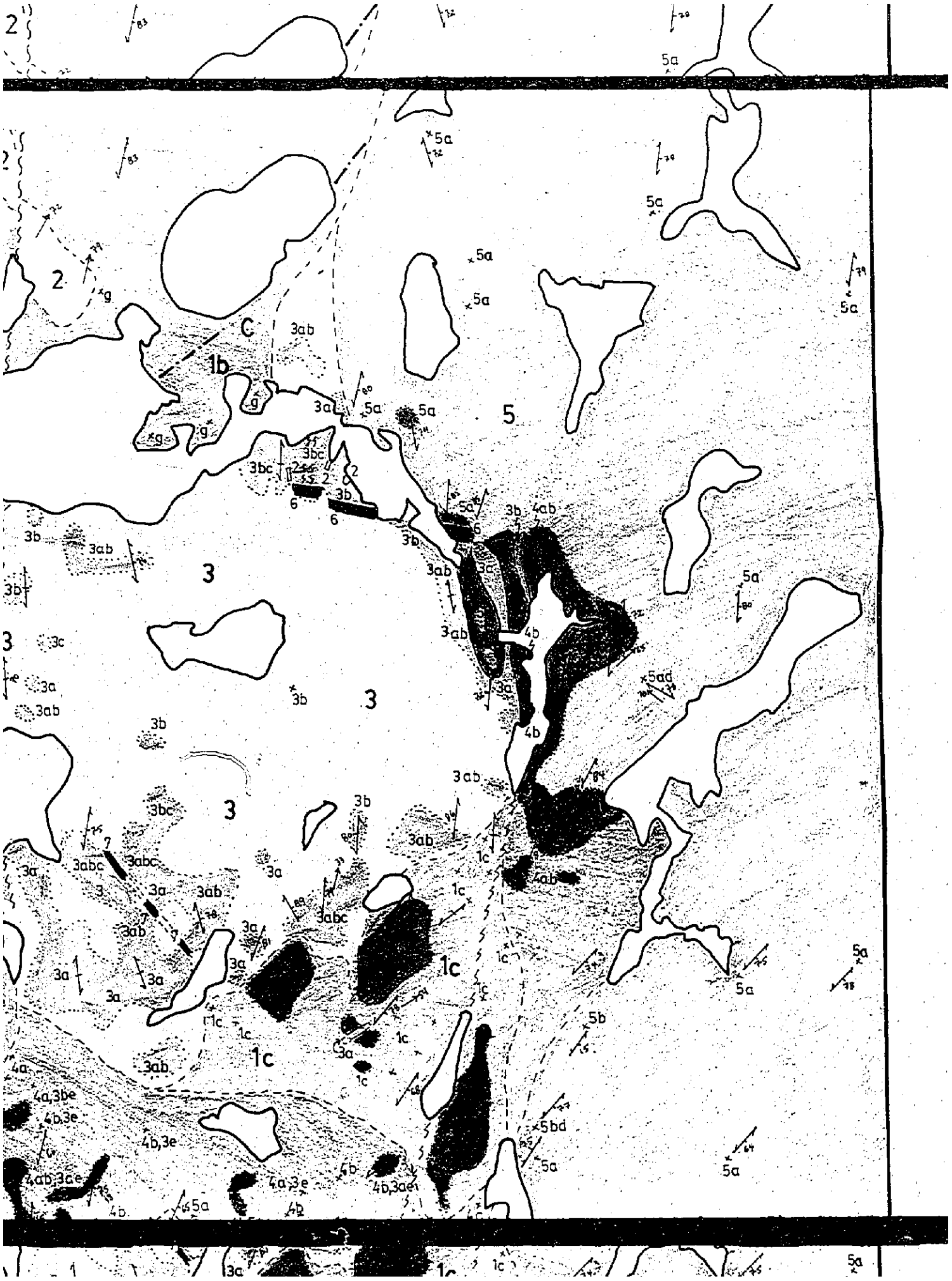
2
5a
2
g
C
3ab
1b
g
3a
5a
5a
5
3bc
3bc
2
2
6
3b
6
3b
5a
6
3b
4ab
3b
3ab
3
3ab
3a
3ab
4b
3b
3
3c
3a
3ab
3b
3
3b
3bc
3
3ab
3b
3abc
3abc
3a
3
3a
3ab
3ab
3a
3abc
1c
1c
4ab
3a
3a
3a
3a
1c
1c
1c
1c
3a
1c
1c
3ab
4a
4a,3be
4b,3e
4b,3e
4ab,3ae
4b
5a
4a,3e
5b
4b,3ae
4b
5a
5a
5a
5a
5a
5a
5a
5a
5a
5a
5a
5a
5b
5bd
5a
5a
5a
1
3a
1c
1c
5a

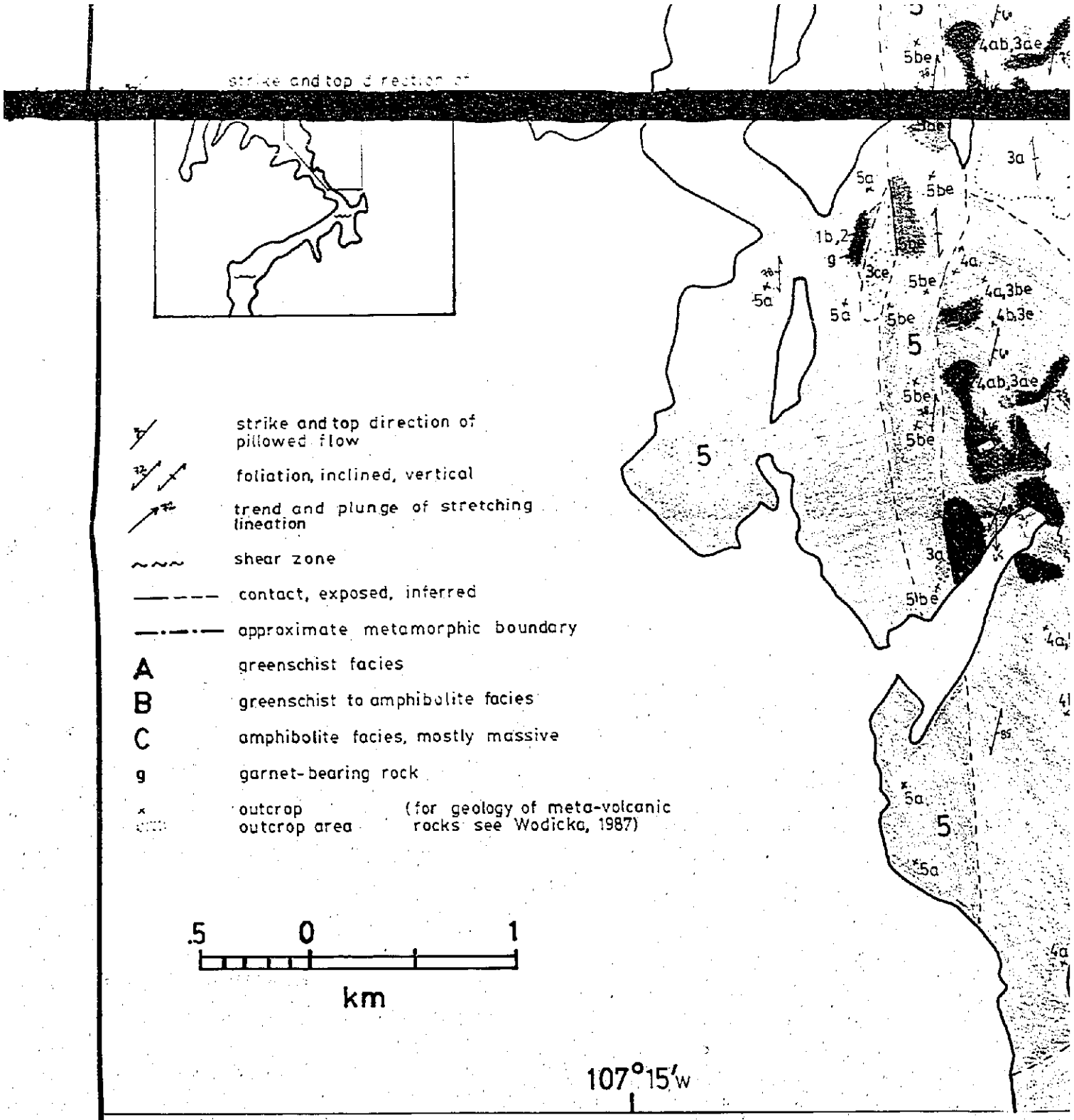

Fig. 2.1

Geology of the Clinton-Colden intrusion and surrou

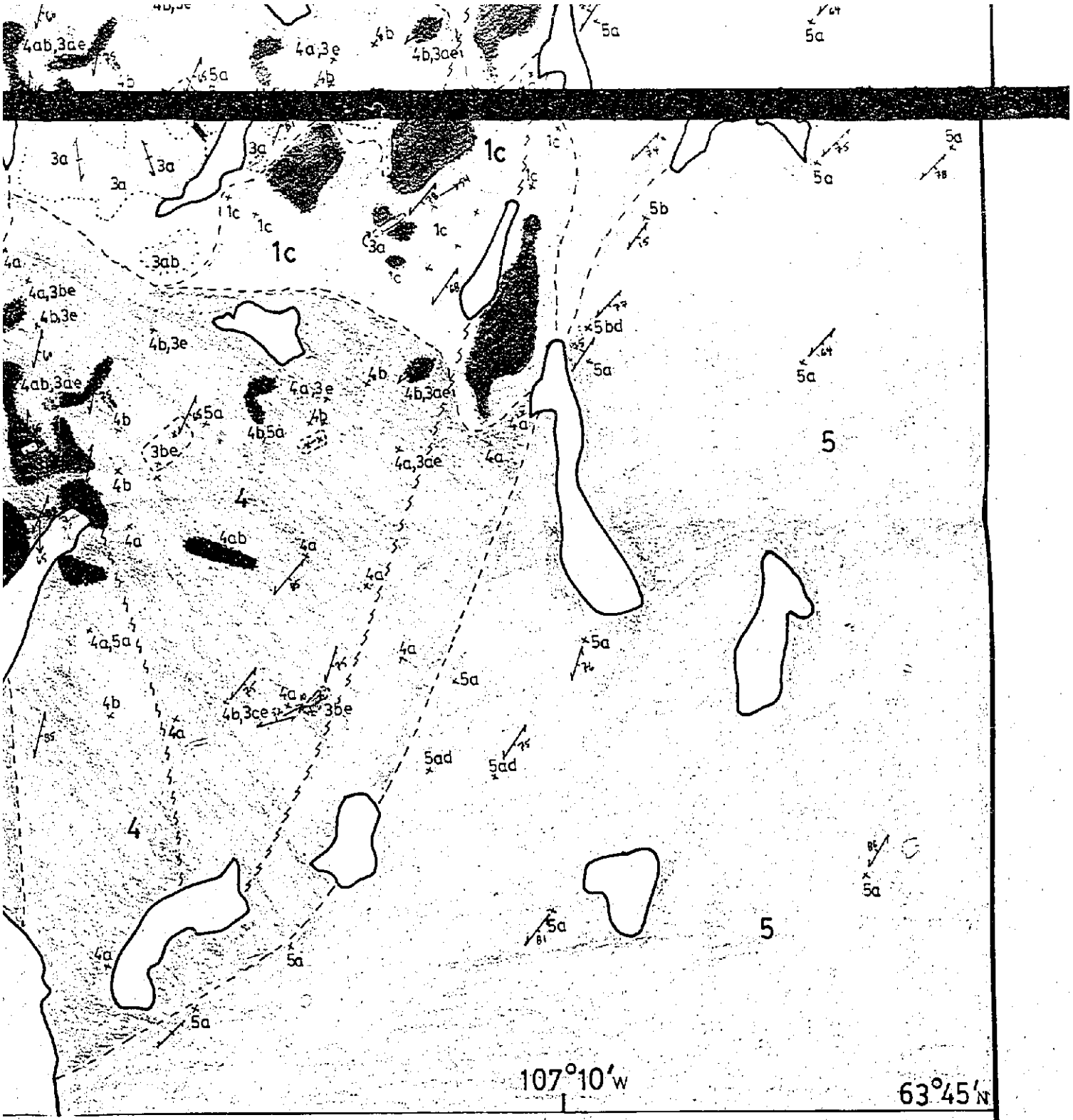

Fig. 2.1

Golden gabbro-anorthosite
surrouding area